UNIVERSITÁ DEGLI STUDI DI MILANO
FACOLTÁ DI MEDICINA E CHIRURGIA

DOTTORATO DI RICERCA IN FISIOLOGIA

SETTORE SCIENTIFICO DISCIPLINARE BIO-09

CICLO XXIII°

Tesi di Dottorato di Ricerca

Investigating the metabolic profile of run-up races and the mechanics of the wobbling visceral mass in vertical jumps

Ph.D student: Ing. Dario CAZZOLA

Matricola: R07722

Tutor: Prof. Alberto E. Minetti
Dipartimento di Fisiologia Umana

Coordinatore: Prof. Paolo Cavallari

Anno Accademico 2009-201

Tesi autorizzata dal coordinatore
Prof. Paolo Cavallari

“…

Barrio,

Il mio barrio,

così lo chiamerò il posto dove mi sentirò uno di voi,

e le voste voci lontane saranno musica per il mio cuore,

Dove amici miei potrete bussare all’ora che volete,

Ci apriranno I bar quando sono già chiusi

E non saremo come numeri sui citofoni

dimenticati come cani di passaggio e senza nomi,

di modo che se fossi nel mio barrio avrei . . .

spalle su cui appoggiare le mani e orecchie a cui confessarmi

e casa, e luna, e stelle che dall’alto sull’angolo del tetto dei miei vecchi mi direbbero…

…

fermati qua . . . fermati qua . . .

…”

Tratto da:

LIVE in VOLVO – Vinicio Capossela

INDEX

Abstract

This Thesis is organized in two parts based on two different investigations about human motion: the metabolic and mechanical analysis of 'skyscraper running', and the estimation of the visceral mass displacement in vertical jumps.

Skyscraper running is a novel sport activity, in which the athletes run on emergency stairs of the tallest building of the world, during the 'run up' races of the world championship circuit. In PART I of this Thesis, this topic has been analysed in terms of mechanical and metabolic requirements, both at general and individual level.

Skyscraper runners'metabolic profile, has been inferred from the total mechanical power estimated in 36 world records (48-421 m tall buildings), ranked by gender and age range. Individual athlete's performance (n=13) has been experimentally investigated during the Pirelli Vertical Sprint, with data loggers for altitude and heart rate. At a general level, a non-linear regression of Wilkie's model relating maximal mechanical power to event duration, revealed the gender and age differences in term of maximum aerobic power and anaerobic energy resources particularly needed at the beginning of the race. The total mechanical power was found to be partitioned among: the fraction devolved to raise the body centre of mass: $\dot{W}_{STA.EXT}$ = 80.4 ± 2.9%, the need to accelerate the limbs with respect to the body: $\dot{W}_{STA.INT}$ = 4.5 ± 2.1%, and running in turns between flights of stairs: $\dot{W}_{TUR}$ = 15.1 ± 2.0%. At the individual level, experiments revealed that these athletes show a metabolic profile similar to middle-distance runners. Furthermore, best skyscraper runners keep constant vertical speed and heart rate throughout the race, while others suddenly decelerate, negatively affecting the race performance.

In PART II of this Thesis another interesting study has been discussed: the mechanics of visceral mass motion in vertical jumps. This internal mass motion could occur in all the locomotion paradigms, and also in all the movements characterized by a high centre of

mass vertical displacement. Moreover, visceral mass shows significant couplings with the respiratory system, as has been discussed in the past in famous studies on quadruped locomotion. Here viscera motion has been analyzed in a simple and well know motor task as the vertical jump, focusing on the effect of respiratory and muscle contractions strategies to limit its displacement, and to improve trunk-pelvis segment stiffness.

A validated method for the estimation of visceral mass displacement has been applied during jump sequences with two different techniques: six subjects before and after a specific training period, executed the natural jump and the "controlled" jump sessions. In that method, the simultaneous measurement of ground reaction forces and spatial coordinates allow the estimation of the relative movement between the 'invisible' abdomen content and the 'container', i.e. the rest of the body as described by the position of external markers.

The results show a significantly higher ($p < 0.05$ – paired t-test) mean of visceral mass displacement (Total = 0.087 ± s.d. 0.021 m) of all the subjects, in normal jumps, compared to the mean of visceral mass displacement (Total = 0.070 ± s.d. 0.027 m) in controlled jumps. An analysis of variance (ANOVA 2-ways) shows a significant effect of jump technique but also of subject and jump-subject interaction, confirming an elevated variability between the subjects. A intraclass-correlation exhibit a significant pattern (ICC= 0.791; $p = 0.017$) and in 5 of 6 subjects, there is a higher mean nominal value of VMD in normal jumps. Also pectorals and low abdominal fat displacements has been measured, showing mean values (weighted by a scaling factor) of 4.5×10^{-4} m and 8.9×10^{-4} m in normal jumps, and 4.5×10^{-4} m and 9.6×10^{-4} m in controlled jumps respectively.

A quantitative and qualitative analysis on visceral mass displacement curve has been completed for both the jumping techniques: a comparison with the 'periodic' curve of body centre of mass show a constant delay ('phase shift') with a mean value of 18.1 ± s.d. 5.73 ms during the aerial phase and 18.8 ± s.d. 9.8 ms in the landing phase.

Finally a preliminary estimation of the internal mass vibration parameters has been showed: the mean values and s.d. of the stiffness in normal and controlled jumps are k_1= 18.2 ± 13.5 KN/m and k_2= 17.9 ± 12.1 KN/m respectively, while the damping constant mean values and s.d. are c_1 300.3 ± 170.7 N/(m/s) is and c_2 is 287.3 ± 129.8 N/(m/s).

For the first time, a method for the estimation of visceral mass displacement, useful in biomechanics and in locomotion-respiratory coupling investigations, has been used in an applied condition. The effects of the "controlled" jumping techniques using respiration and muscles contraction strategies to limit viscera displacement has been demonstrated. The displacement of visceral mass and the body frame have been quantified and compared, and a preliminary estimation of vibration parameter of the internal system has been showed. We foresee an increasing interest in sports biomechanics to improve athletes jumping performance, as well as in the energetics and biomechanics of locomotion.

Prologue

This prologue would be a brief description of the three projects started during my Ph.D. Two of them will be discussed in next chapters: 'Skyscraper running' and 'The visceral mass displacement in vertical jumps'. The first study has been published on the 'Scandinavian Journal of Medicine and Science in Sport'.

The third is based on the design of a knee-exoskeleton for downhill running, to relief joints of mechanical stress and to assist the muscle-skeletal system to dissipate energy. The exoskeleton has been designed to assure a valid assistance for obese subjects and old man in downhill locomotion (stairs, downhill walking), but also to give a further enhancement for long and frequent eccentric exercises in not-pathologic subjects.

It's made up of two custom-fitted cases for the shank and the thigh, connected by two knee-pad allowing the rototraslatory movement as in the biological structure. An oleodynamic circuit, assembled by an electron-valve and a fluidodynamic resistance, is connected to piston damper, to resist knee flexion and allow free knee extension. The electron-valve is actually controlled by a switch, but it will be driven according to quadriceps EMG signal, in future development. This prototype is ready to be tested, but because of the lack of experimental data, it couldn't be analyzed in this thesis.

Future experiments based on kinematic and electromyographic measurements will test exoskeleton mechanical support in human downhill running.

CHAPTER 1

INTRODUCTION

Introduction

The need to move in the most efficient manner has always been a priority in the animal kingdom. The main reason was to survive, both by escaping from predators and by migrating to search for more welcoming e wealthy lands. Locomotion is a ancestral function characterized by a high level of versatility with respect to the different environments. While animals can move with different gaits and speeds along a straight or curvilinear path, on level surface or along positive and negative gradients, natural locomotion has been proven to occur most of the time as to minimize the metabolic energy consumption needed to travel a unit distance (Alexander: Principles of Animal Locomotion).

Humans certainly adhere to this principle during 'natural' locomotion, but there are reasons to suspect that some deviations from that rule could occur. On one side, the erect posture implied bipedalism, which involved a vertical movement of visceral mass as opposed to the horizontal one developed in millions of years of quadrupedalism. This could affect, for instance, how respiration and locomotion are mutually coupled. On the other end, humans invented new forms of locomotion, as walking or running on stairs, which have been invented to facilitate the steep gradient locomotion typical of buildings in high density urban environments. Stairs allow the foot to be flat with respect to the gradient and potentially assist propulsive muscles to avoid overstretch and to use a low efficacy contraction length. To this ancient invention we have to add a very recent sport activity, consisting in reaching the top of the building as fast as possible by running along emergency stairs in skyscrapers (Run-Up Races). This further deviates from ancestral locomotion, by incorporating turns between flight of stairs, by recovering some quadrupedalism in supporting propulsion via the

use of hand-rails, and by forcing the respiratory pattern to perform at a rate imposed by running on every other step.

The aim of this PhD Thesis is to investigate, among all the potential deviations from the ancestral locomotion, these two aspects. They will be studied individually and part of the final remarks will be devoted to link them together.

In the following, a short review of the advances in the understanding of locomotion, relevant to the present project, will be provided.

The study of all forms of terrestrial legged locomotion passes through the concepts of mechanical energy generation and dissipation, as caused by the shortening and lengthening contractions of skeletal muscles, and the metabolic energy associated to it. and delineates every specific locomotion paradigm. Mechanical energy generated or dissipated (i.e. positive or negative work) is normally due to a change in the total mechanical energy of the system, which in turns is the result of a combination of potential (PE) and kinetic energy (KE) of the body centre of mass (BCOM) and of body segments. In some gaits, some elastic energy (EE) can be stored in tendons and other deformable biological structures, which then return that energy in a different phase of the gait cycle. Mechanical energy forms exchange among each other, allowing to save mechanical, and thus metabolic, energy. In walking, as mentioned below, a portion of PE is exchanged with KE, as in a pendulum, while in running PE+KE exchange with EE.

The positive total work (WTOT) is the sum of the external work (WEXT), or the work associated to raise and accelerate the BCOM within the environment, and internal work (WINT), needed to accelerate body segments with respect to the BCOM (Cavagna & Kaneko 1977; Cavagna et al. 1963; Cavagna et al. 1964; Cavagna et al. 1976; Minetti 1998; Minetti & Ardigo 2001; Minetti et al. 1993;

Minetti et al. 1994; Minetti et al. 1994; Minetti et al. 1995; Minetti & Saibene 1992; Minetti et al. 1994; Willems et al. 1995; Williams & Cavanagh 1983; Winter 1979).

Historically, human locomotion has been modelled as an inverted pendulum/rolling egg for walking (Cavagna, Thys 1976) and as a mass-spring system (pogo-stick or bouncing-ball) for running (Margaria 1976). The main characteristic of the inverted pendulum is a continuous exchange of PE and KE, showing a resulting total energy (TE is the sum of KE and PE) with a lower excursion with respect to the one of its individual components. This peculiarity suggested to introduce a parameter called energy recovery that quantifies this ability to behave like a pendulum (in a ideal pendulum the energy recovery is 100%) (Cavagna, Thys 1976). Running is described by the bouncing ball paradigm where KE and PE change in phase, and EE is stored and released in every step, saving a large amount of energy needed to move. Those differences in the mechanical paradigm possibly contribute to explain the existence of an optimal speed for walking (at which the metabolic cost per unit distance is lowest) and an independent cost of transport for running (Figure 1).

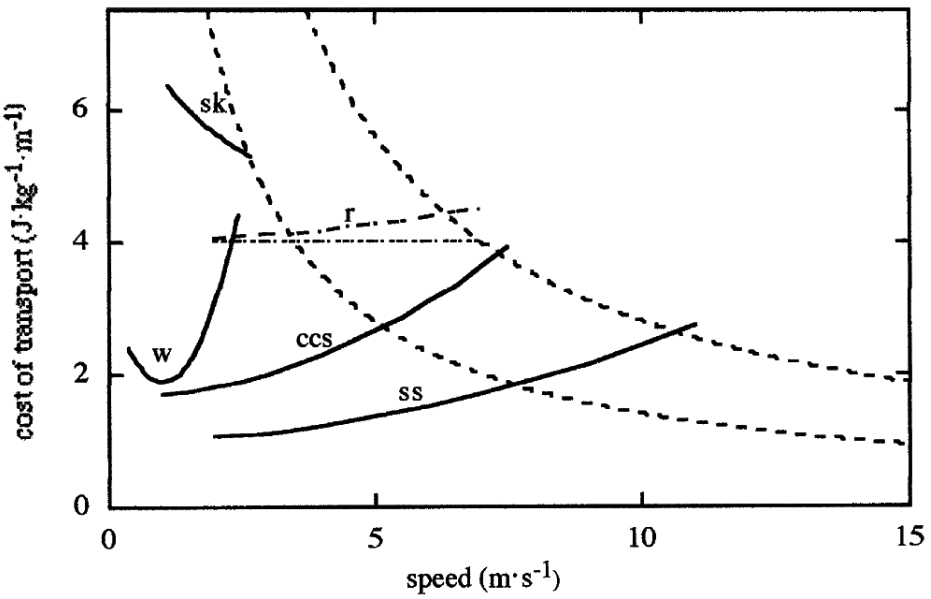

Figure 1: Cost of transport as a funcion of speed for different types of human locomotion. W Walking, r Running, ccs Cross country skiing, ss ice skating, sk skipping. The dashed curves represent the iso-metabolic poer limit for healthy normal subject (14 W.Kg-1, lower curve) and an athlete (28 W.kg-1, upper curve).

Muscle contractions combine to maintain a constant amount of BCOM mechanical energy in level gaits (Donelan et al. 2002; Laursen et al. 2000; Minetti, Ardigo 1993), where the positive and negative external work performed are equal, while in non-level, ascending or descending, gaits the more gradient change, the more total mechanical work needed increases or decreases (Daley & Biewener 2003; Gabaldon et al. 2004; Gottschall & Kram 2006; McIntosh et al. 2006; Minetti, Ardigo 1994).

In particular, Minetti (Minetti, Ardigo 1993), measured the mechanical work in level and non-level gaits, walking on a treadmill and evidenced that the fraction of positive work decreased in a sigmoidal pattern from 100% at 15% gradient to almost nil at -15% gradient, regardless of speed (Saibene & Minetti 2003).

During running uphill at very steep gradients positive mechanical work is the only work carried out (Minetti et al., 1994), and the absence of negative work

tells us that BCOM will not be lowered enough in the first half of the foot contact phase for some elastic energy storage to occur, with no successive chances to save energy by elastic release. Thus we could say that the bouncing ball paradigm does not apply in high gradient uphill running.

Running uphill on stairs, and especially on emergency stairs of the tallest building of the world, could be modelled in the same way: elastic energy intervention is negligible and the work to increase the gravitational potential energy [the prevalent portion of the WEXT, needed to accelerate and lift BCOM] considerably exceeds the work to move limbs with respect to the centre of mass (WINT). Hence, the required metabolic energy (or the metabolic energy rate) has to be strictly proportional to the total mechanical work (WTOT or power) generated by muscles during the ascent, the last being an easy variable to calculate (Minetti et al. 2009).

In the 'Part I' of this Thesis the overall mechanics of this emerging activity, called skyscraper running (or run-up races) is delineated, and a physiological profile of the athletes who compete in buildings of very different height is drawn.

The difficulty to outline a complete description of this sport is in accurately modelling all the phases of the race. For example, the mechanical total work WTOT, has been expressed as the classical sum of WEXT, WINT with the addiction of WTURN, that is the mechanical work estimated to running in turns between successive flight of stairs. Another aspect is the presence of handrails that maximize the muscle mass involved and, consequently, the mechanical/metabolic power of the ascent. Moreover, kinematic and physiological variables have been monitored during the race, showing an attractive correlation. For example, discontinuous velocity profile corresponds to

a heart rate overshoot, or the point of speed deflection during the race is related to the average vertical speed value.

All this insights are useful to define the best race strategy, avoiding the conditions that could jeopardize the race performance, and could shed lights on biomechanical and physiological couplings. For example, an athlete running chooses a determinate stride length and step frequency depending on the adopted speed, but at the same time drives his respiration frequency to be in 'phase', often locked with that movement. In run-up races the vertical speed and the number of stair-steps covered implies a given step frequency, not necessary to be optimally linked to the required respiration frequency for that effort.

In literature, this coupling has been analysed in quadruped and humans. Quadrupeds (horses and dogs, mainly) synchronize the locomotor and respiratory cycles at a constant ratio of 1:1 (strides per breath) in both the trot and gallop, and this results from the constraints put on the thoracic region from the repeated impact loading when the forelimbs strike the ground (Alexander 1993; Bramble & Carrier 1983; Young et al. 1992).

These interactions appear to be different in human runners: because of our upright posture and bipedal locomotion, we employ several phase-locked patterns (4:1, 3:1, 2:1, 1:1, 5:2, and 3:2), although a 2:1 coupling ratio appears to be favoured (Bernasconi & Kohl 1993; Bramble & Carrier 1983). These coupling ratios are often more variable than in animals and humans appear to have further greater variability in respiration during locomotion. It has been suggested that tighter coordination between limb rhythms and respiration may reduce the metabolic cost of a movement (Hill et al. 1988; Paterson et al. 1986) or at least the perception of the workload (Bonsignore et al. 1998).

Hence, when two rhythmical components of a system interact in a way so that one (locomotory rhythm) imposes its on the other (respiration rhythm), consequently a frequency and phase locking could be shown.

This could become a key factor in a race strategy, and in run-up races it mainly depends on the number of stair-step in a stride, that leads the athlete respiration. A 'coupling determined' respiratory training could bring to an efficient respiration-locomotion coupling, supporting a winning race-strategy. Also, it should be interesting to relate that coupling to athlete's fitness: neither the frequency coupling nor the phase coupling are normally addressed by running training or specific motor ability, but trained runners show a greater level of adaptability of the locomotor and/or respiratory systems to changing speed and metabolic demands (McDermott et al. 2003). These respiration-locomotor couplings, as a consequence, could be seen just like a physiological responses to dynamic stimulus on the human system.

Analysing both these interactions and the anatomy of the examined biomechanical model, another attractive coupling, already discussed in literature, could be exhibited: it pertains with cyclical motion of visceral mass during locomotion, described as a 'visceral piston' (Bramble & Carrier 1983; Young, Alexander 1992), mainly studied in animals so far.

In quadrupedal locomotion this 'visceral piston' drives ventilation by moving with a specific phase in respect to the musculoskeletal frame, but can also have an effect on bipedal gaits or specific human movements. In the case of stairs ascent, it is clear that respiration and viscera motion are potentially connected toeach other, and a periodic and almost vertical BCOM displacement emphasizes this relation. A simple example tof this important link consists in jumping vertically while trying to breathe completely out of phase with respect

to BCOM motion: normally we expire during contact phase and inspire during flight phase, and it is in practice impossible to do the opposity. Hence, in human running and especially in all the motion characterized by a high BCOM vertical displacement, as vertical jumps, the 'visceral piston' could be a critical factor.

Unfortunately, there are not many studies on human visceral mass motion, and usually are just theoretical or clinical-anatomical analysis. Some of them show a quantitative analysis of viscera motion based on MRI or CT imaging technique measurements, but exclusively during free-breathing or related to different trunk positions (static measurements). From a biomechanical approach, instead, it becomes interesting to evaluate the dynamics of viscera mass system in specific movements, using a method to estimate its motion in the simplest possible way.

In the 'Part II' of this Thesis a validated method for the estimation of visceral mass displacement in periodic movements has been improved and applied on repeated vertical jumps. This method (Minetti & Belli 1994) estimates visceral displacement through a simultaneous force platform and motion capture data acquisition, instrumentation historically utilised for locomotion analysis.

The choice of vertical jump movement simplifies the analysis focusing the study on method refinement and its adaptability for other applications, in addition to lead the viscera up to its maximal excursion.

The aim of this second study is to verify the effects of different jumping techniques, based on particular respiration and muscle contraction strategies, in limiting the vertical excursion of the body visceral mass. In literature there are a lot of studies, mainly related with sport activity, about the ability to control the abdominal or thoracic respiration in a way to get a more compact abdomen during the exercises. With the abdominal muscles intervention, the viscera could be further packed together, and the athlete could potentially be more performing.

As a matter of fact, none quantitative study has been carried out to confirm this idea, even if athletes' and trainers' experience seems to support it.

Anyway, the possibility to link viscera displacement with a long studied movement as the vertical jump allows to check the real effect on that technique and brings to other speculations: this approach allows to easily analyze visceral mass displacement, and to refine what we know about the real value of the BCOM displacement. In fact the viscera could be considered as a further anatomical segment, characterized by a definite weight on BCOM computation, and consequently on the total mechanical work of the system. In this way the vertical BCOM displacement during uphill running could present a higher excursion oscillation, strictly in phase with the respiration signal, in its monotone positive ascent.

As far as the Thesis structure is concerned, "Part I" will describe an investigation on skyscraper running (paper "Skyscraper running: physiological and biomechanical profile of a novel sport activity" (Minetti, Cazzola 2009), while "Part II" will discuss the "Effects of different jumping techniques in limiting the vertical excursion of the body visceral mass".

CHAPTER 2

2. PART II

SKYSCRAPER RUNNING: PHYSIOLOGICAL AND METABOLICAL PROFILE OF A NOVEL SPORT ACTIVITY

The content of this chapter has been published as:

Minetti A. E., Seminati E., Cazzola D., Giacometti D. and S. G. Roi. Skyscraper running: physiological and biomechanical profile of a novel sport activity. Scand. J. Med. Sci. Sports. 18 DEC 2009 | doi: 10.1111/j.1600-0838.2009.01043.x.

2.1 INTRODUCTION

Running uphill on steep emergency stairs (Run-Up races), today a rapidly expanding sport activity performed on the tallest buildings of the planet, has been an interesting motor act to physiologists since Rodolfo Margaria's time, when he designed the rapid ascent test to evaluate the individual maximum anaerobic power (Margaria et al. 1966). Only a few studies previously discussed stair climbing, some of them considering kinetics and kinematics (Larsen et al. 2009; McFadyen & Winter 1988; Yu et al. 1997) or metabolic aspects of slow walking on stairs, or in particular conditions as running while wearing firemen robes (O'Connell et al. 1986; Teh & Aziz 2002). The particular appeal in this new sport discipline resides in the fact that mostly positive work is done (Minetti, Ardigo 1994), that the elastic energy storage and the consequent release in running is practically nil at steep gradients, and that the work to increase gravitational potential energy (the prevalent portion of the external mechanical work (W_{EXT}), needed to accelerate and lift the body centre of mass) greatly exceeds the work to move limbs with respect to the centre of mass (the mechanical internal work - W_{INT}). Thus the required metabolic energy (or metabolic energy rate) has to be strictly proportional to the total mechanical work (W_{TOT} or power) generated by muscles during the ascent, the last being an easy variable to calculate. Another attractiveness relates to the presence, in most skyscrapers, of handrails that maximize the muscle mass involved and, consequently, the mechanical/metabolic power of the ascent, giving to the race the character of a global, maximal effort as in rowing. Since the duration of the events ranges from a few dozens seconds to 14 minutes and runners attend many different races, both anaerobic and aerobic skills are simultaneously required. Thus the athlete's choice in terms of the sustainable 'engine set-point' is crucial to the overall performance, as an excessive initial power could negatively affect aerobic pathway enzymes and jeopardize the rest of the competition.

Run-up races, as they are usually called, are organized on buildings of very different height, and they allow to test predictions about the maximum mechanical power sustainable for a given exercise duration (e.g. Wilkie, 1980) in a wide range of performances. This analysis will also (see below) provide the 'typical' profile of run-up male and female athletes of very different age in terms of aerobic and anaerobic resources available.

Aims of this paper are: 1) to define a research methodology for this new sport, 2) to measure physio-mechanical variables of a group of athletes during a real run-up race, and 3) to infer from them the climbing strategy, if any. We will introduce the topic, in the following, by reviewing and analysing world records in this expanding sport activity.

2.2 ANALYSIS OF WORLD RECORDS

2.2.1 Mechanical work in skyscraper running

As shown in Fig. 2, races so far were organized in buildings of very different height, ranging from a few dozen metres to the tallest skyscrapers on the planet (KL Tower, Malaysia, 421 m). The event duration ranges from 50 s to about 14 min and the race conditions vary a lot, not just for climatic reasons. In some cases a short, level approach to stairs is included and the staircase steps, while being quite similar, are not exactly of the same size/geometry in the different buildings. Runners are often divided in groups, to avoid overcrowding the race terrain, and the group size can affect the overall performance. In addition, the stairs width affects the usage of handrails as pushing aids, and the number of floors implies a different number of 'running turns', for the same vertical distance travelled.

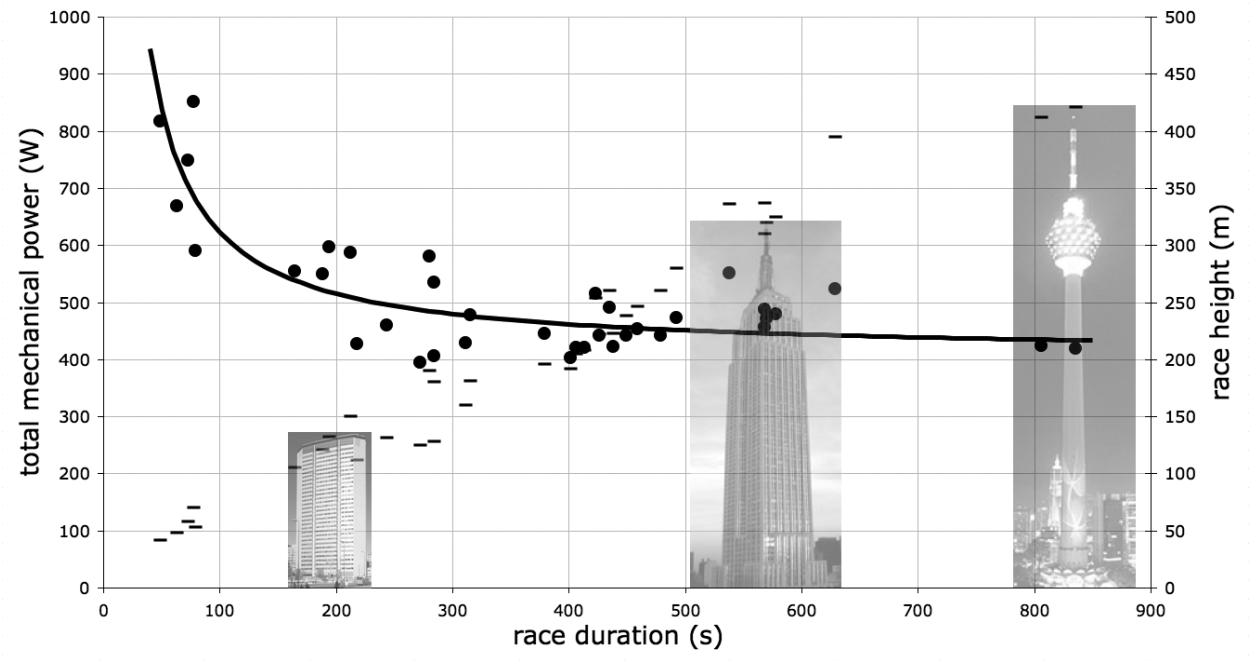

Figure 2: Current world records of male athletes in run-up races are represented as the 'minimum' mechanical power ($\dot{W}_{TOT}$) needed to set them (solid circles, see text), together with the building height (minus symbols) shown for each record on the right hand side ordinate, as a function of race duration. The curve represents a non-linear regression of world records ($\dot{W}_{TOT}$) based on Wilkie's model (see eq. 5).

As anticipated in the Introduction, run-up races seem easier to be mechanically analysed than other sports as, for example, level running, because the power to move vertically is expected to be the predominant fraction of the total power needed. In order to consider the most comprehensive list of determinants, though, we modelled the total mechanical power required to complete the ascent as:

$$\dot{W}_{TOT} = \dot{W}_{STA} + \dot{W}_{TUR} \quad (1)$$

i.e. the sum of the power necessary to run up the stairs ($\dot{W}_{STA}$) and the one related to running in turns between successive flight of stairs ($\dot{W}_{TUR}$).

The first term is classically partitioned into the external and internal portion of the mechanical power:

$$\dot{W}_{STA} = \dot{W}_{STA.EXT} + \dot{W}_{STA.INT} \quad (2)$$

$\dot{W}_{STA.EXT}$ is estimated as:

$$\dot{W}_{STA.EXT} = \frac{mg\Delta h}{\Delta t} \quad (3)$$

where m, g, Δh and Δt are the subject mass (made equal to 70 kg), the gravity acceleration, the height of the race inside the building (m) and the race time (s), respectively. We disregarded both the vertical and forward kinetic energy changes of the body centre of mass (BCOM) because they are supposed not to affect the overall mechanical work, being 'buried' in the monotonically ascending curve of the total energy of BCOM when running at very steep gradients (Minetti et al., 1994).

The term $\dot{W}_{STA.INT}$ reflects the mechanical internal power necessary to accelerate limbs with respect to BCOM (Cavagna & Kaneko 1977). Normally obtained by processing kinematics data, here we estimate its real value by using a model equation that have been previously tested for gradient locomotion (Minetti, 1998):

$$\dot{W}_{STA.INT} = m f \bar{\dot{s}}^2 \left(1 + \left(\frac{d}{1-d}\right)^2\right) q \quad (4)$$

where: f is the stride frequency (Hz), $\bar{\dot{s}}$ is the (diagonal) speed (m/s) on the stairs, d is the duty factor, i.e. the fraction of the stride period at which one foot is in contact with the ground, and q reflects the inertia properties of the four body limbs. Depending on the building height, the race time, the reported number of steps and previous data from our group about gradient running (Minetti et al., 1994; Minetti, 1998), we estimated for each record f and $\bar{\dot{s}}$, while d and q were assumed to be equal to 0.45 (extrapolated for a gradient of about 50% from the $\dot{W}_{INT}$ model) and 0.15, respectively. Stride frequency was deducted from the number of stair steps and from observing that athletes run on every other step, and $\bar{\dot{s}}$ was estimated by dividing the vertical speed by *sin(atan(i))*, where i is the stairs gradient (assumed equal to the one we measured on the Pirelli building, about 50%).

The mechanical power involved in running in turns between flights of stairs ($\dot{W}_{TUR}$) and its metabolic energy consumption have never been studied in the past. A set of preliminary experiments provided the metabolic equivalent of $\dot{W}_{TUR}$ (see Appendix). A curvature radius of 1 meter describing the body trajectory to the next floor, as measured on the Pirelli building in Milan (see below), has been assumed for all the builings involved in world Run-Up records. Because of this methodological approach, we can expect that estimated $\dot{W}_{TUR}$ reflects the sum of the external and the internal power of running in circles.

The total mechanical power ($\dot{W}_{TOT}$) needed to achieve the world records on 36 skyscrapers, calculated according to the above equations, is shown as solid circles in Fig. 2. The prediction is supposed to be reliable due to the expected absence of elastic energy stored and released during the contact phase (Minetti et al., 1994). In any case, the estimated $\dot{W}_{TOT}$ and the related metabolic energy consumption, obtained by dividing by the muscle contraction efficiency, represent the 'minimum' work rate and energy consumption for each ascent. Additional components of $\dot{V}_{O2}$ could include, for example, the effect of antagonist muscles, the need to stabilize the trunk during uphill running and the acceleration at the beginning of each flight of stairs.

When the 3 main components of $\dot{W}_{TOT}$ are plotted vs. race height, as in Fig. 3, it appears that their contribution is quite constant, being 80.4±2.9%, 4.5±2.1% and 15.1±2.0% for $\dot{W}_{STA.EXT}$, $\dot{W}_{STA.INT}$ and $\dot{W}_{TUR}$, respectively.

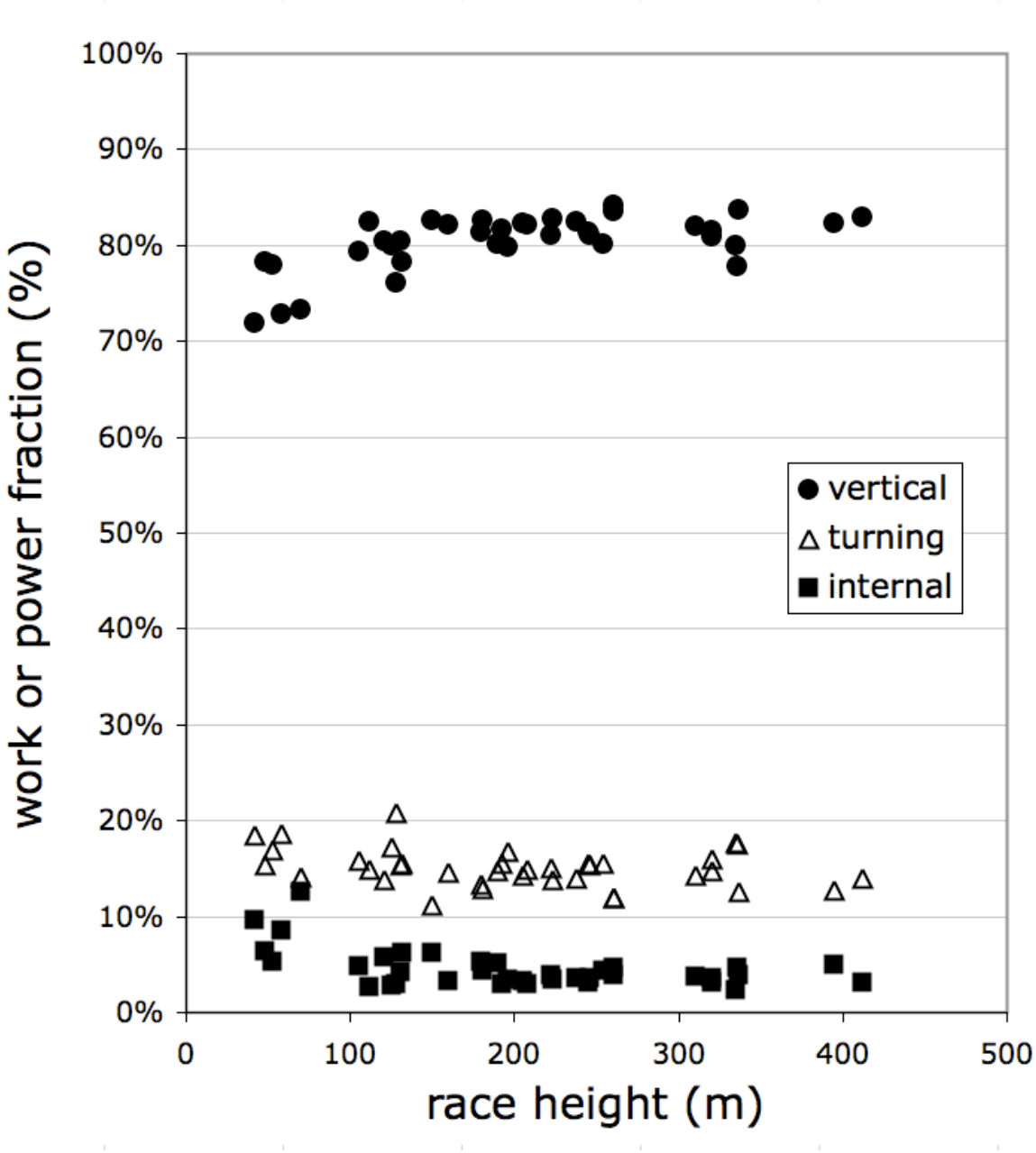

Figure 3: The 3 components of the estimated mechanical power (vertical: $\dot{W}_{STA.EXT}$, turning: $\dot{W}_{TUR}$, internal: $\dot{W}_{STA.INT}$, see text) are shown as fractions of $\dot{W}_{TOT}$, for the different race heights.

2.2.1 Maximum human mechanical power: Wilkie's model

While in early days run-ups participants were amateur runners, more recent records have been established by professionals, thus $\dot{W}_{TOT}$ data in Fig. 2 represent performances of top male athletes in the age range 20-35 yrs who often attend multiple events, on skyscrapers with very different height (and race duration). It is apparent that the total mechanical power generated is much greater for smaller buildings, where the shorter performance allows to exploit more powerful, high energy phosphate sources.

Wilkie (1980) tried to capture this phenomenon by proposing an equation predicting the available average mechanical power ($\dot{W}_{MECH}$ (W) - same of our $\dot{W}_{TOT}$) as a function of the event duration (t (s), same of our Δt) with the assumption that subjects reach exhaustion at the end of the exercise:

$$\dot{W}_{MECH} = A + \frac{B}{t} - \frac{A \cdot \tau \left(1 - e^{-\frac{t}{\tau}}\right)}{t} \tag{5}$$

where A is the maximum long-term mechanical work rate (W), B is the mechanical equivalent of the available energy from anaerobic sources (J) and t is the time constant (s) reflecting the inertia of the system. Wilkie modelled this equation to be accurate for durations ranging from 40 s to 10 min, which very closely match run-up competitions.

Fig. 2 also shows a curve obtained by performing a non-linear regression based on Wilkie's model on the $\dot{W}_{TOT}$ data. The software, written in LabView programming language (downloadable at albertominetti.it/MathModCompMeth), has been tested with mock data series created according to known A, B and t values. The resulting coefficients were A = 416.4 W, B = 23002.3 J and t = 5.5 s.

A and B, once converted into metabolic units according to an efficiency value for muscle contraction of 0.25, define the metabolic profile of this class of athletes. These parameters

correspond to the maximum sustainable aerobic power (1.67 kW or 71.4 mlO_2/(kg min), compatibly with typical values of middle distance runners (Saltin et al., 1967) and the anaerobic capacity, respectively, above resting conditions. As mentioned by Wilkie (1980), t is much shorter than the time constant of metabolic transient (typically in the region of 40 s) because it reflects the speed at which the mechanical output raises at the beginning of the exercise.

2.2.3 Athletes metabolic profile: effect of age and gender

The analysis of world records gave us also the opportunity to indirectly study the metabolic profile of athletes of different gender and age. The same non-linear regression applied above on the absolute winners was replied on clusters of data pertaining to male and female athletes (female mass assumed to be 55 kg) of different age ranges (from 10 to 80 years, step 10 years). The results are shown in Fig. 4, where the decay of A and B at increasing age is apparent.

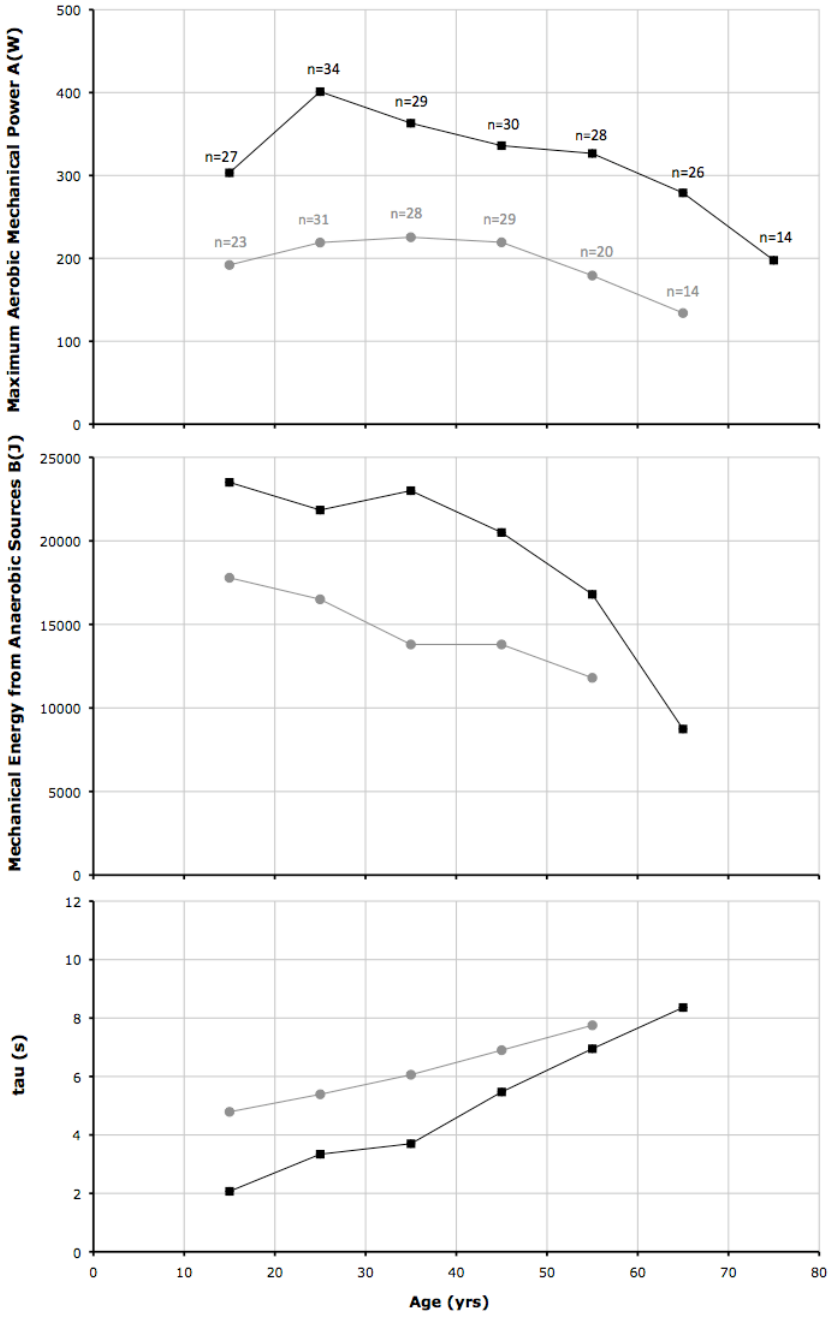

Figure 4: Effects of age and gender (n is the sample size) on the mechanical equivalent of maximum aerobic work rate, of the anaerobic work capacity and time constant (A, B and t, respectively, in equation 5), as obtained by using non-linear regressions based on Wilkie's model. The B and t values in the oldest age ranges have not been shown because the paucity of records in smaller skyscrapers for those athlete cohorts suggests caution about their reliability.

The data scatter observed in Fig. 2 is caused by the heterogeneity of building heights and race features. The variability can be reduced by considering the results from just one race, performed in a given time span. The oldest competition was the Empire State Building Run-Up in New York (320 m height, 1576 steps, 86 floors), which runs since 1978. Because of the relevant number of male and female athletes of all ages attracted by that race (upper panel of Fig. 5), the variability in terms of event record from 2003 to 2006 (expressed as $\dot{W}_{STA.EXT}$ and shown in the middle panel, Fig. 5) is further reduced. Again, the effect of age is apparent in reducing the available mechanical power. As a curiosity, even the oldest participant (aged 91 in 2003) had worse performances in successive competitions (the 3 rightmost points for males).

Inferences about the amount of mechanical work sustained by each heart beat (J/beat) as a function of age have been calculated by dividing the mechanical vertical power ($\dot{W}_{STA.EXT}$) by the heart rate (80% of the maximum, estimated according to age, minus the basal value, assumed to be equal to 55 bpm). The lower panel of Fig. 5 shows that up to the age of 65-68 yrs in males the work per beat is quite constant, as to suggest that the most crucial factor in mechanical power reduction with age could be the heart rate. The consistent drop for older athletes would imply that other factors, as the decreases of both maximum heart rate and stroke volume or a lower oxygen extraction, collaborate to lower the available mechanical power.

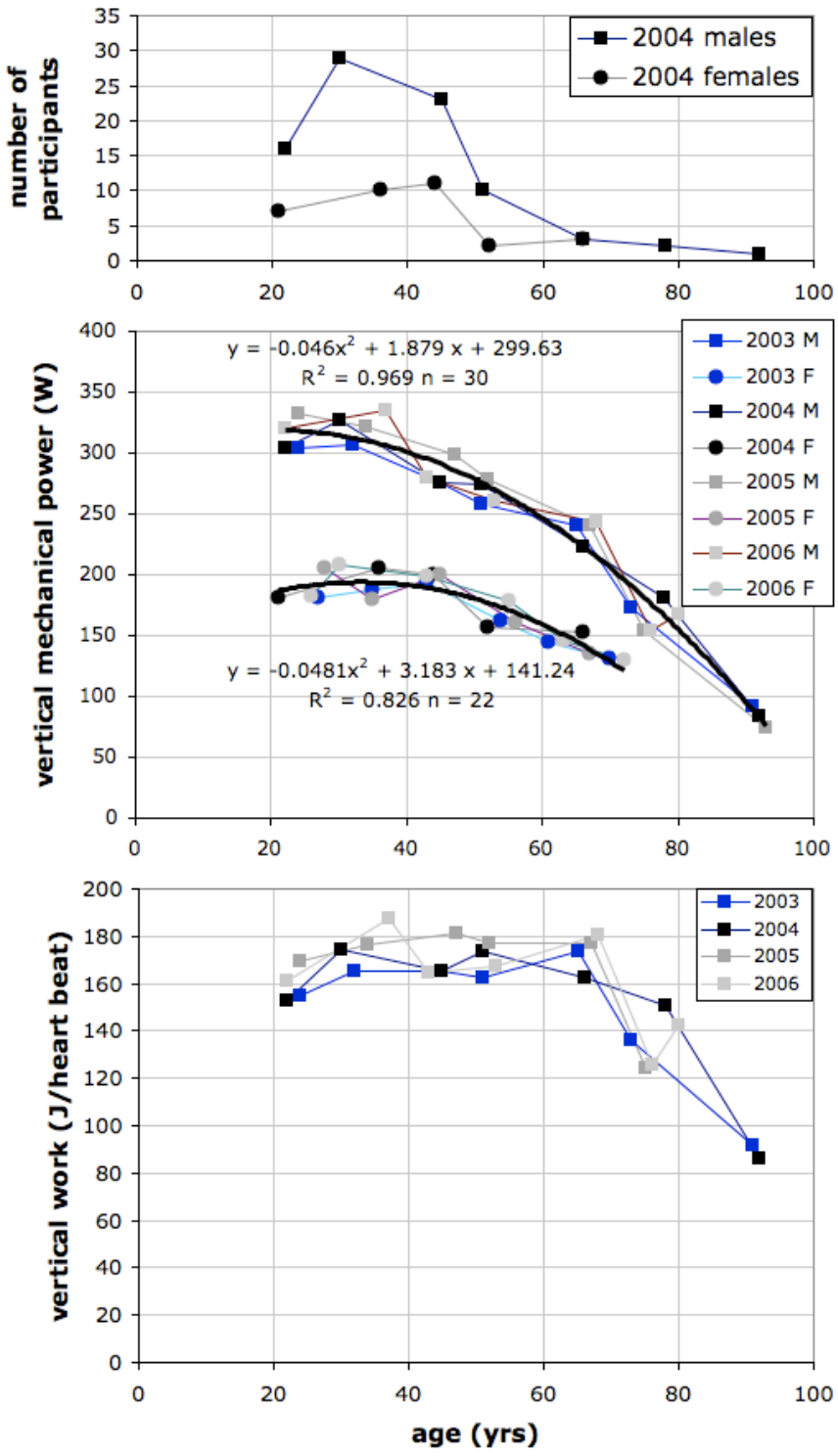

Figure 5: Upper panel: age distribution of participants to the Empire State Building Run-Up Race held in 2004. Middle panel: vertical mechanical power of female and male winners of run-up races held in 4 subsequent years. Lower panel: vertical mechanical work per heart beat of male winner of the 4 run-up races (see text for details).

2.2.4 Experiments during Pirelli run-up

As shown in the preceding paragraphs, exercise physiology and locomotion biomechanics provide sufficient information to analyse run-up performance just from record times. Those inferences are valid for the average runner, be a male or female of a given age. Individual athletes, though, need to be monitored during training and sport events by a proper research protocol. In the following we describe a simple set of preliminary measurements based on the above analysis of run-ups that we used during a real race.

2.3 METHODS

2.3.1 Experimental protocol and data acquisition

The ascent speed of 13 male athletes (see anthropometric data in Table 1), who gave their written informed consent about the experimental procedure, was investigated during the run-up races on Pirelli building (121 m height, 710 steps, 30 floors) occurred in Milan on February 24th 2008 and on March 1st 2009. The study was approved by the ethics committee of the University of Milan. Altitude was measured on five athletes by using an altimeter+logger device, designed to monitor model aircrafts and rockets, capable of 0.4 m resolution and a sampling rate of 10 Hz (LoLo/Alti2, Roman Vojtech, www.lomcovak.cz). The ascent of 4 other athletes was measured by the internal barometric altimeters of GPSs (Geko 301 and Edge 305, Garmin) at a lower resolution (1 m) and sampling rate (1 Hz maximum). Also, heart rate was monitored during the race (Edge 305 by Garmin; Vantage, RS800 and S810 by Polar). Ascension and HR data of other 4 elite athletes (including the winner (Thomas Dold) of this and many other run-ups) were provided from their own monitoring equipment after the race.

Subjects	Age (years)	Body mass (kg)	Stature (m)	Ascent time (s)	Vertical speed (m/s)	$\dot{W}_{STA.EXT}$ (W_{MECH})	$\dot{W}_{STA.INT}$ (W_{MECH})	$\dot{W}_{TUR}$ (W_{MECH})	$\dot{W}_{TOT}$ (W_{MECH})
1	23	69	1.78	188	0.642	435.7	30.663	75.26	541.6
2	22	68	1.79	209	0.579	386.9	22.121	66.85	475.9
3	38	68	1.77	222	0.544	363.6	18.352	62.81	444.8
4	31	60	1.65	255	0.473	279.0	10.647	48.19	337.8
5	28	59	1.64	270	0.447	259.6	8.872	44.85	313.3
6	37	72	1.76	249	0.484	342.8	13.721	59.22	415.8
7	42	77	1.78	258	0.468	354.3	13.239	61.20	428.7
8	28	72	1.52	314	0.384	272.2	6.867	47.02	326.1
9	48	75	1.76	329	0.367	270.6	6.219	46.75	323.6
10	64	69	1.75	335	0.360	244.5	5.419	42.24	292.1
11	58	78	1.67	362	0.333	255.6	4.847	44.16	304.6
12	47	72	1.74	365	0.331	234.1	4.372	40.45	279.0
13	49	53	1.68	428	0.282	147.0	1.997	25.40	174.4

Table 1: Antropometric data of the investigated Run-Up runners are shown in the table, together with the estimated partitioning of their total mechanical power (see text).

Lactate was measured (Lactate Analyser YSI Sport, Yellow Spring, USA) 3-6 minutes after arrival in 21 male amateur athletes (mass 68.2 ± 10.0 kg, stature 173.8 ± 6.6 cm, age from 26.5 to 68.6 yrs), to check their anaerobic status and to estimate the lactate contribution to the work production.

2.3.2 Data analysis methods

In order to mathematically describe the 2-segment shape of the time course of vertical speed observed in many athletes (see Results), a statistical algorithm fitting a single data set with two successive regression lines was used (Jones & Molitoris 1984). The method searches, among all possible two-lines combinations, the optimum one in terms of the minimum residuals across the entire data set and statistically assess whether two lines fit better than a single one. A derived result is the optimum breakpoint, i.e. the point in the abscissa (and the corresponding ordinate) at which the second regression line comes into action. The method has been translated into a computer program (LabView, National Instrument, US) and additional features have been added. Since it is expected that points lying on a (concave or convex) monotonous curve are better fitted by two lines than by a single one, we added a subroutine checking whether a 2^{nd} degree polynomial fits better than two adjacent lines, again based on the minimization of the sum of residuals (a more detailed description and the program is downloadable at albertominetti.it/MathModCompMeth). The single line and the 2^{nd} degree polynomial represent continuous time courses of the vertical speed, while the 2-segment model describes a discontinuous performance. While a parabola regression provides 3 parameters, the 2-segment model would involve 4 of them (2 intercepts and 2 slopes) but, due to the constraint imposed by the intersection, the effective parameters reduces to 3, and the adherence of the two models to the same data can be compared

2.4 RESULTS

In the male amateur athletes the average lactate concentration at the end of the race was 5.3 ± 1.4 mM (range 2.50-7.75), with no significant effect of race speed on it.

Table 1 reports the partitioning of the total mechanical work rate for the 13 individually studied runners according to the rationale described in the Introduction (Analysis of World Records). Nine of them, monitored through digital altimetry during the ascent, showed a sudden change of vertical speed, as significantly detected by the 2-segment regression. For eight of them the change was a reduction of vertical velocity (see an example in Fig. 6 column A), while one subject increased his vertical velocity in the last part of the race. This sudden change was confirmed by the ratio between the residuals related to a 2nd degree polynomial and the residuals obtained with the 2-segment model, which resulted to be greater than 1 in nine cases.

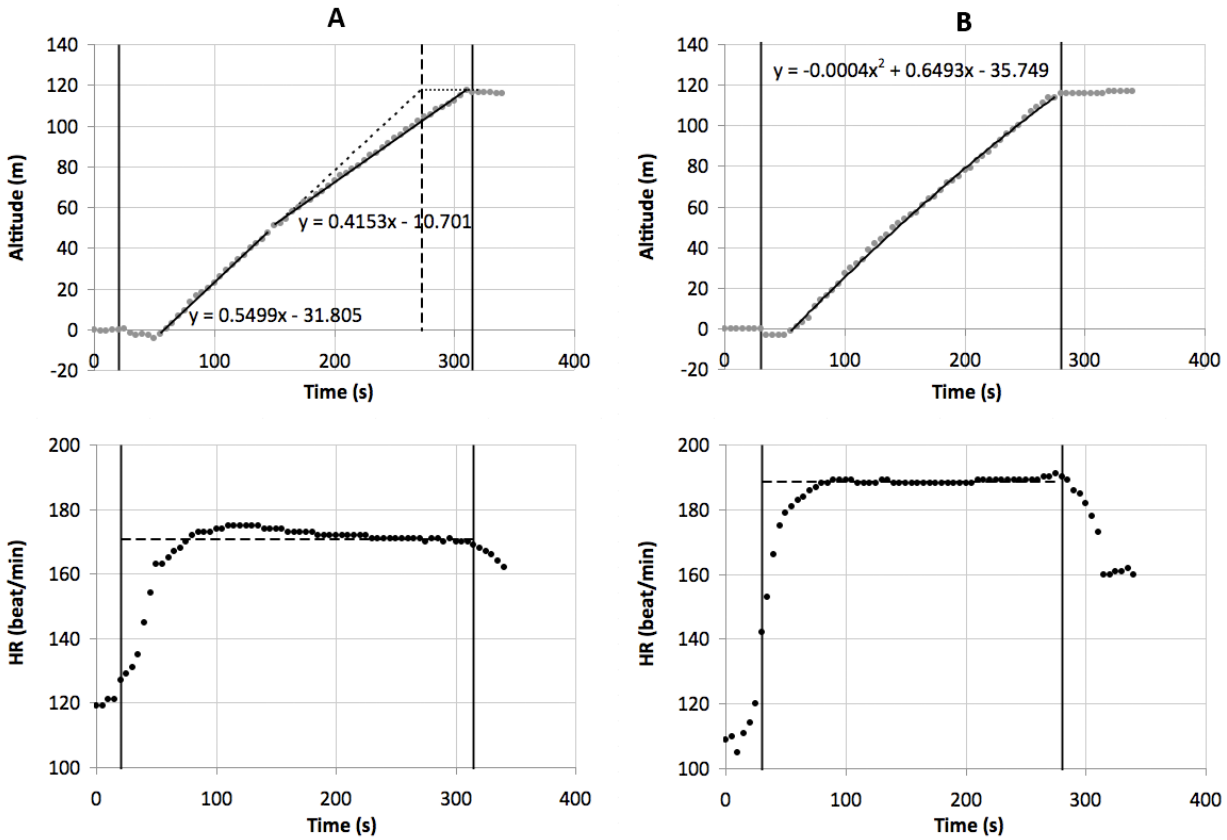

Figure 6: Two examples of ascent profile and concurrent heart rate time course (upper and lower panels, respectively) are shown for two typical athletes: a discontinuous profile and a very steady ascent (left and right hand side, respectively). It can be noted that the discontinuous profile corresponds to a heart rate overshoot that could jeopardize the rest of the race performance.

Two of these nine athletes showed high ratio values, underlining their considerable speed reduction, as showed by the correlation coefficient of the 2-segment model (Fig. 7). In the 4 remaining athletes, who were the highest in the race ranks for both the under-40 and over-40 years old categories, that ratio was lower than 1, indicating that a continuous function (a line or a parabola), with no abrupt change in vertical speed, better described their uphill motion. This ascent profile index (the residuals ratio) shows an inverse relationship with the average vertical speed in both athlete categories (Fig. 7).

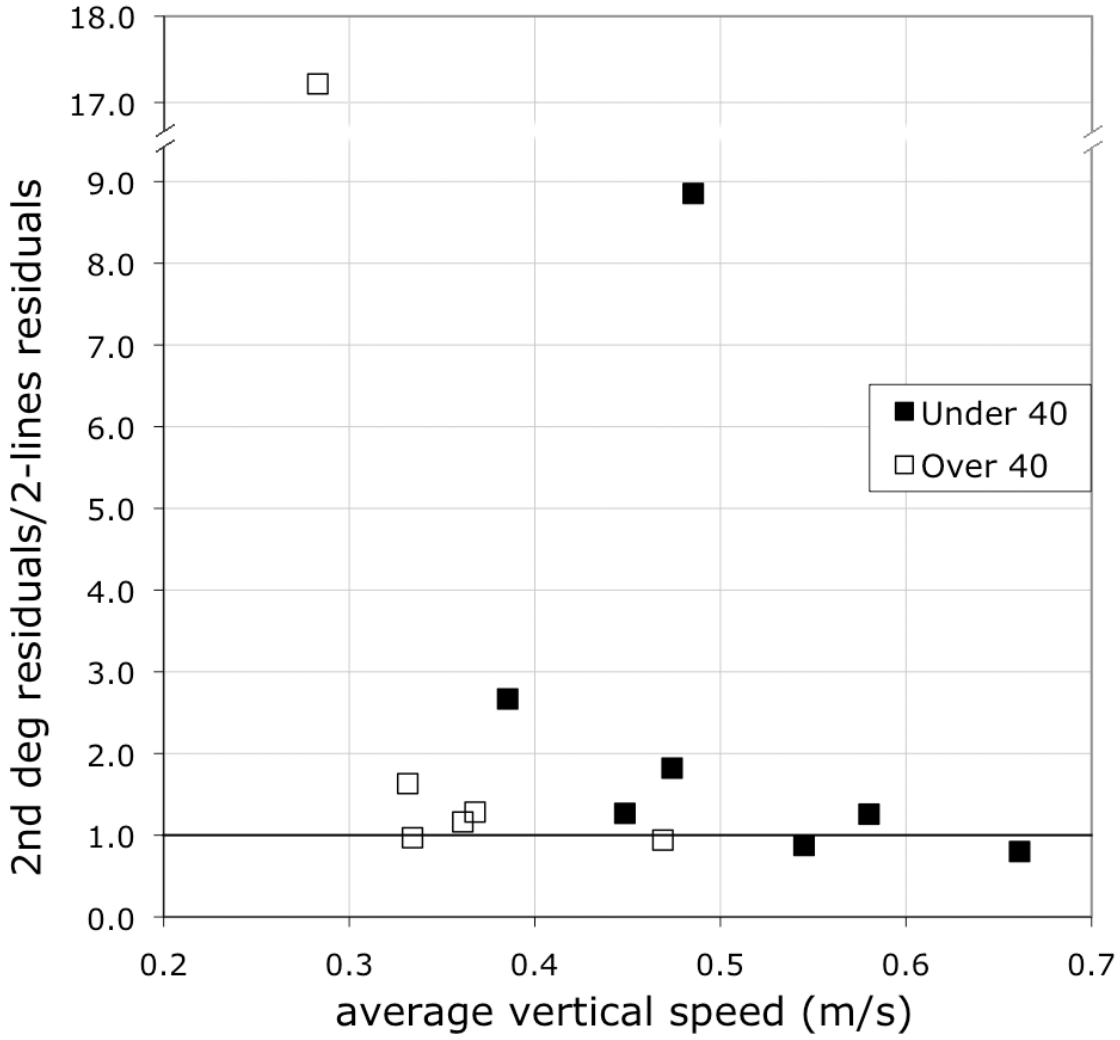

Figure 7: The ascent profile factor is plotted against the average vertical speed for 7 under-40 (solid squares) and 6 over-40 (open squares) years old athletes. The ascent profile factor has been calculated as the ratio between the residuals obtained from using the 2nd degree polynomial and the ones related to the 2-segment regression. The horizontal line located at the value 1 represents the threshold between continuous ascents (below the line) and discontinuous ones (above the line). In both groups there is a tendency for faster athletes to perform ascents without sudden vertical velocity change (see text).

When the time of inflection, expressed as a fraction of the individual race time, is plotted against the average vertical speed, a positive trend is apparent (Fig. 8). In synthesis, the more discontinuous ascent occurred in an earlier phase of the race, the worse the overall performance.

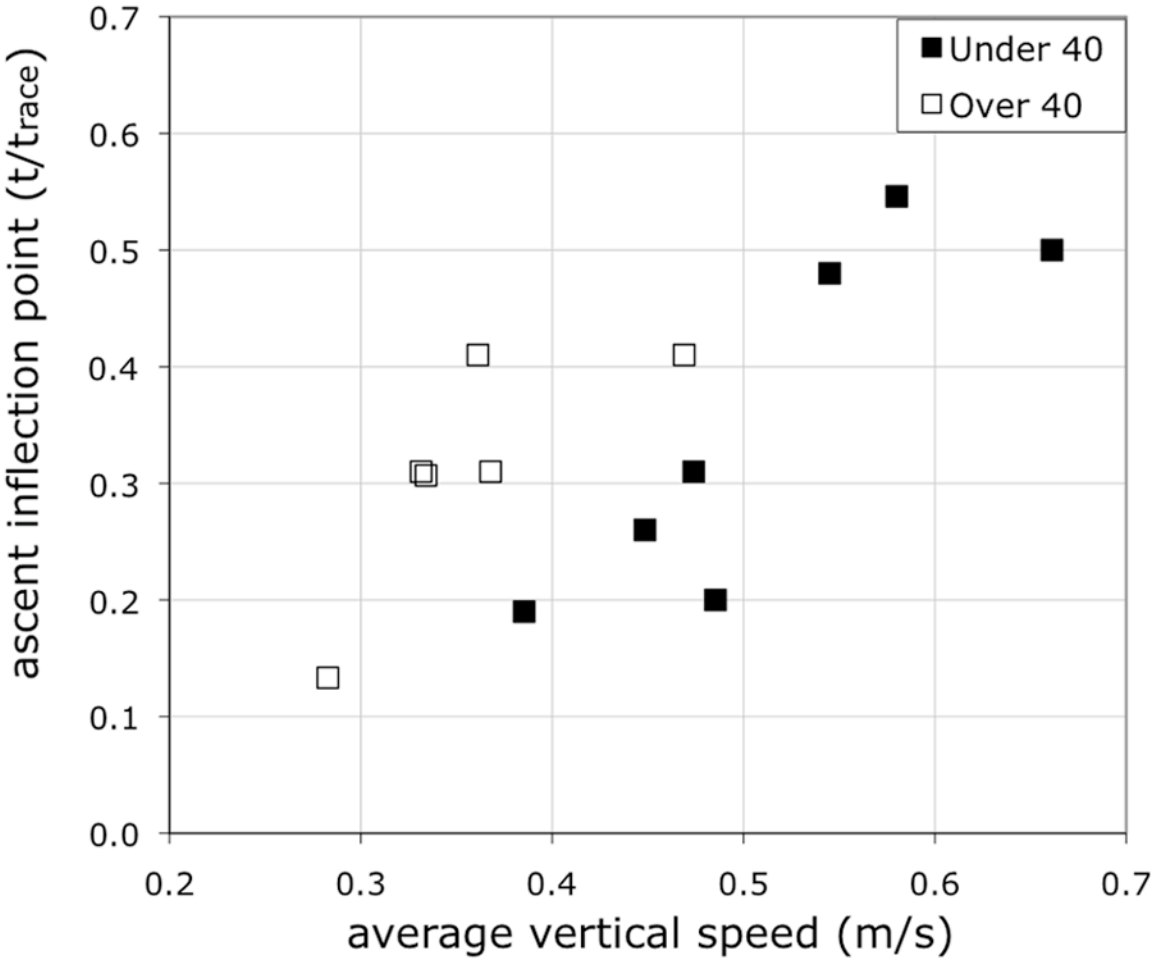

Figure 8: The ascent inflection time, calculated by the algorithm for the 2-segment regression and expressed as a fraction of the total race duration, is plotted against the average vertical speed for 7 under-40 (solid squares) and 6 over-40 (open squares) years old athletes.

2.5 DISCUSSION

2.5.1 Aerobic and anaerobic profile

As indicated in the 'Analysis of World Records' section, the physiology and biomechanics of run-ups are supposed to be quite straightforward. Eighty percent of the total mechanical/metabolic work or power is determined by the increase of body potential energy inherent to ascending upstairs at a gradient of about 50%, the rest being caused by the cost of running in circles between flights of stairs (15%) and by the acceleration of upper and lower limbs with respect to the body centre of mass (5%). However, differently from the high consistency of records of running on a level surface (Minetti, 2004) or runup records in the same building across many years (Fig. 5), the maximum estimated performance in different buildings, in terms of mechanical work, seems quite scattered (solid circles in Fig.2). This can be due to building heterogeneity (quoted above), including the variable length of the level approach to stairs, the variable number of floors height (and number) and the actual vertical distance travelled, which is not always properly reported.

Despite of such variability, which will never be alleviated by race field standardization in this sport, information on the aerobic and anaerobic profile of competitors can be obtained. It is well known the decay of the physiological funtional human capacity due to the aging (Jones & Molitoris 1984). In the present work, published race results, ranked by age ranges and gender, together with the model proposed by Wilkie (1980), allow to show the decay of the (mechanical equivalent of the) aerobic and anerobic capacity of male and female athletes with age (Fig. 4).

Furthermore, the age-related decline of anaerobic capacity is more pronunced than that of aerobic power, as recently confirmed by Kostka (Kostka et al. 2009). This evidence

partially explains the lower participation of master athletes in short run up races (less tall skyscrapers).

The results from the present study about the time constant (t), despite their predictable increase with age in both genders, should be taken with caution. Since Wilkie's model deals with mechanical power, the time constant is only loosely related to the transient on-phase of the 'global' oxygen uptake, reflecting preferentially the mechanical and 'local' biochemical transient from rest to maximal exercise levels. Also, Wilkie (1980) warns about the applicability range of his model, from 40 s to 10 min, which almost excludes the influence of the tiny t obtained from his study and the present investigation (ranging from 63 to 835 s). The present t values are even smaller than Wilkie's results, and this could depend on the difference between the two exercise forms: more muscle mass is activated in stair ascending than in pedalling on a cyclo-ergometer. Anyway, obtaining t values much smaller than the shortest event measured suggests that those estimates have to be considered as 'extrapolated' results, with little effect on the overall dynamics. However, a mechanical delay in the off-on transient is expected to increase with age, just as it happens for the on-response time of the oxygen uptake (on average from 25.0 ± 3.4 s to 42.0 ± 5.1 s, from 24.2 ± 1.8 yrs to 69.4 ±1.7 yrs), (DeLorey et al. 2005; DeLorey et al. 2007; di Prampero 2003; Gurd et al. 2008; Sabapathy et al. 2004).

The reliability of the three model parameters depends both on the number of athletes competing in a given age range (general reliability), and on the attendance to short duration events (B and t reliability). In this respect we observed, as mentioned, that old athletes tend not to compete in short run-up races.

2.5.2 Race strategy: what's the best ascending profile?

Down to the scale of individual athletes, this study shows that a digital altimeter and a heart rate monitor, both with logging capabilities, are enough to capture and partially explain the race result (lactate concentration at the arrival was positively but not significantly correlated to the average mechanical power). The time course of the ascent deserves some attention, since many of the investigated runners showed a biphasic profile: the first part of the ascent was performed at a higher vertical speed than the rest of the race, with an abrupt point of inflection (Fig. 6, column A). A deeper analysis seems to indicate that best runners (higher average vertical speed) are associated to a more uniform ascent profile, without inflection point (Fig. 7). Also, an early inflection point seems to be negatively related to the overall performance. Only one athlete decided to change his profile in the second half of the ascent, by increasing his velocity. Probably he saved some energy for the last part of the race, but he did not win the race despite having increased the average vertical speed, underlining our hypothesis that best performance is associated to a uniform ascent profile (Fig. 8).

These observations refer to the individual strategy of conduct during the race. As in many other competitive sports, the final result depends both on the size of the engine and on a proper management of energetic resources during the whole event. It is evident from column B in Fig. 5 how it is possible to climb the building in a shorter time by keeping a very steady heat rate and mechanical power output (the slope of the ascent profile), rather than starting at a pace that cannot be maintained throughout the entire race (column A).

Our study is the first investigation about this new sport activity, therefore we cannot draw ultimate conclusions on the true determinants of the observed points of inflection in the ascent profile, which represents an index of power switch, a phenomenon not easily detectable in other sport disciplines. Speculative candidates include: 1) negative effects of

anaerobic metabolism, particularly lactate accumulation and low tolerance, on the aerobic pathways, as partially witnessed by the initial HR overshoot, and 2) central or peripheral fatigue, presumably affecting the propulsive contribution of upper limbs (lower muscle mass), too.

Also, it is possible that less experienced athletes tend to initially outperform to get a leading position in their battery, being convinced that the progression along narrow stairs could be slowed down when moving within a crowd.

Those aspects certainly deserve further investigation. The still limited specialization of athletes and the competition ground heterogeneity, mentioned above, are reflected by the wide scatter of current world records. A strict standardization of ascent characteristics in future run-up events is out of question, but in a few years time the records of this relatively novel sport activity could display much less variability due to a more focussed selection of athletes and more specialized/specific training regimes.

2.6 PERSPECTIVES

This investigation represents an applied physiology study where a novel motor activity is 'dissected' into its metabolic and mechanical aspects and their determinants. Also, the analysis of run-up world records and experiments conducted during two of those races allowed to reach conclusions both at the general and the individual level.

The novel approach to performance estimation suggests that vertical speed and heart rate logging are the keys to explain and predict performances in this recent sport discipline, on which there is no scientific literature at present. The developed algorithm to identify the inflection point in the ascent speed could be incorporated, together with a high resolution digital altimeter, into portable heart rate monitors. The resulting device would guide athletes during the training sessions and even during races towards the optimization of metabolic resources.

2.7 Appendix: Running in circles

2.7.1 Running in circles: energy consumption estimation

There have been a few studies of curved path running, or maneuverability during controlled conditions (Walter, 2003; Usherwood and Wilson, 2005) and natural predator avoidance (Alexander, 1982; Howland, 1974), but more detailed biomechanical data such as ground contact forces generated by the limbs, or metabolic data as energy consumption in 'turning' are lacking.

Because of the lack of relevant literature on this topic, the metabolic energy consumption involved in running in circles, needed to approximate the total work of skyscraper running, has been obtained by the following procedure.

In two trained male subjects, the relationships between heart rate (HR monitor S810i, Polar, Finland, 1 beat resolution) and oxygen consumption (Vmax, Cardinal Health, USA) were assessed by level running on a treadmill at increasing speed (from 0.8 to 2.8 m/s, step 0.33 m/s). After 8 min of warm-up at slow pace, each speed lasted 4 min, at the end of which measurements took place. The average values of the two variables at all speeds were correlated using a type II linear regression ($R^2 = 0.957$, $n = 7$).

Two weeks later, the same subjects, equipped with HR monitors, underwent an experimental session involving running in circles. On the flat roof of our department, two 1m radius circles were drawn as to produce a ''figure-of-8'' path. This was arranged to prevent the inevitable dizziness after a few minutes of running along a single circle. After a period of practicing, subjects were asked to run for 5 min at three speeds, individually selected from preliminary

attempts as to involve an HR in the range of 135–170 b.p.m. The stride frequencies

during the preliminary tests were measured and later reproduced by a metronome. The tests, preceded by a 15-min warm-up at leisure speed, were repeated three times, 10-min intervals between them.

From the average HRs measured, the corresponding $\dot{V}_{0_2}$ values were estimated according to the $\dot{V}_{0_2}/HR$ relationship obtained previously in the laboratory.

To calculate the metabolic cost of transport for running in circles, the net $\dot{V}_{0_2}$ was divided by the speed of the BCOM.

This speed is lower than the one (of the feet) along the figure-of-8 path according to the different leaning of the body, necessary to counteract the centrifugal effect of running in circles.

It can be demonstrated that the relationship between leaning angle (α, deg.), circle radius (r_f, m) and tangential speed along the path (v_f, m/s) is

$$\tan\alpha = \frac{r_f^2 g}{\left(r_f - l\cos\alpha\right)v_f^2}$$

where (m) is the average height of the BCOM. We used again the equation graphing software 'Grapher', to calculate that at the measured v_f range (1.64–2.49 m/s), as measured, and for an r_f of 1m, as expected in the transition between stair ramps, a ranged from 78° to 68°. Then, the speed of the BCOM (v_{cm}, m/s)

$$v_{cm} = v_f \frac{r_{cm}}{r_f}$$

where $r_{cm} = r_f - l\cos\alpha$ (Fig. 9), was in the range from 1.37 to 1.79 m/s.

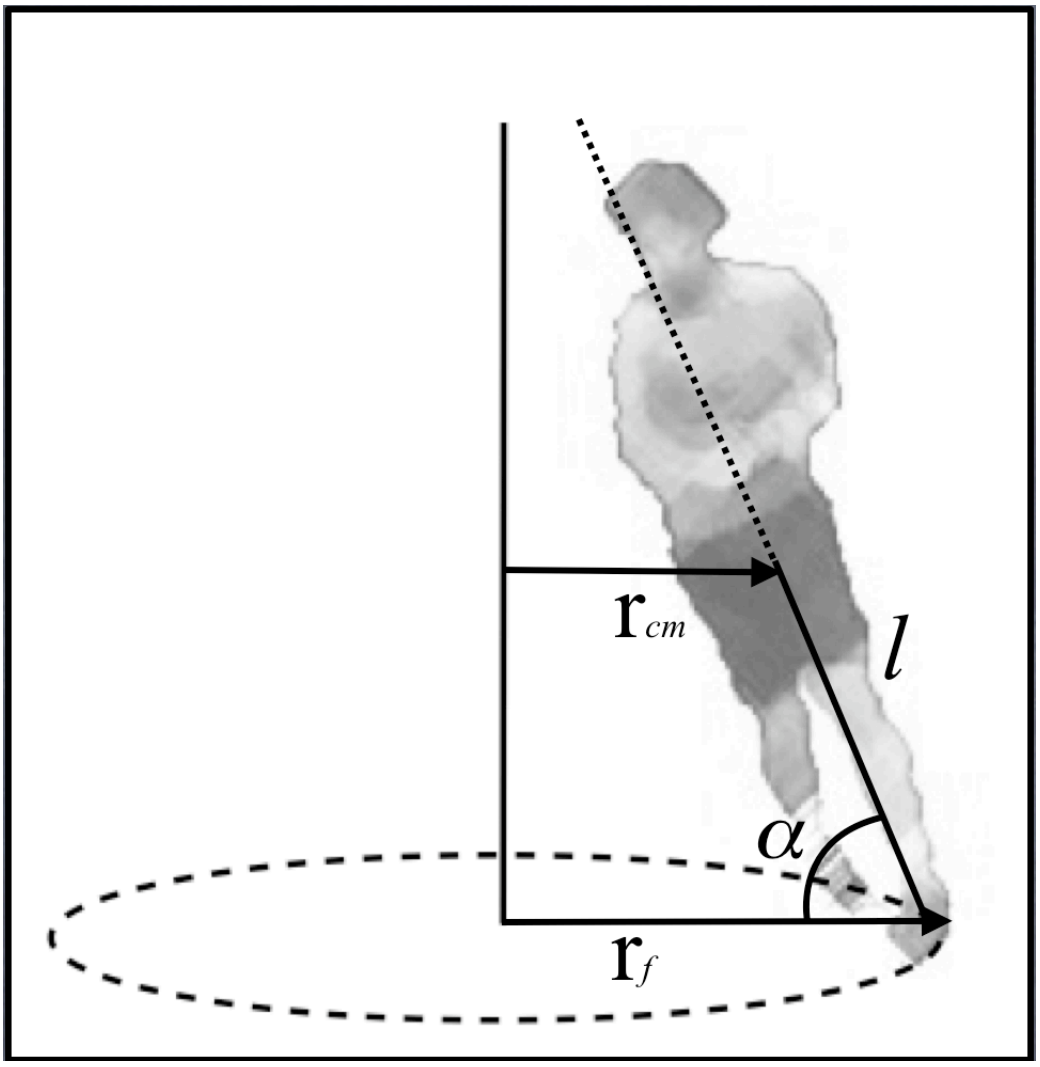

Figure 9: Sketch of the variables involved in the calculation of leaning angle of the body during running in circle.

Finally, the cost of running in circles with a 1m radius was found to be almost speed independent, and equal to 283.1 ± 64.1 mlO2/(kg km). The mechanical equivalent work [J/(kg m)] was obtained by multiplying the metabolic cost by the muscle efficiency (0.25), and expressed as J/(kg floor) by assuming that two half-circles are normally expected to be travelled for each floor of the building.

2.7.2 Running in circle: biomechanical data analysis

The biomechanical approach is well represented by Chang and Kram (Chang & Kram 2007), who measured on a dynamometric platform the GRF during running on circles of five (1,2,3,4 and 6 meters) different radii. They compared the maximum extension force in curved paths and straight path, focusing on the asymmetry between the 'inside' and 'outside' leg.

In this way, the comparison is based mainly on GRF analysis and its relation with the addiction of centripetal acceleration component in curved paths. An interesting investigation making use of these platform data is the computation of BCOM displacement and external mechanical work of an ideal circle of 1 meter radius: for this study a digitizing software (GraphClick, Apple Inc) has been used to get inside and outside leg platform data (referring to 1 m radius data), in coherence with the original sampling frequency (1 kHz). The first step is to design the ideal path positioning eight virtual platforms on the circle, and assuming that the subject step length matches with the platforms position (Fig. 10). Moreover, starting with the inside leg from the non-rotated platform (0° in figure 10), and inside and outside leg contacts have been coupled with the corresponding platforms.

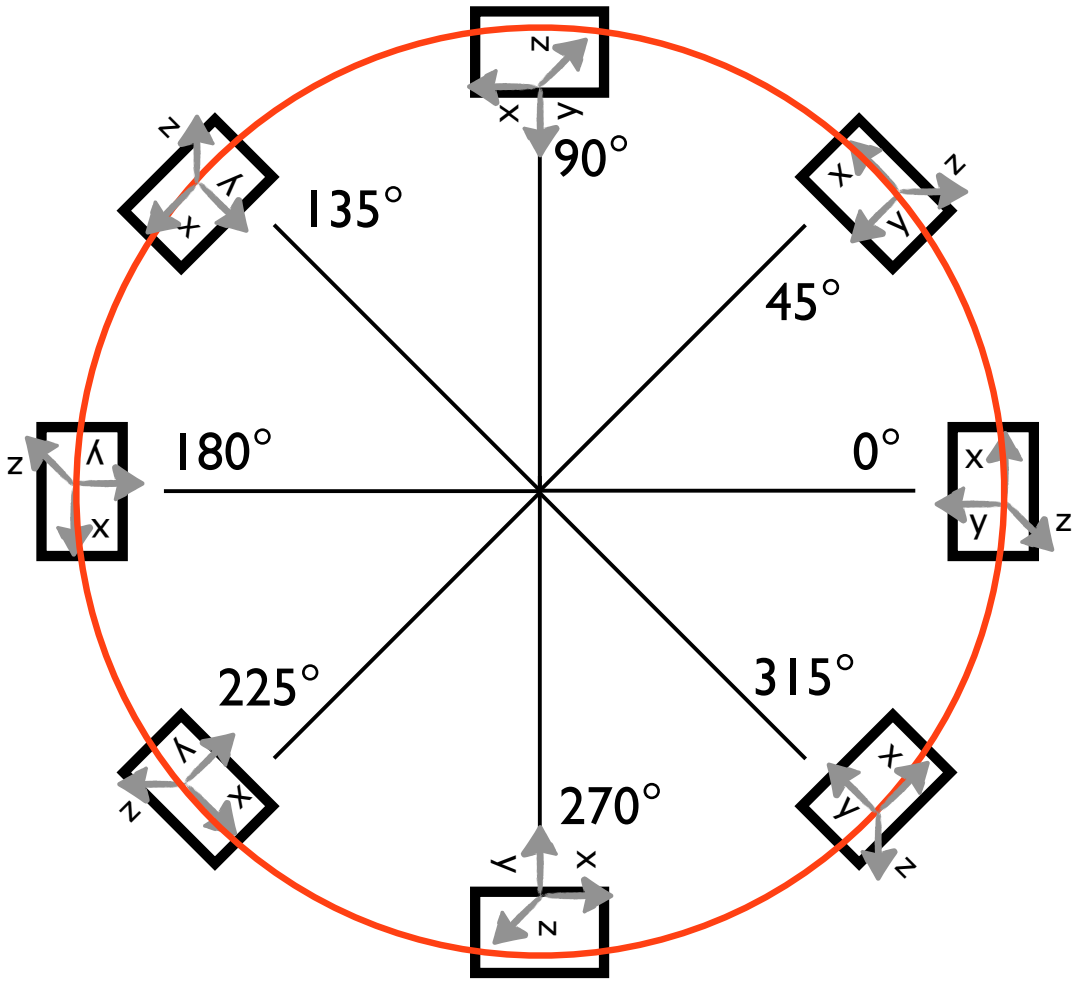

Figure 10: Ideal curvilinear path with eight virtual dynamometric platforms.

The measured mean value of inside and outside leg step length is 0.77 and 0.80 meters respectively, hence 4 steps for each leg complete exactly the circle (6.28 m). After that, a rotational matrix containing the cosine directors has been utilized to compute the simulated force vectors for every platform position. These matrix products allow to complete all the running simulation, and to calculate the BCOM displacement and the total external work.

We used an equation graphing software (Grapher, Apple Inc., Cupertino, California, USA) to plot the 3D BCOM displacement, calculated double integrating every platform signal (Fig. 11).

The mean speed value measured in the paper, for a circle of 1 m radius, is 2.99 ± 0.07 m/s, but as demonstrated above the v_{BCOM} depends on the inclination of the

body. In this case, considering the same range of inclination angle previously used (78° - 68°), v_{BCOM} is 1.71 m/s. The computed BCOM displacement is shown in 'figure 3' and, using a scaling factor $\frac{r_{com}}{r_f}$ of 0.57.

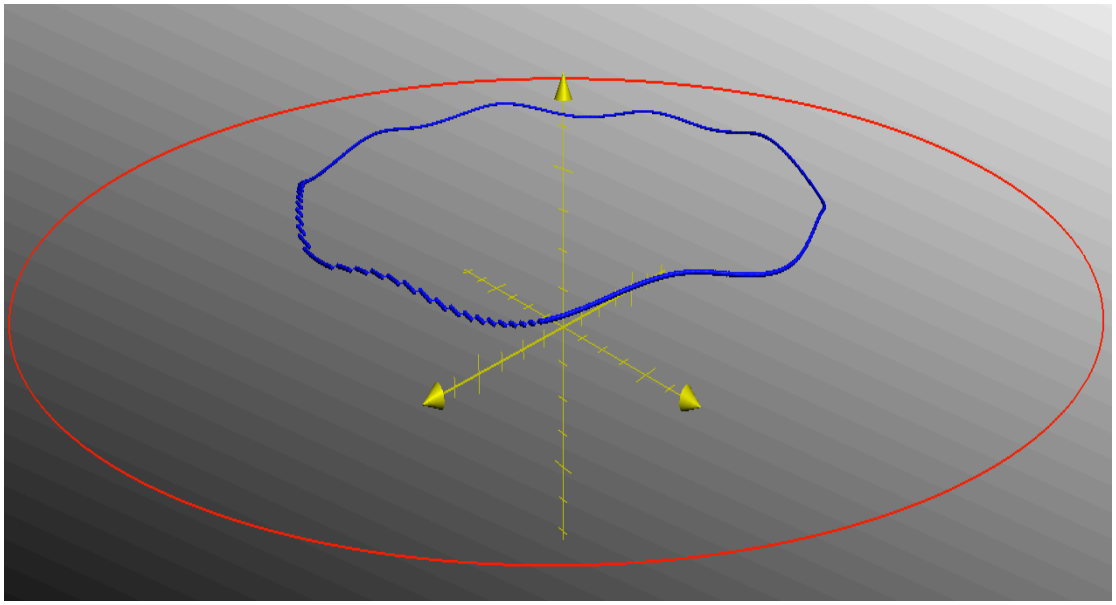

Figure 11: BCOM displacement running on a circular path of 1 m of radius.

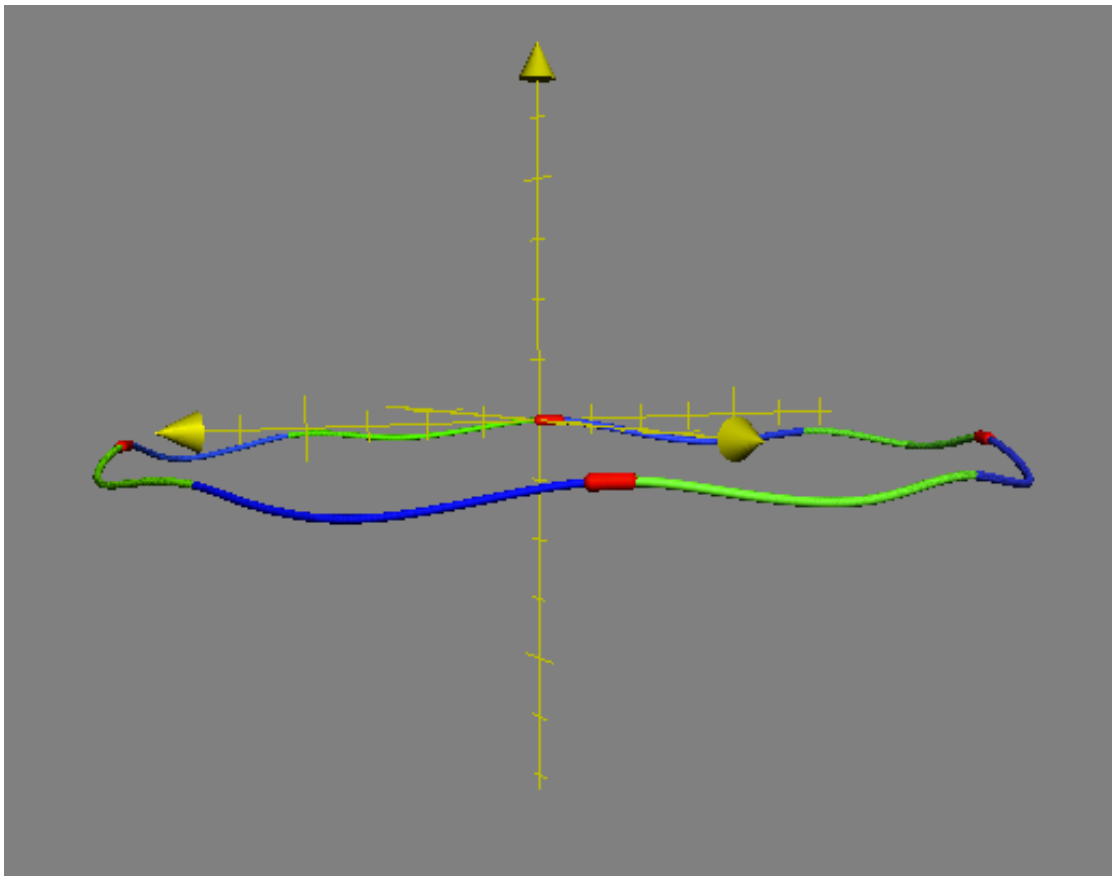

Figure 12: starting from axis origin the inside leg contacts are represented in green, the outside leg contact in blue and the flight-time in red. As shown in figure, the flight time is present only during the stride starting with the outside leg contact.

The mean value of measured inside leg step frequency is 3.82 ± 0.12 s^{-1} (with a related step duration of 0.261 s) and of the ground contact time is 0.290 ± 0.022 s, while for the outside leg are 3.56 ± 0.26 s^{-1} (step duration 0.281 s) and 0.261 ± 0.004 s respectively.

For this reason the flight time mean value of 0.02 s (regarding on a single step value of the simulated path) is remarkable just in the outside leg stride (from an outside leg contact to the following outside leg contact), confirming different biomechanical response of the legs during running in circles. On that account, also duty factor changes in relation with the two legs: the stride starting with inside leg shows a duty factor of 0.53 (typical of walking), while the one starting with outside leg of 0.48

(proper of running).

This asymmetry constrains the inside leg to be more on contact with the ground but also to express less resultant force and to be less effective at making quick changes in running direction (Rand & Ohtsuki 2000).

Hence, the inside leg is more affected by the curved path, limiting the maximal speed, but its intervention in turning the BCOM has to be discussed. In fact we can turn the body only during the contact phase generating lateral and fore-aft forces, while in the flight phase we have to go straight.

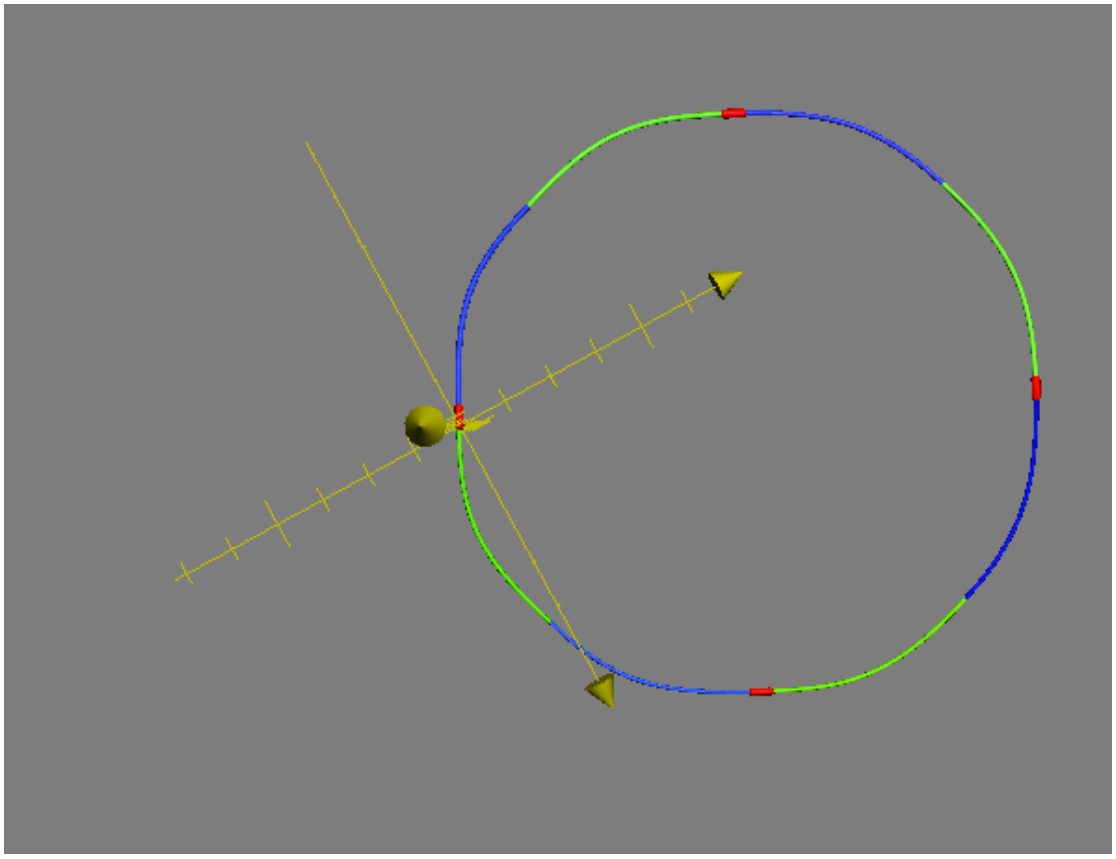

Figure 13: BCOM displacement in the transversal plane. The inside step is green and the outside step is blue.

Little differences are exhibited in step length of the outside leg that is 0.03 m greater than the inside one (leading to a 0.12 m turning asymmetry for all the circle), and in vertical BCOM displacement (0.02 m), due to the greater vertical force generation of the outside leg that lifts more the BCOM.

Further experiments should be done to accurately measure these differences, analyzing more then two steps and simulating the others. Anyway some biomechanical speculations could be done: in particular, it could be said that there isn't an absolute leading leg but only a limiting one, even if the outside leg generates an higher external work than the inside leg (Fig. 14).

The external work has been calculated considering the positive increments of the total energy (KE + PE) (Cavagna and Kaneko, 1997; Minetti et al. 1993).

Furthermore, outside leg shows kinetic and potential energy curves exactly in phase, describing a classical running energy exchange, while the inside leg energy exchange presents the kinetic and potential energy not perfectly in phase (Figure 6).

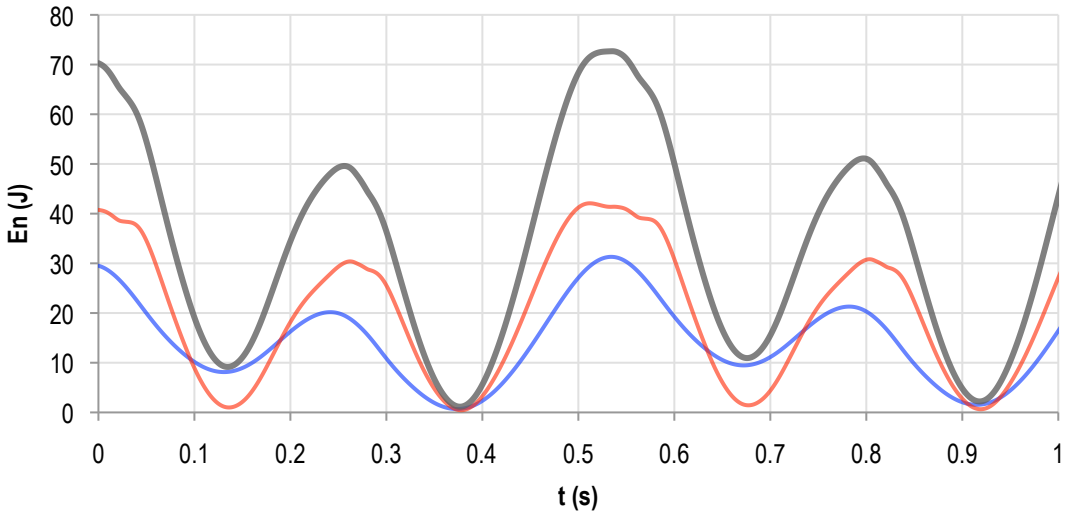

Figure 14: Kinetic energy (KE) and potential energy (PE) curves are plotted in red and blue respectively, while the total energy (TE=KE+PE) in grey.

The lack of a complete kinematic analysis doesn't allow to precisely describe the biomechanics of inside leg and its function in turning, but the energetic analysis could be useful.

This leg seems to give more support than propulsion, especially with small radii, working as a hub (pivot): the potential energy variation (ΔPE) during the step is low

(1/3 of the outside leg ΔPE) and the initial PE is one half of the PE peak. The KE and PE are not exactly in phase but the energy recovery is in reality nil. Unfortunately the elastic energy (EE) effort couldn't be obtained from these data, but with reference to straight running data, BCOM vertical displacement shows a smaller variation for both the legs, and hence the storage and release of EE should have less influence. This fact has an important impact on energy consumption, increasing the cost of transport of running on curves.

In this way even if the inside leg could largely turn the body showing a longer contact time, the BCOM displacement on the coronal plane related to both legs activity is almost equivalent (Fig. 13). Finally the estimated external mechanical work, considering a subject of mass m (80.7 kg), and a circular path s_c of 6.28 m is computed as

$$W_{tot} = \frac{\sum_{0}^{T} \Delta TE}{m\left(s_c * 0.57\right)}$$

where ΔTE are the positive total energy increments during the period of time T, required to cover the circumference of radius 1 m, with a speed v_c. The body CoM displacement is weighted by the factor 0.57 because of body inclination, as discussed before.

The estimated value of mechanical cost of transport is 2.5 (J_{mech}/(Kg.m)), higher in respect with the value of 2 (J_{mech}/(Kg.m)) of running on straight paths.

CHAPTER 3

3. PART II

EFFECTS OF DIFFERENT JUMPING TECHNIQUES IN LIMITING THE VERTICAL EXCURSION OF THE BODY VISCERAL MASS

3.1 INTRODUCTION

Humans and animals minimize their mechanical work and improve their motion efficiency in different ways. The ability to transfer a force impulse from lower limbs to all the body, without any dispersion of energy, is a key motor strategy for all the dynamic muscular activity related to lower limbs. The visceral mass displacement could play a role in impulsive motor activity like jumping or running, as it potentially interferes between the force production and the final performance of the body centre of mass.

In the past, Bramble (Bramble & Carrier 1983) and Alexander (Alexander 1987; Alexander 1989), investigated the role of visceral piston in locomotion-respiration coupling in quadrupeds.

They suggested that a resonant mechanism may be operating: during periods of fast cursorial locomotion, many animals are observed to maintain an almost constant stride and respiratory frequency (Alexander, 1989; Ardigo et al. 1995; Baudinette et al. 1987; Bramble & Carrier 1983; Giuliodori et al. 2009; Lafortuna et al. 1996), increasing their speed and respiration by simply lengthening their stride and increasing their tidal volume. One of the mechanism proposed by Bramble and Carrier (1983) and later expanded by Alexander (1989) using mathematical models, is based on the viscera piston: the viscera may be regarded as a mass suspended by elastic structures within the body wall rather like a piston within a cylinder. Forward/backward accelerations acting upon the body must cause displacements of this visceral piston relative to the body wall and the amplitude and the phase of these displacements will be determined by the mass and the visco-elastic properties of the viscera and their supporting structures. If this piston were to behave as a tuned oscillator, its displacements could drive ventilation (Alexander, 1989).

Recently, Daley and Usherwood (Daley & Usherwood 2010) described bouncing viscera effect on the mechanical work of running, and its relation with the 'cost of force'. In that study, for compliant gaits, hysteresis losses owing to loading viscera and any other compliant non-locomotor tissue, have been investigated. Their model assumes that the viscera deflect in the direction of the leg force, dissipating energy. The legs produce net positive work to restore energy dissipated by the viscera, and energy lost depends on the properties of the viscera (stiffness, hysteresis and mass), and of the legs (stiffness and sweep angle). The idea is that stiffer legs lead to higher leg forces and greater energy dissipation by the viscera, increasing the mechanical cost of transport (figure 2.1).

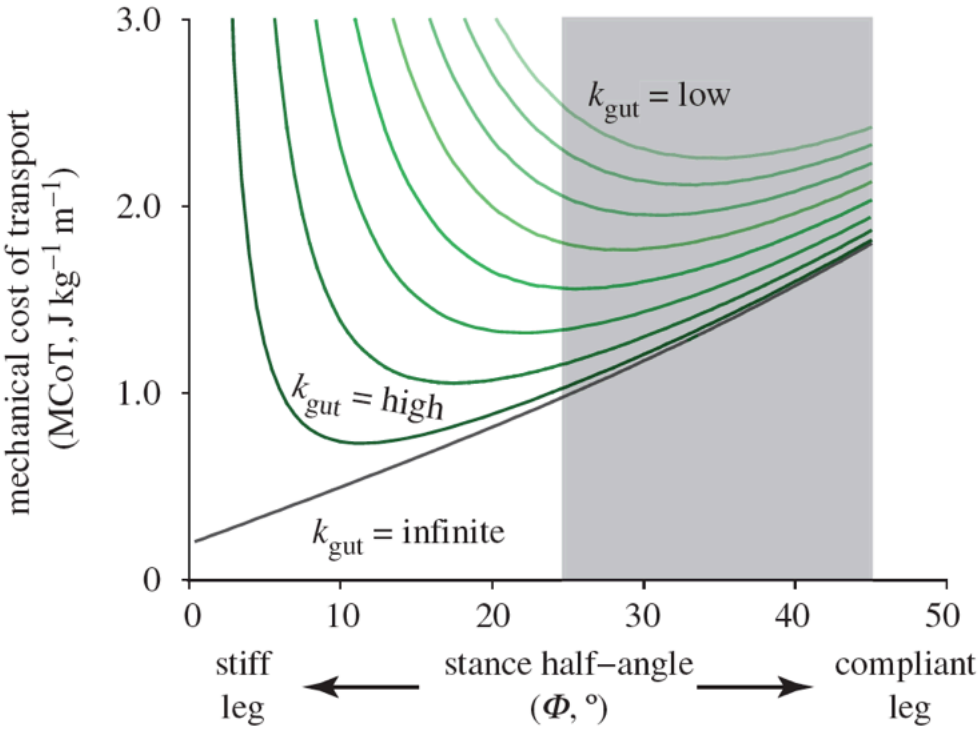

Figure 2.1: The mechanical cost of transport in function of the stance half-angle, and depending on different leg stiffness (Daley & Usherwood 2010).

Remodeling viscera properties, the more are relatively massless, elastic or stiff, the more their losses are low, so stiff legs are favourable, while if viscera dissipate substantial energy, compliant legs are favoured. That model is consistent with the finding that metabolic cost relates to the timing and magnitude of ground forces (Kram & Taylor 1990;

Pontzer 2007; Pontzer 2007), and suggests that compliant viscera with hysteresis may be one of the primary ultimate sources for this 'cost of force'.

In literature, values for viscera stiffness, or viscera motion have not empirical evidence in locomotion activity. There are only some anatomical studies, showing a quantitative analysis of internal organs motion during respiration or in different trunk position. Precisely Beillas (Beillas et al. 2009) presented a method to quantify, using a positional MRI scanner, the volume deformation, centre of mass translation and rotation of soft organs in addition to thoracic and abdominal cavities. The results shown a no significant variation of kidneys, spleen, liver and abdominal object volumes, and the organs movements were coherent with the effect of gravity.

The other anatomical study is based on a real time reconstruction with 3D computed tomography images, and simulation of the abdominal organ position and motion during free breathing (Hostettler et al. 2010; Hostettler et al. 2010).

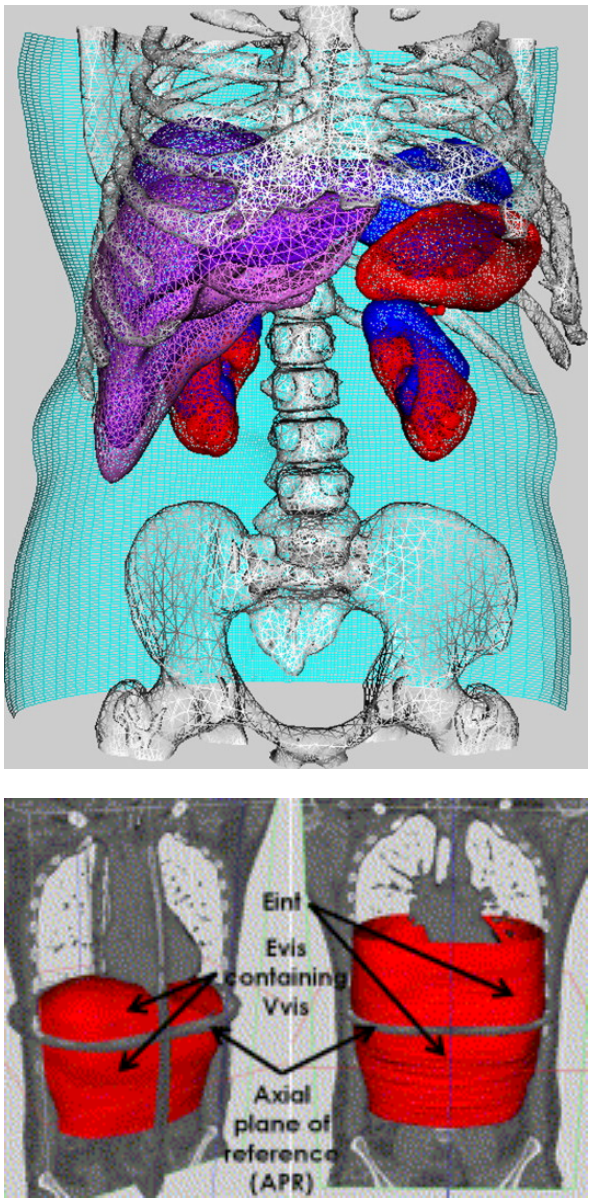

Figure: 2.2 Upper organs and abdominal viscera 3D reconstruction (Hostettler, Nicolau 2010).

From a mathematical and mechanical point of view, in the seventies Muskian and Nash (Muksian & Nash 1974) described a theoretical model to predict human response to specifics inputs. They developed multi-degree-of-freedom (MDOF) lumped parameter model with linear and non-linear passive elements (springs and damper), in respect to the vibration frequency. In these two works, the human model is divided in different mass-spring-damper systems, including head, diaphragm, thorax, abdomen, vertical column and spring and damper constants have been estimated, revealing for the first time a frequency response approach on a biomechanical model.

The final step toward a complete biomechanical approach have been done by Minetti and Belli in 1994 (Minetti & Belli 1994), showing the unique quantitative method for the estimation of the visceral mass displacement in periodic movements. Starting from the basis of concurrent cinematographic and dynamometric measurements, this method allows to improve the prediction of the true body centre of mass (CoM) displacement, and the computation of the 'external work' related to the total CoM energy changes (Minetti & Belli 1994). The only restrictions imposed by that method are that the periodicity of the movement patterns and the mass of the internal viscera has to be known (or estimated) in advance.

In this thesis, this validated method (Minetti & Belli, 1994) for the estimation of visceral mass displacement has been applied, during jump sequences with two different techniques: a natural jump and a "controlled" jump technique, based on peculiar respiration and abdominal muscles contraction strategies (Kapandji 1977, Caufriez 1997). The last strategy was meant to improve trunk–pelvis segment stiffness and minimize visceral mass displacement.

In that method, restricted to periodic movements, the simultaneous measurement of ground reaction forces and spatial coordinates allow the estimation of the relative movement between the 'invisible' abdomen content and the 'container', i.e. the rest of the body as described by the position of external markers.

3.2 MATERIALS

3.2.1 Experimental protocol

Six subjects (age 23.3 ± 2.5 years, trunk length 0.570 ± 0.110 m and weight 659.43 ± 53.0 N) have been selected to jump, in two different sessions on a dynamometric platform (KISLER, CH), synchronized with a six-camera motion capture system (VICON MX, Oxford Metrics, UK) (Fig. 2.3).

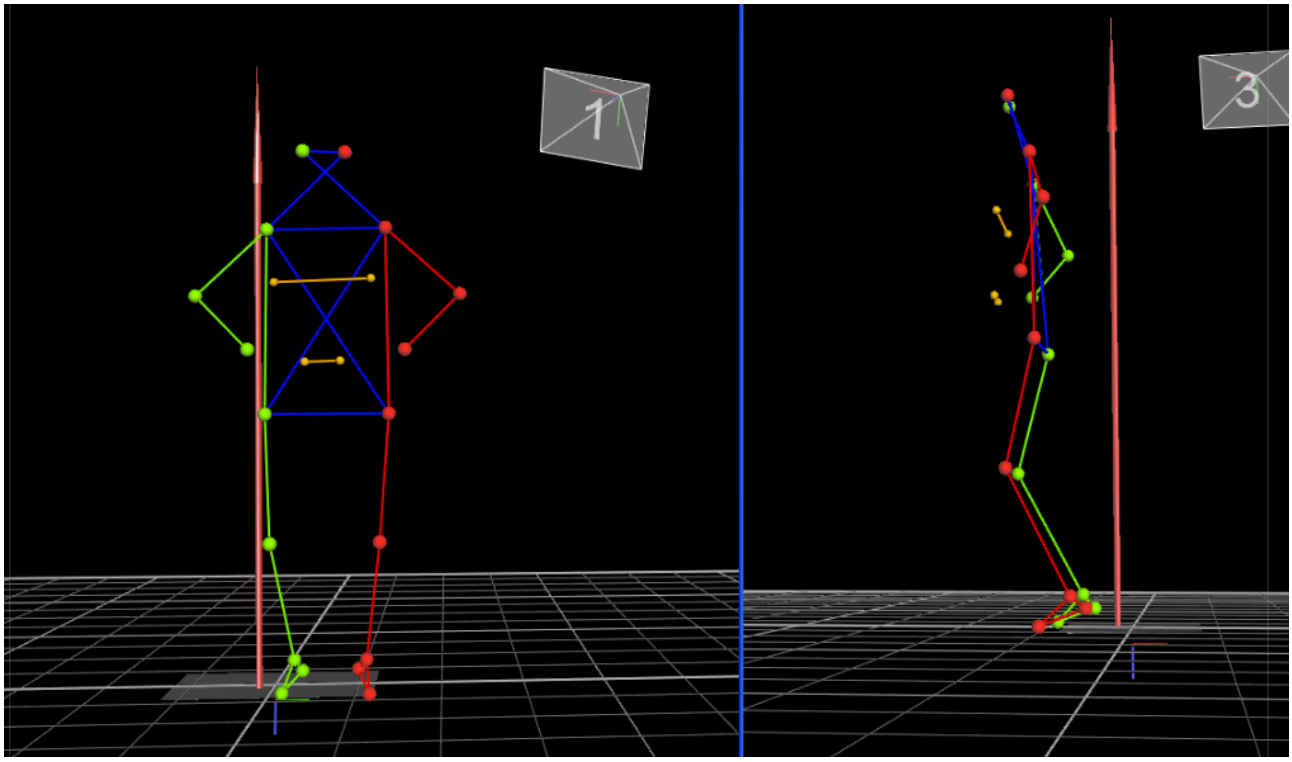

Figure 2.3: Two different views of a synchronized acquisition of VICON motion capture system and KISTLER platform. The 22 markers biomechanical model shows the right side in green, the left in red and the pectoral and low abdomen in yellow.

The platform signal has been sampled at 1200 Hz, while the optoelectronic system sampling frequency was 400 Hz. The human body has been modelled as a series of linked, rigid segments: eighteen reflective markers (Ø = 14 mm) were placed bilaterally on anatomical landmark points (Fig. 2.4), nine per each side (Koopman et al. 1995; Mian et al.

2006), while four technical-markers were placed on the estimated centre of mass position of pectoral muscles and low abdomen.

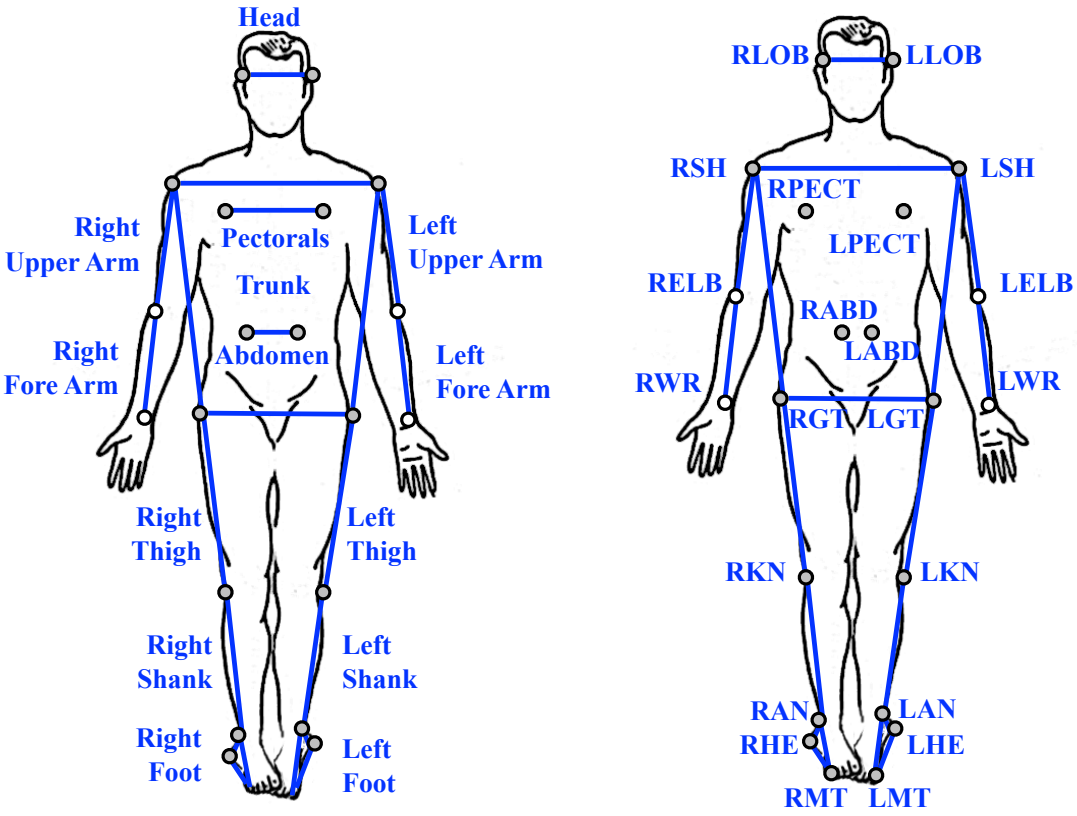

Figure 2.4: Human body modelled with 14 segments ad 22 reflective markers.

In this way, 14 body segments were defined: head, trunk, right and left upper arm, right and left fore arm, right and left thigh, right and left shank, right and left foot, pectorals, and abdomen.

Segment mass fraction and proximal distance of the centre of mass were taken from Dempster et al. (1959). All the subjects were students of Motor Science faculty of the University of Milan, chosen for their motor/jumping skill.

During the first session, the subjects jumped barefoot, with the hand on their pelvis, without any advice, to facilitate a natural jump execution. Every session was made up of 5

trials, at least of 20 jumps, spaced out by an adequate recovery period between every trial. The second experimental phase started after a training period of one month, while the subjects learned to jump in the "controlled" way, following the learning progression described above.

3.2.1 Jumping technique: normal and controlled jumps

In the literature, respiration is described as a rhythmic variation of pulmonary volume, controlled by the respiratory neurons. In such activity many muscular groups are involved in pulmonary volume variation: the first ones are pharyngeal and laryngeal muscles that control the upper airway resistance, the second ones, involved in the inspiration, are diaphragm, chest, spinal and neck muscles.

Other abdominal wall, chest and spinal muscles are involved again when active expiration is needed. Many of these muscular groups have in common origin and insertion, hence their activity is complex and reciprocally dependent, and in addition they are influenced by many other factors as posture, locomotion and voluntary activities (Lumb A.B., 2005).

Consequently, there are different ways to breathe and various technique of thorax expansion: in such way the respiration is adapted to the several situations of psycho-physical activity that the subject is living. (Calais-Germain B, 2005)

These notions could be applied on specific physical activities, as jumping or running, where respiration is considerably influenced by mechanical interactions. The athletes learn to optimize their movements and all the respiratory-motion couplings to improve their performance.

In fact, the ability to transfer a force impulse from inferior limbs to all the body, without any dispersion due to asymmetry, is a key motor strategy of jumping and of all the dynamic muscular activity related to inferior limbs. In this respect, visceral mass

displacement could represents a good body-stiffness index, during impulsive motor activity.

Jumping in a natural way causes a physiological viscera motion strictly linked to respiration frequency, which could influence the movement of the centre of mass. The idea is to find a "controlled" way to jump, minimizing this motion and improving the stiffness of the body. In this way specific respiration techniques and abdomen muscle contractions are necessary to control viscera displacement during a vertical jump.

Hence, a hip-trunk rigid segment is critical to improve abdominal belt stiffness (Le Boulch, 1973). This is possible through a limited hip anteversion position, due to a low diaphragmatic inspiration (Fig. 2.5), with a contemporary dorsum-lumbar expansion due to an endo-abdominal pressure improvement, amplified by trunk expiration during the impact phase (Caufriez, 1997, Kapandji 1977).

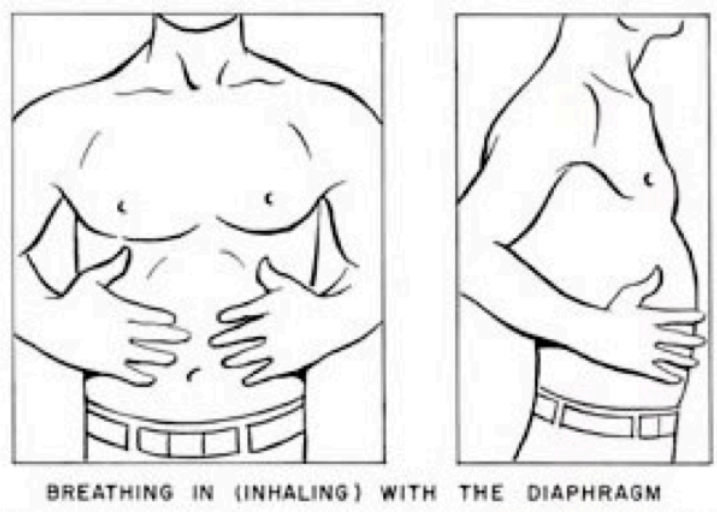

Figure 2.5: Low diaphragmatic inspiration, before the endo-abdominal pressure improvement.

The learning progression used by the subjects of this study was:

1. Diaphragmatic respiration learning, from sitting to standing position.
2. Same respiration in standing position, with the dorsal-lumbar trait holding on a wall.
3. Jumping, after a diaphragmatic inspiration, executing trunked expiration on every metatarsal contact.

3.3 METHODS

3.3.1 Mechanical model

In this study, the method for the estimation of visceral mass displacement previously described has been applied: in periodic movement, as repeated jumps, the simultaneous measurement of ground reaction forces and spatial coordinates of all but one segment (of know mass), allow the estimation of the relative movement of the last one, with respect to the centre of mass of the others (Minetti & Belli 1994).

The present method is based on a model made up of an empty container with mass M, holding in a hidden mass m, oscillating periodically in the vertical and horizontal direction. In respect to the previous study, we included an external wobbling mass linked to the container, and the new equation of motion is:

$$\left(M + m + m_e\right)\ddot{y}_{CoM}(t) = F_v(t) - \left(M + m + m_e\right)g; \qquad (1)$$

Equation (1) is the result of the system of equation

$$\begin{aligned} M\ddot{y}_1(t) &= F_v(t) - Mg - f_v(t) - f_e(t) \\ m\ddot{y}_2(t) &= f_v(t) - mg \\ m\ddot{y}_3(t) &= f_e(t) - m_e g \end{aligned} \qquad (2)$$

where f_v and f_e are vertical internal forces, unknown, exerted by the internal and external masses respectively (Fig. 2.6), M the container mass, m the internal visceral mass and m_e the external mass.

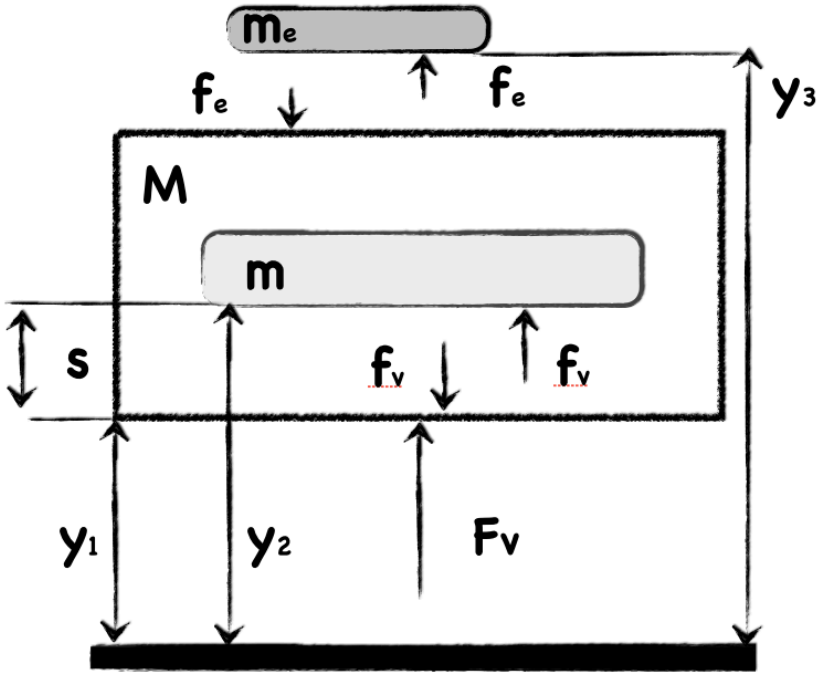

Figure 2.6: Model for the estimation of visceral mass displacement. M is the container mass, m the internal visceral mass, and me is the external mass. Then y_1, y_2 and y_3 are distances from ground level and $s=y_2-y_1$. The whole system oscillates vertically and exerts a vertical ground reaction force Fv, while internal and external mass exert a force f_v and f_e respectively on the container.

The magnitude of the internal visceral mass 'm' was estimated to be 14% of body mass (Scientific Tables, Ciba Geigy), while the external masses 'm_e' was evaluated to be 2% of body mass (Winters&Woo, Multiple Muscle System).

3.3.2 Data analysis software

An "ad hoc" software (LABVIEW 8.6, National Instrument) (Fig. 2.8) elaborates data and calculates the visceral mass vertical displacement, as shown in the equation (3).

$$s(t)-s_0=\frac{(M+m+m_e)}{m}\left[\int_0^t\left(\int_0^t\left(\frac{F_v(t)}{M+m+m_e}-g\right)dt\right)dt-\frac{t}{T}\int_0^T\left(\int_0^t\left(\frac{F_v(t)}{M+m+m_e}\right)dt\right)dt\right]-\left(\frac{M+m}{m}\right)\left(y_1(t)-y_1(0)\right)-\left(\frac{m_e}{m_e+m}\right)\left(y_3(t)-y_3\right.$$

(3)

At first, we tested our software loading kinetics data of a model, generated by a simulation software (Visual Nastran 4D, MSC Software) (Fig 2.7). The model was a mechanical conservative system made up of a rectangular prism (container), linked at the top of its inner part, with a sphere (visceral mass) by a Hooke's spring, without any collision. In this way, we compared the sphere vertical displacement, generated by Visual Nastran 4D, with the one computed by the implemented software.

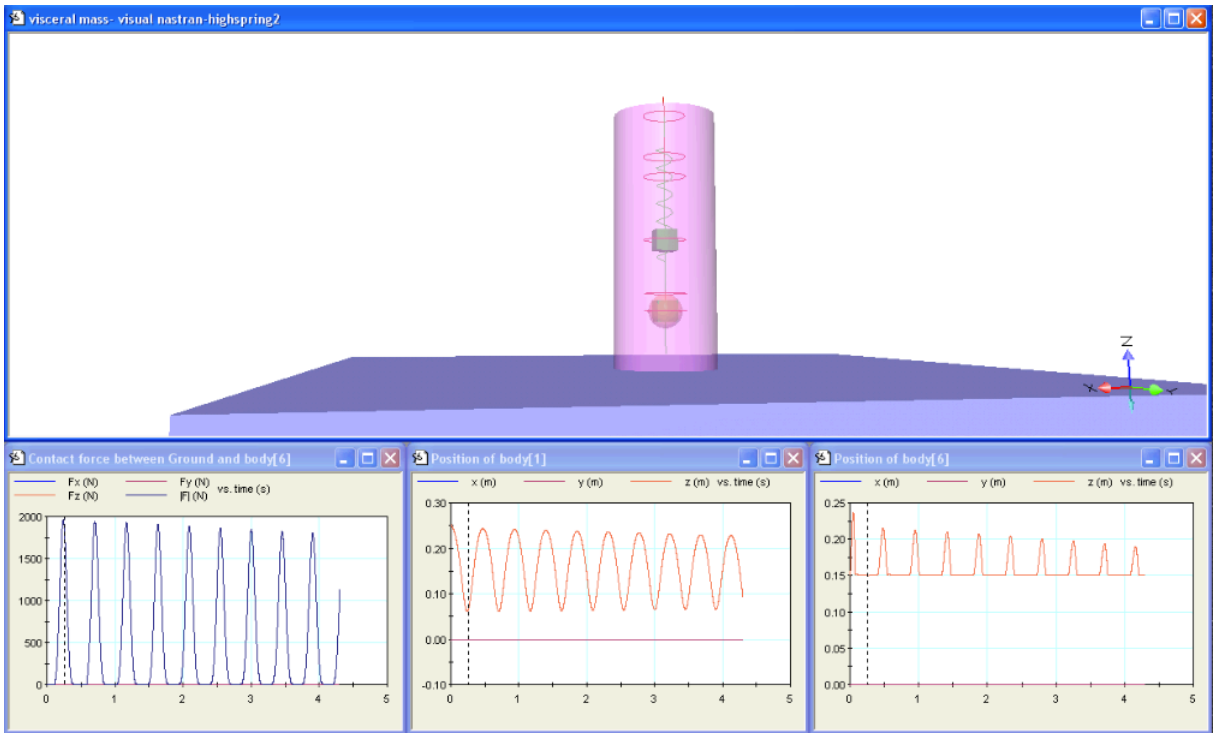

Figure 2.7: A frame of the simulation software VISUAL NASTRAN 4D is shown. The container has been modelled as a cylinder including an inner sphere representing the visceral mass. The motion is due to a free vibration of the system after an initial input force.

The Labview software automatically recognizes and isolate every jump, double integrate using the trapezoidal rule, and then decimates platform data from 1200 Hz to 400 Hz. Data analysis started after 4-5 hopping cycles, in order to process just stable hopping oscillations (Rousanoglou & Boudolos 2006). Ground reaction force signal is shifted backward to cover a 1,66 ms ($2\Delta t$) time gap, due to double integration, in order to synchronize this data with cinematography acquisition.

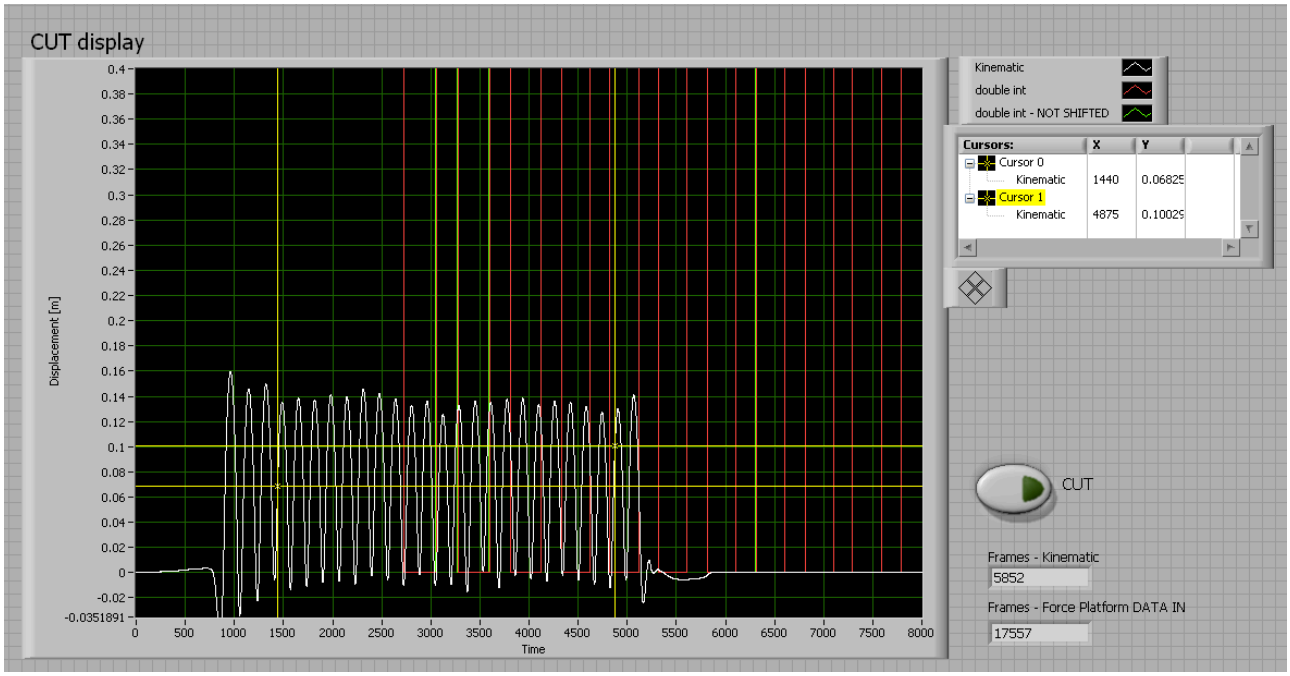

Figure 2.8: A frame of the user interface of LABVIEW software.

The kinematics data analysis, evaluates the container centre of mass vertical displacement from the eighteen anatomical markers position, while the four technical markers quantify the estimated pectoral and abdomen masses vertical displacement. Their difference represents the relative displacement of the external masses (pectorals and abdominal fat), with respect to the container centre of mass. In the model equation (1) of motion, this value is weighted by the scaling factor me/(m+me).

3.3.3.1 Frequency analysis data processing

Kinematic and force data have been cut to extract the signal during the contact force period Tc, and the FFT has been performed for every jump, using a rectangular windows of period Tw ≤ Tc. Force data and visceral displacement data have been filtered by a low-pass Butterworth filter with cut-off frequency of 40 Hz and 30 Hz respectively. The mean values of FFT amplitude and phase have been calculated for every trial.

3.3.3 Vibrational analysis: frequency response of the model

3.3.3.1 Frequency response function

It's well known that many real systems motion could be modelled with a specific vibration or a harmonic motion. Vibration can be classified in several ways: a free vibration without externally applied forces, or a periodic, aperiodic or random forced vibration. Both free and forced vibration can be damped, which is the term used in the study of vibration to denote dissipation of energy. The classical model selected in vibration analysis is the mass-spring-damper model (Fig. 2.9).

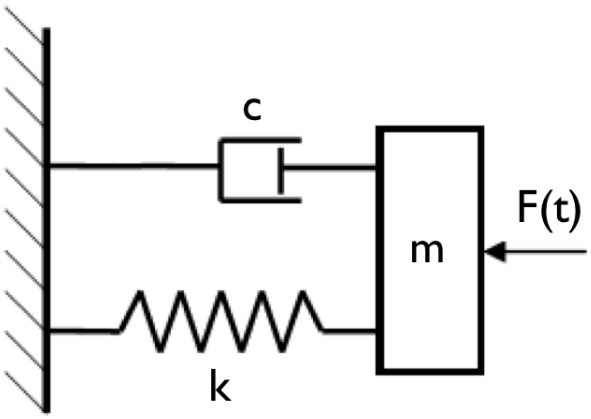

Figure 2.9: A SDOF (single-degree-of-freedom) Mass-Spring-Damper model system, forced by a force F(t).

Vibrations are also classified by the number of degree of freedom of motion. The number of degrees of freedom, correspond to the number of independent coordinates needed to completely describe motion, and is obviously linked with the number of model (or masses) in motion.

In the case of a harmonic oscillator, forced by an external impulse, pulses with a frequency dependent exclusively to physical system parameters, as the elastic constant k and the

mass. This frequency is called natural frequency of the system, or resonance frequency of the oscillator:

$$f_n = \frac{1}{2\pi}\sqrt{\frac{k}{m}}$$

At this frequency, an external force transfers energy to the system with the maximal efficiency. For this reason the more an external force is applied with a frequency close to the natural frequency, the more the oscillation amplitude will rise, while for frequency larger or lower, the force obstructs the oscillation. This is of engineering interest in the prediction of maximum stress, or mechanical failure, but could be also of great pertinence in biomechanical modelling.

In fact, our mechanical model can be analyzed as a classical mass-spring-damper model, referring to the fundamentals of vibration analysis and modal testing: even a complex structure can be modelled as a "summation" of simple mass–spring–damper models, and in our case, a periodic motion as repeated jumps, can be modelled with a classical forced damped vibration.

There are many tools available to perform vibration analysis and testing, and one of those is based on the frequency response function analysis. This approach allows to compute the frequency response function (FRF) and then to estimate the natural frequencies (resonance frequency), damping ratios and mode shape of a structure.

In this way, the solution of a vibration problem is an input/output relation where the force is the input and the output is the vibration. If we represent the force and vibration in the frequency domain (magnitude and phase) we can write the following relation:

$$X(\omega) = F(\omega).H(\omega) \quad (4)$$

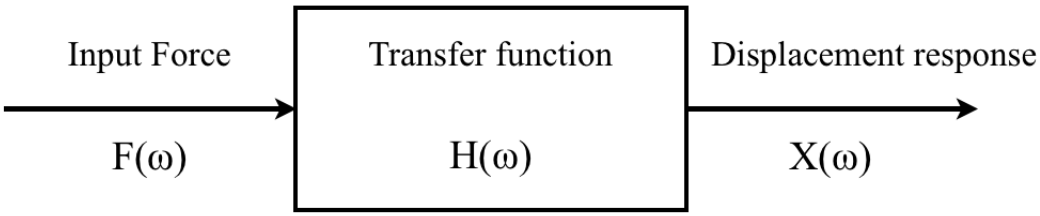

H(ω) is called the FRF and expresses the structural response to an applied force as a function of frequency. Every function is a complex function, which may also be represented in terms of magnitude and phase. The magnitude of the FRF and the phase are shown in the following equations:

$$H(\omega) = \frac{X(\omega)}{F(\omega)} = \frac{1}{k} \frac{1}{\sqrt{\left(1 - r^2\right)^2 + \left(2\xi r\right)^2}},$$

where $r = \frac{\omega}{\omega_n}$ is the frequency ratio and ω_n is the natural frequency,

where $\xi = \frac{c}{2\sqrt{km}}$ is the damping ratio,

and the phase is $\phi = \arctan\left(\frac{2\xi r}{1 - r^2}\right)$

In this way, it could be very interesting to find the characteristic frequency curve, i.e. the frequency response of human body and to infer its response to specific stimulus. In the next paragraph, the frequency response method will be described, but we can anticipate the significance of this mechanical paradigm on biomechanical models. The muscle-tendon vibration parameters could change becoming more stiff or damping, depending on the stimulus that is exactly generated by the same muscles.

This could means that human body system is used to response to natural stimuli, closed in a limited frequency range, probably not far from its natural frequency to minimize energy loss. This frequency will depend on all the mass-spring-damper models composing human

body, and not only to lower limbs, even if are the main element of that system. An example is actually the visceral mass, because of its mass amount and possible displacement. Moreover, visceral mass could change its response depending on diaphragm or abdominal muscles vibration parameters, and its motion could influence the vibration 'modes' of human model.

The main usual stimulus occur in human locomotion or jumping, and could be described, in the frequency domain, with distinctive frequencies. That said, delineating the frequency response of whole human body, the response relative to the principal natural stimulus could be inferred, showing the most dangerous or the optimal frequencies.

3.3.3.2 Frequency response function (FRF) method

The frequency response function (FRF) analysis, is a fast and useful method to estimate vibration parameters, converting the stimulus and the response of the system in the frequency domain. The vibration is represented as an input/output and the FRF does not necessarily have to be calculated from the knowledge of the mass, damping, and stiffness of the system, but it can be measured experimentally. It's exactly our instance, where we applied a measured force and sweep the frequency and then calculated the resulting vibration, solution of equation (1), to obtain the frequency response function and then characterize the system:

$$H(\omega) = \frac{X(\omega)}{F(\omega)}$$

In a classical forced vibration example, only a simple harmonic force is applied to the model, but this can be extended to other situations using the Fourier transform and "the principle of the superposition.

The Fourier transform takes a signal as a function of time and breaks it down into its harmonic components as a function of frequency, generating a frequency spectrum that presents the magnitude of the harmonics that make up the same wave, and the phase. The Fourier transform can also be used to analyze non-periodic functions such as transients (e.g. impulses) and random functions. With the advent of the modern computer the Fourier transform is almost always computed using the Fast Fourier Transform (FFT) computer algorithm in combination with a window function. Hence, the Fourier transform allows interpreting also “complex” forces as a sum of sinusoidal forces, with frequency and amplitude of the found harmonics.

The second mathematical tool, "the principle of the superposition”, permits to sum the solutions from multiple forces if the system is linear. In the case of the spring–mass–damper model, the system is linear if the spring force is proportional to the displacement and the damping is proportional to the velocity over the range of motion of interest. Consequently, the solution to the problem with a non-periodic wave is summing the predicted vibration from each one of the harmonic forces found in the frequency spectrum of that wave.

3.3.3.3 Vibrational model

Hence, FRF method to study the vibration of our mechanical model has been chosen. It's a system with two degree of freedom and forced by the GRF force $F_v(t)$ (Fig. 2.10).

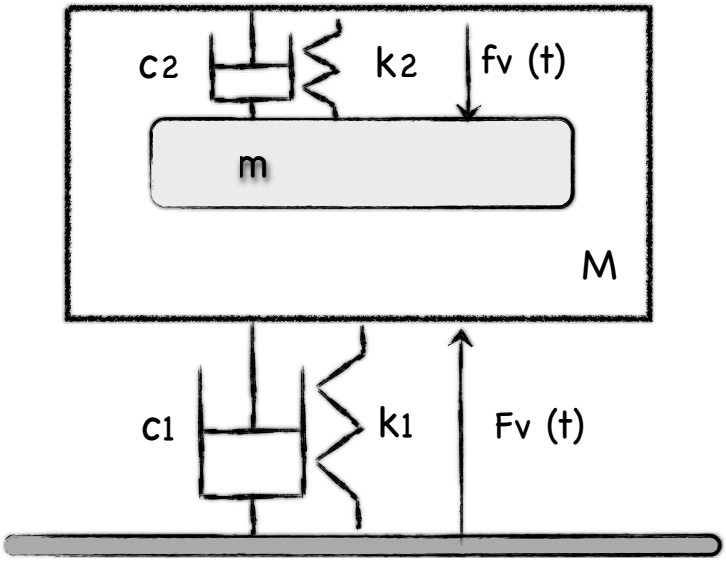

Figure 2.10: MDOF model, with two degree of freedom, forced by Fv(t).

This system is made up of two mass-spring-damper models: the first is composed by a container of mass M, a spring of elastic constant k_1, and a damper of damping constant c_1, as well as the second one represented by a mass m, a spring of elastic constant k_2, and a damper of damping constant c_2.

The first model is forced by the GRF Fv(t), and describes the container motion related to lower limbs stiffness and damping parameters.

The second model, has been designed observing viscera anatomy, and its retaining structures: sub-diaphragmatic organs are closely joined to upper abdominal wall (diaphragm), as the liver by three ligaments and vena cava inferioris and vena porta; sovra-mesocolic organs like stomach and duodenum have limitation in relative down-warded

movements given by the hepato-gastric and hepato-duedenal ligaments and the oesophagus (Fig. 2.11).

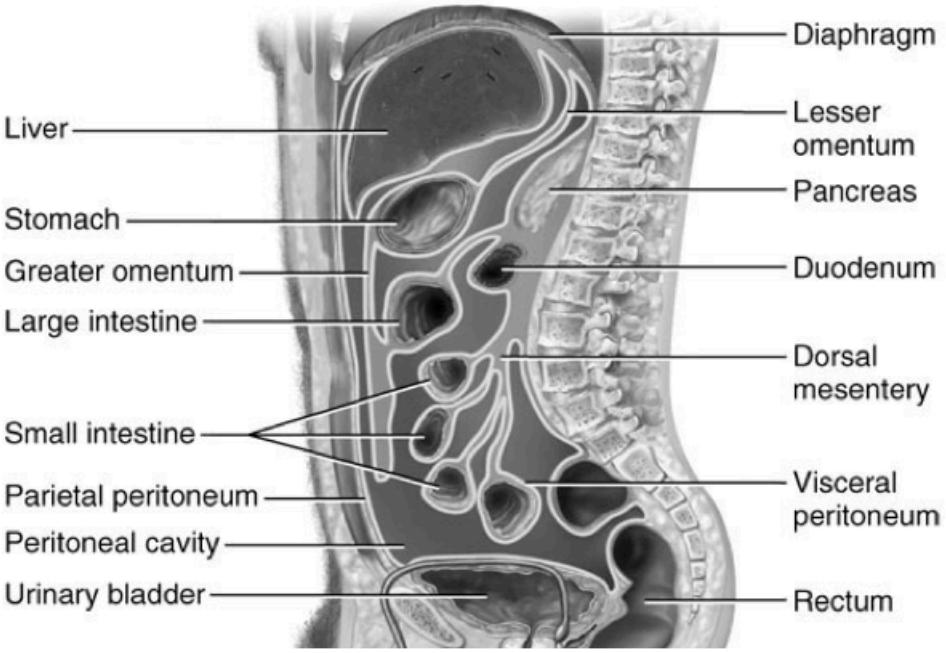

Figure 2.11: Anatomy of human viscera.

The main moving mass is the greater omentum and the transverse colon and can be seen as a festoon placed in the middle of the abdomen, pending between ascending and descending colon, with a low possibility to move downward but almost to rise. The same could be said about small intestine and its connection to the posterior wall, the mesentery. Hence, we decided to model viscera as a ball in a fluid connected to the posterior-upper wall, at one third of the upper wall region, by a spring and a damper. The spring represents the elastic component as ligaments or diaphragm response while the damping represents the friction between internal organs and their pliability.

The MDOF system described above is absolutely the best model to fit the vibration studied. In this Thesis, I decided to present only the preliminary data of a simplified SDOF

(single-degree-of-freedom) model, because the vibration analysis based on the system identification method of the MDOF system is not still completed. An exhaustive analysis of the new method is described in the 'Perspective' paragraph.

In this case, the model is represented by a single mass system (visceral mass) with a spring of constant k_2 and a damper of coefficient c_2 (Fig. 2.12).

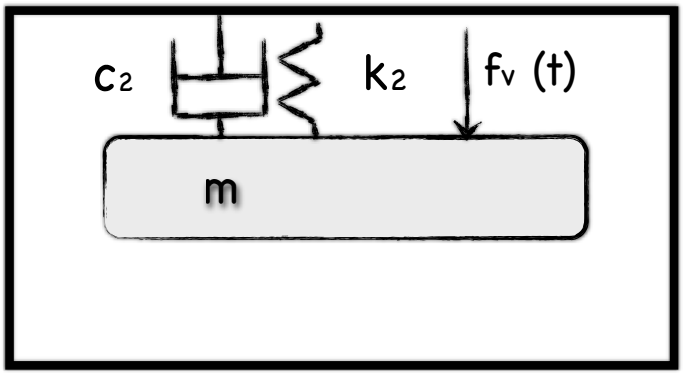

Figure 2.12: A SDOF system, force by an impulse $f_v(t)$. The mass m represents the visceral mass, while k_2 and c_2 are the vibrational parameter of the simplified system.

The impulse f_v derives from the equation of motion (2) and is applied directly on mass m, while the response is the relative viscera vertical displacement in respect of CoM (Fig. 2.12).

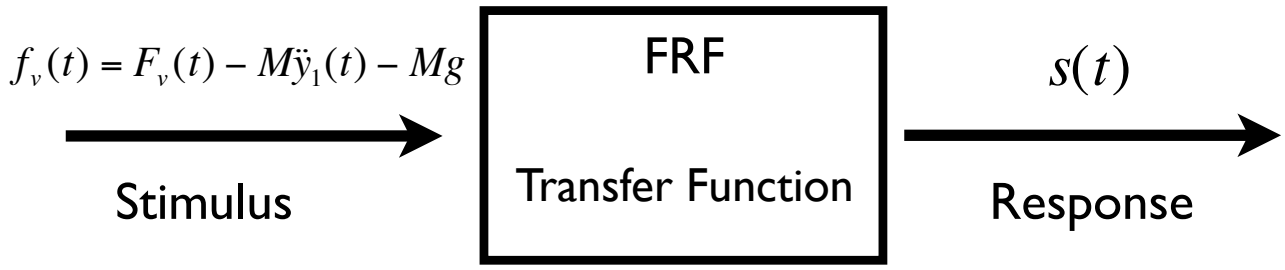

Figure

Finally we considered negligible the external mass contribution owing to its low influence in overall system motion, as described in results paragraph.

3.3.3.4 Estimation of vibration parameters

The vibration parameters estimation, starts analysing an ideal free vibration of the model (Fig. 2.13). In this way the damping effect is null, and the mechanical model is dependent simply to its elastic component. This form of vibration is called harmonic motion, and the system is vibrating at its natural frequency f_n.

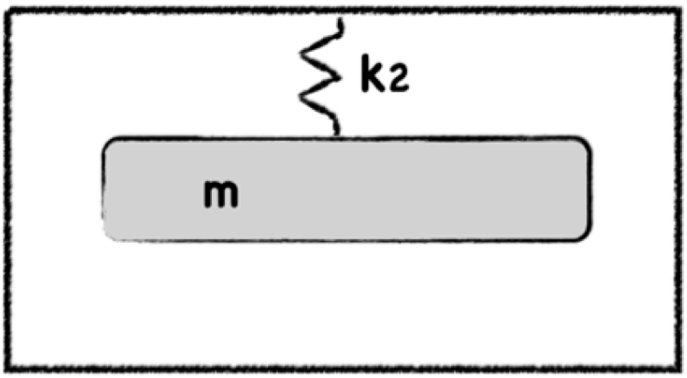

Figure 2.13: The free vibration model of the system. Considering damping null, the system will vibrate with two different natural frequencies dependent to the parameters k_2, and m.

It's a well known method in mechanical of vibration, demonstrating how is crucial to prevent any vibration close to the natural or resonance (natural and resonance frequency are approximately the same when damping is null) frequency.

In fact the resonance is a tendency of the system to oscillate with the highest amplitude, storing and transferring mechanical energy without any losses (as potential and kinetic energy exchange in an ideal pendulum). These losses are caused by damping that attenuates the vibration amplitude with a specific damping ratio ξ (figure 2.14).

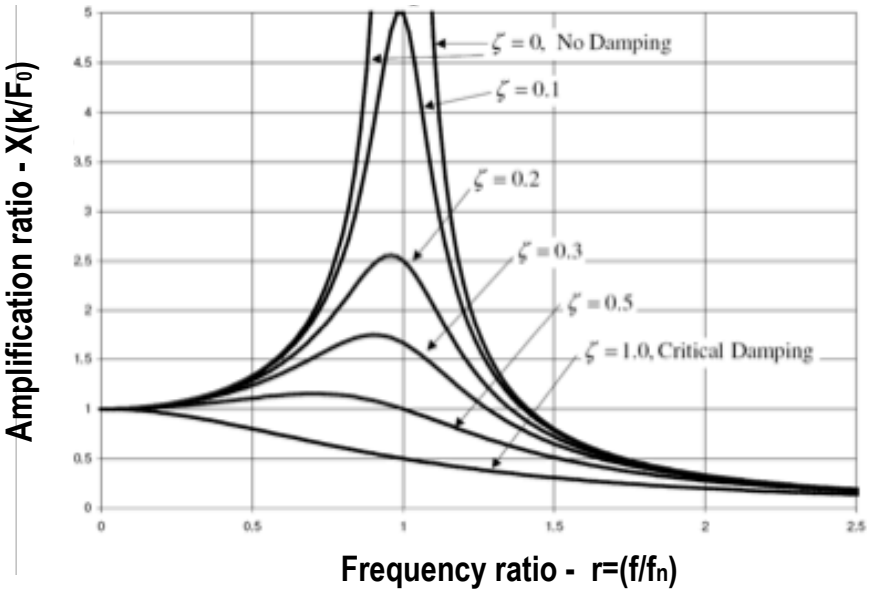

Figure 2.14: The frequency response of a mechanical system: the maximum amplitude ratio occurs at the resonant frequency while the damping decrease the amplitude ratio for all the frequencies, in proportion to the amount of damping.

Damping estimation is the second step of this method, and could be expressed with the 'quality factor' Q.

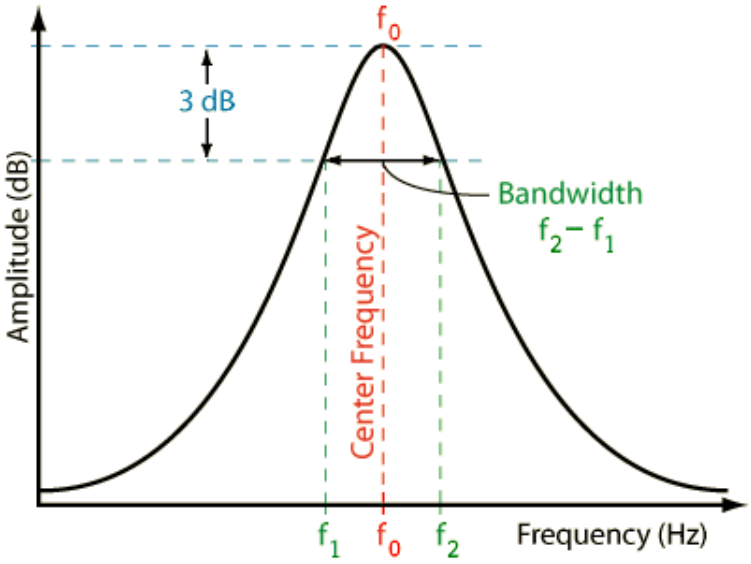

Figure 2.15: The bandwidth, $\Delta f = f_2 - f_1$, of a damped oscillator is shown on a graph of amplitude (dB) versus frequency (Hz). The Q factor of the damped oscillator, is f0 / Δf. The higher the Q, the narrower and 'sharper' the peak is.

The quality factor or Q factor is a dimensionless parameter that describes how under-damped an oscillator or resonator is, or equivalently, characterizes a resonator's bandwidth relative to its center frequency. A high Q brings to longer and higher oscillation while a low Q described a damped oscillation. The physical interpretation is $Q = \frac{1}{2\zeta}$ and in respect of damping, a system with a $Q < \frac{1}{2}$ is over-damped, $Q > \frac{1}{2}$ is under-damped and $Q = \frac{1}{2}$ is critically damped.

At last, knowing the influence of these parameters on the response of the system, it's possible to analyse the FRF to estimate them.

The resonant frequency can be estimated from the frequency response data by observing the frequency at which any of the following trends occur:

- The magnitude of the frequency response is a maximum.

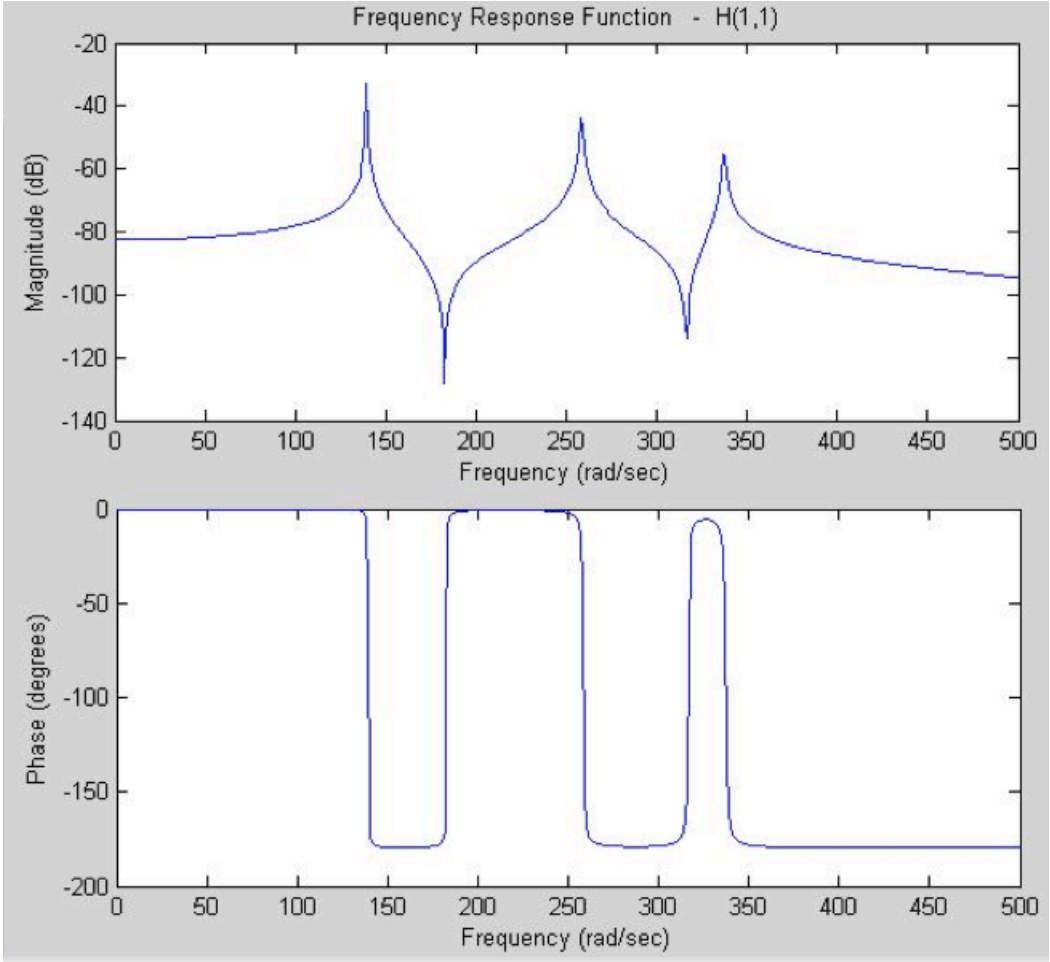

Figure 2.16: Example of a multiple degree of freedom FRF. Tree resonant frequencies have been found in correspondence of a coherent phase.

- The imaginary pat of the frequency response is a maximum or minimum.
- The real part of the frequency response is zero.
- The response lags the input by 90 phase.

It was discussed earlier that the height of the resonant peak is a function of damping. The damping factor can be estimated by the half power method by determining the sharpness of the resonant peak, as in the figure 2.15.

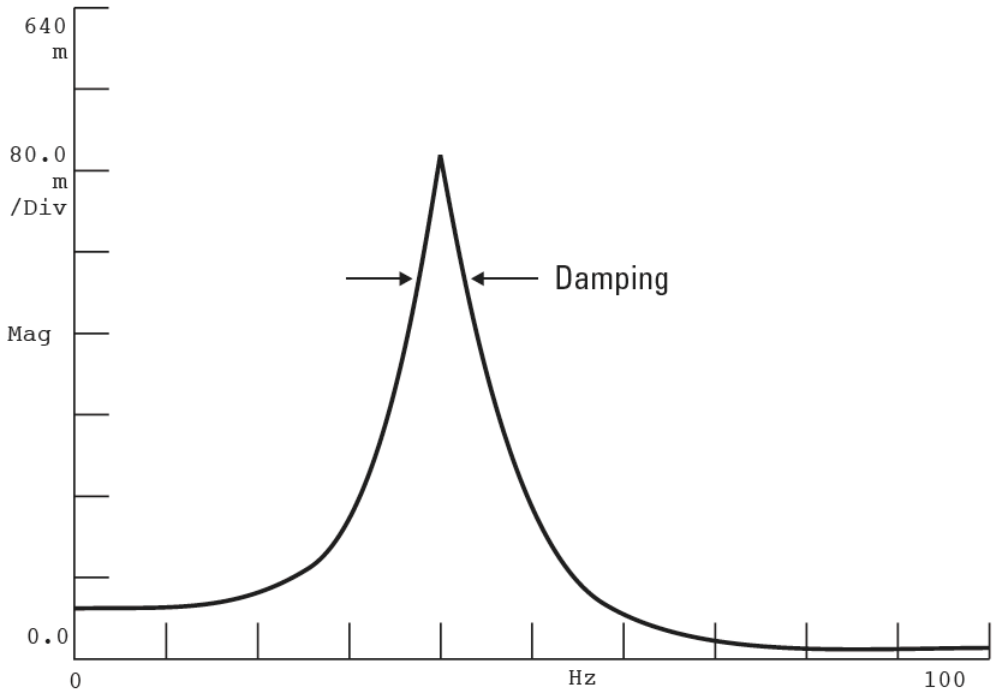

Figure 2.17: Half power method utilized to estimate the damping factor.

3.4 Results

3.4.1 Internal mass displacement values in normal and controlled jumps

In Table 2.1 results of all the experiments, divided for every subject, are shown.

JUMP	Subjects	Mean (m)	St. Dev (m)	N
Normal	*S1*	0.0656	0.00644	88
	S2	0.1016	0.01759	89
	S3	0.0782	0.01	73
	S4	0.1011	0.01178	87
	S5	0.0625	0.01947	95
	S6	0.1159	0.01374	55
	Total	0.0855	0.02399	487
Controlled	*S1*	0.0515	0.00574	101
	S2	0.0712	0.01788	84
	S3	0.0492	0.00871	100
	S4	0.1143	0.01282	84
	S5	0.046	0.00487	94
	S6	0.0921	0.01627	61
	Total	0.068	0.02744	524
Total	*S1*	0.0581	0.00931	189
	S2	0.0868	0.02334	173
	S3	0.0614	0.01711	173
	S4	0.1075	0.01394	171
	S5	0.0543	0.01643	189
	S6	0.1034	0.0192	116
	Total	0.0764	0.02726	1011

Table 2.1: The mean value and SD values in normal and controlled jumps are showed for every subject. A further total mean value and SD for both the jumping techniques for every subject is exhibited.

The mean of visceral mass displacement (VMD) (Total = 0.087 ± 0.021 m), for all the subjects, measured during normal jumps, is significantly higher ($p < 0.05$) performing a paired t-test, compared to mean of VMD (Total = 0.070 ± 0.027 m) in controlled jumps

(Fig. 2.26). An analysis of variance (ANOVA 2-ways) shows a significant effect of jump technique but also of subject and jump-subject interaction, confirming an elevated variability between the subjects (Table 2.2).

Tests of Between-Subjects Effects

Source	Type III Sum of Squares	df	Mean Square	F	Sig.	Partial Eta Squared	Noncent. Parameter	Observed Power
Corrected Model	0.586[a]	11	0.053	322.649	.000	0.780	3549.136	1.000
Intercept	6.117	1	6.117	37059.489	.000	0.974	37059.489	1.000
Jump	0.069	1	0.069	417.176	.000	0.295	417.176	1.000
Subjects	0.452	5	0.090	548.121	.000	0.733	2740.607	1.000
Jump * Subjects	0.054	5	0.011	65.973	.000	0.248	329.865	1.000
Error	0.165	999	0.000					
Total	6.656	1011						
Corrected Total	0.751	1010						

Table 2.2: Jump, subject and jump*subject interaction from an ANOVA 2-ways. (a) R Squared = 0.780 (Adjusted R Squared = 0.778)

In this way the paired t-test shows a low significance of mean values difference between the two techniques for all the subjects, even if the mean values in 5 of 6 subjects are higher in normal jumps then in controlled jumps.

Multiple Comparisons						
(I) Subjects	(J) Subjects	Mean Difference (I-J)	Std. Error	Sig.	95% Confidence Interval Lower Bound	95% Confidence Interval Upper Bound
S1	S2	-.0288*	.00135	.000	-.0328	-.0248
	S3	-.0034	.00135	.190	-.0074	.0006
	S4	-.0495*	.00136	.000	-.0535	-.0455
	S5	.0038	.00132	.063	-.0001	.0077
	S6	-.0453*	.00152	.000	-.0498	-.0409
S2	S1	.0288*	.00135	.000	.0248	.0328
	S3	.0254*	.00138	.000	.0213	.0295
	S4	-.0207*	.00139	.000	-.0248	-.0166
	S5	.0326*	.00135	.000	.0286	.0366
	S6	-.0165*	.00154	.000	-.0211	-.0120
S3	S1	.0034	.00135	.190	-.0006	.0074
	S2	-.0254*	.00138	.000	-.0295	-.0213
	S4	-.0461*	.00139	.000	-.0502	-.0420
	S5	.0072*	.00135	.000	.0032	.0111
	S6	-.0420*	.00154	.000	-.0465	-.0374
S4	S1	.0495*	.00136	.000	.0455	.0535
	S2	.0207*	.00139	.000	.0166	.0248
	S3	.0461*	.00139	.000	.0420	.0502
	S5	.0533*	.00136	.000	.0493	.0573
	S6	.0042	.00155	.107	-.0004	.0087
S5	S1	-.0038	.00132	.063	-.0077	.0001
	S2	-.0326*	.00135	.000	-.0366	-.0286
	S3	-.0072*	.00135	.000	-.0111	-.0032
	S4	-.0533*	.00136	.000	-.0573	-.0493
	S6	-.0491*	.00152	.000	-.0536	-.0447
S6	S1	.0453*	.00152	.000	.0409	.0498
	S2	.0165*	.00154	.000	.0120	.0211
	S3	.0420*	.00154	.000	.0374	.0465
	S4	-.0042	.00155	.107	-.0087	.0004
	S5	.0491*	.00152	.000	.0447	.0536

Table 2.3: Results from ANOVA 2-ways, Post-Hoc Bonferroni. The comparison between subjects is shown.

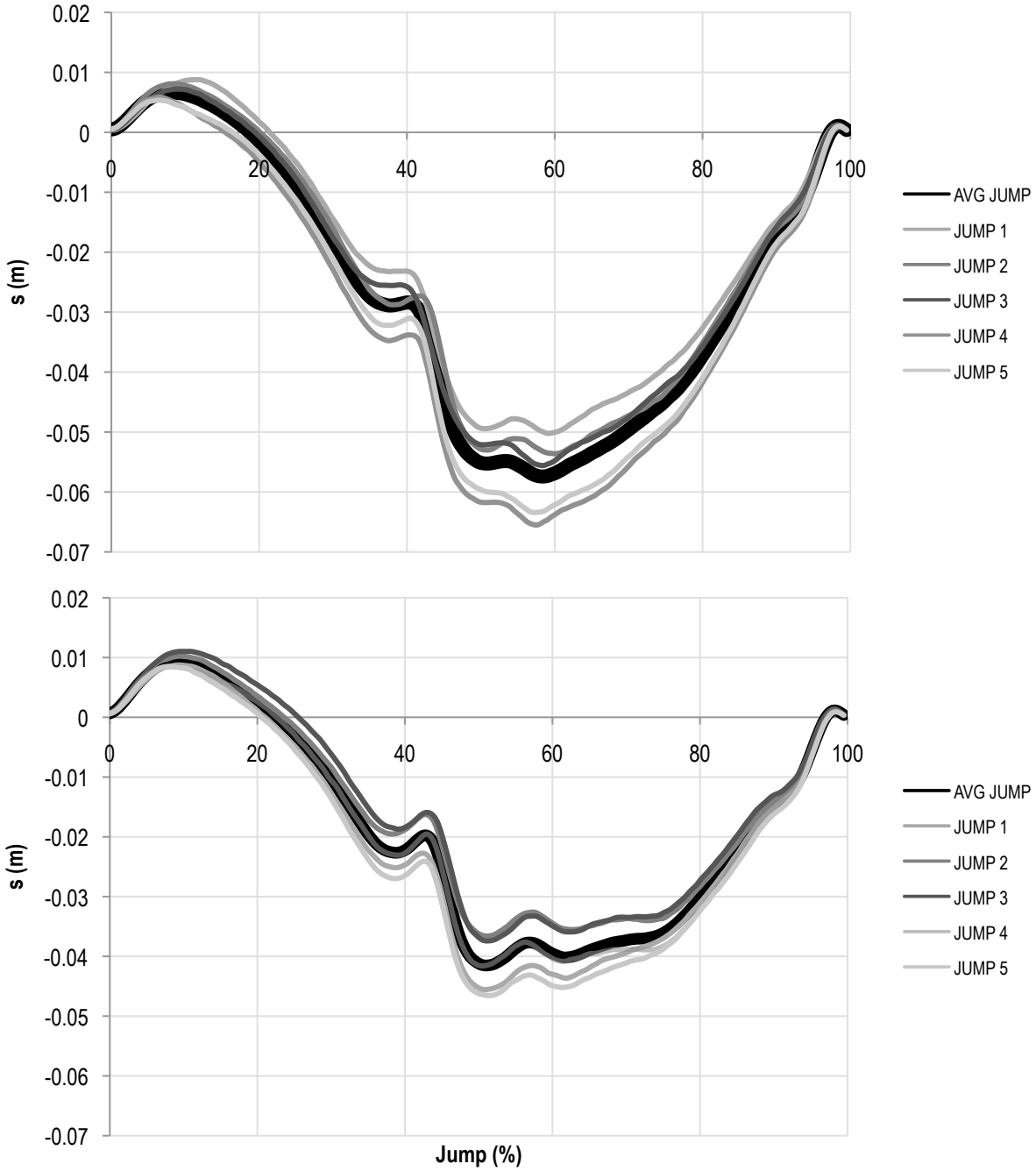

Figure 2.18: Subject 1 normal (upper graph) and controlled (lower graph) jumps. The mean curve of s (visceral mass displacement) for every trial and the mean of all the trials curve are shown for both the techniques.

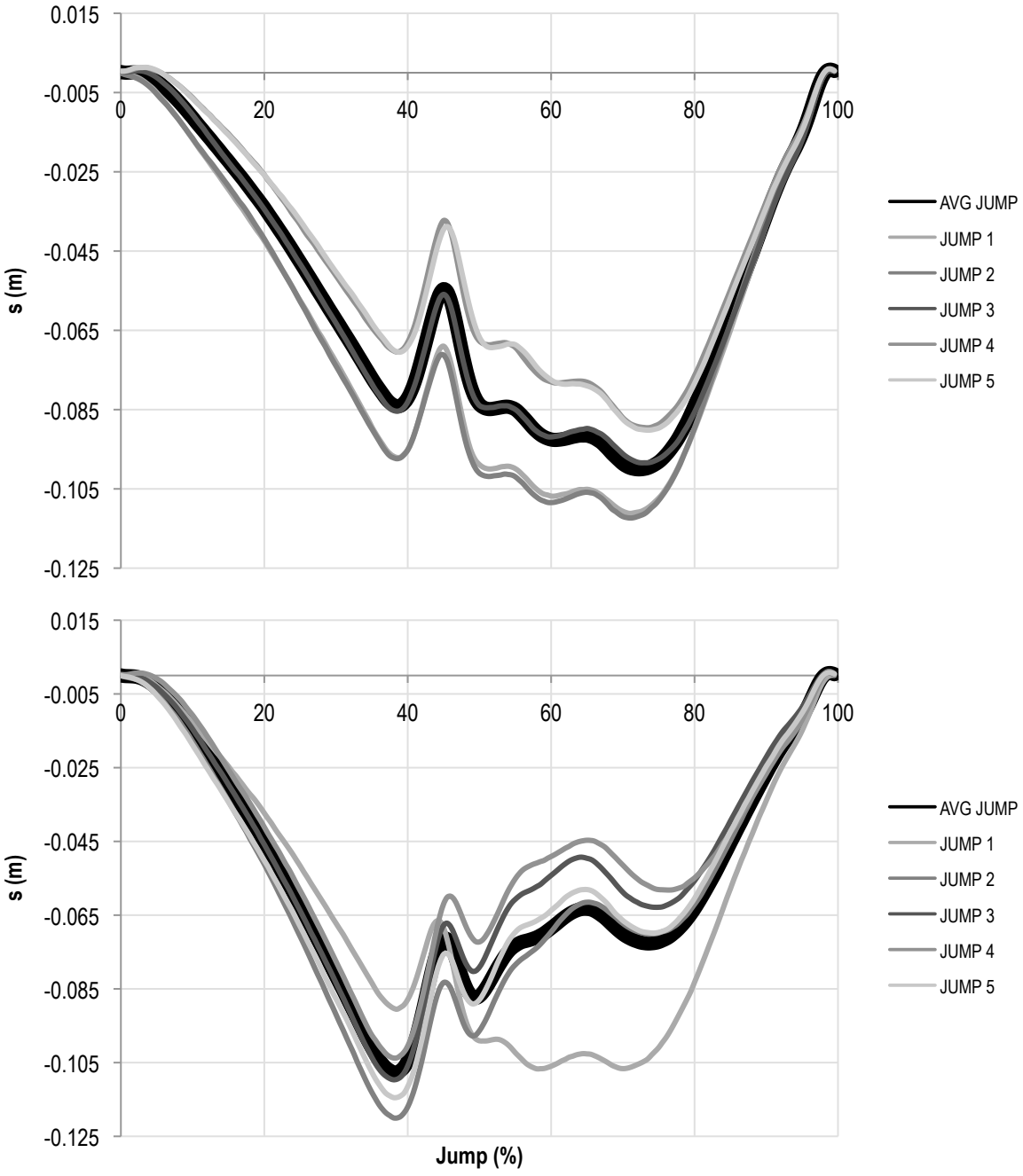

Figure 2.19: Subject 4 normal (upper graph) and controlled (lower graph) jumps. The mean curve of s (visceral mass displacement) for every trial and the mean of all the trials curve are shown for both the techniques.

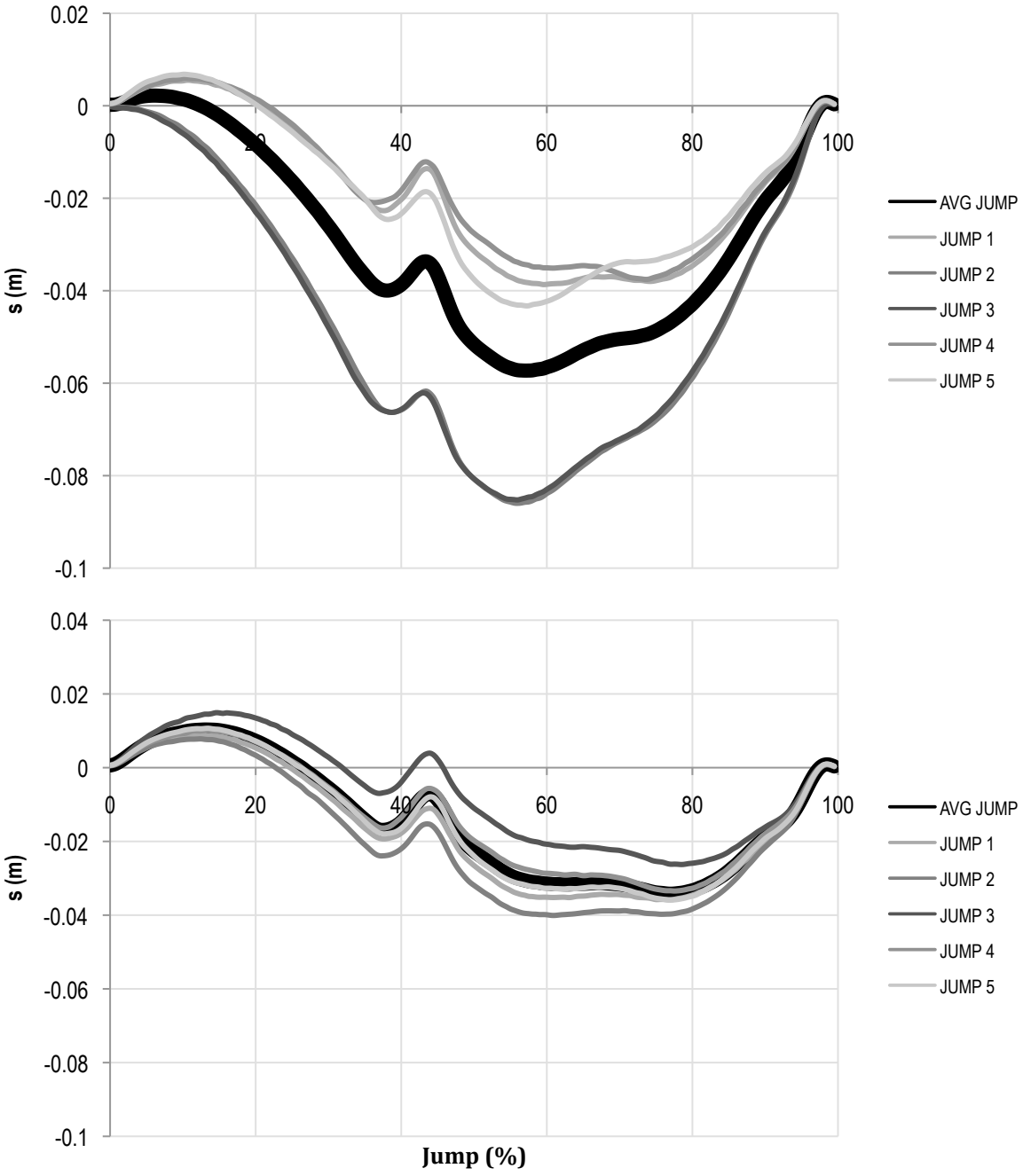

Figure 2.20: Subject 5 normal (upper graph) and controlled (lower graph) jumps. The mean curve of s (visceral mass displacement) for every trial and the mean of all the trials curve are shown for both the techniques.

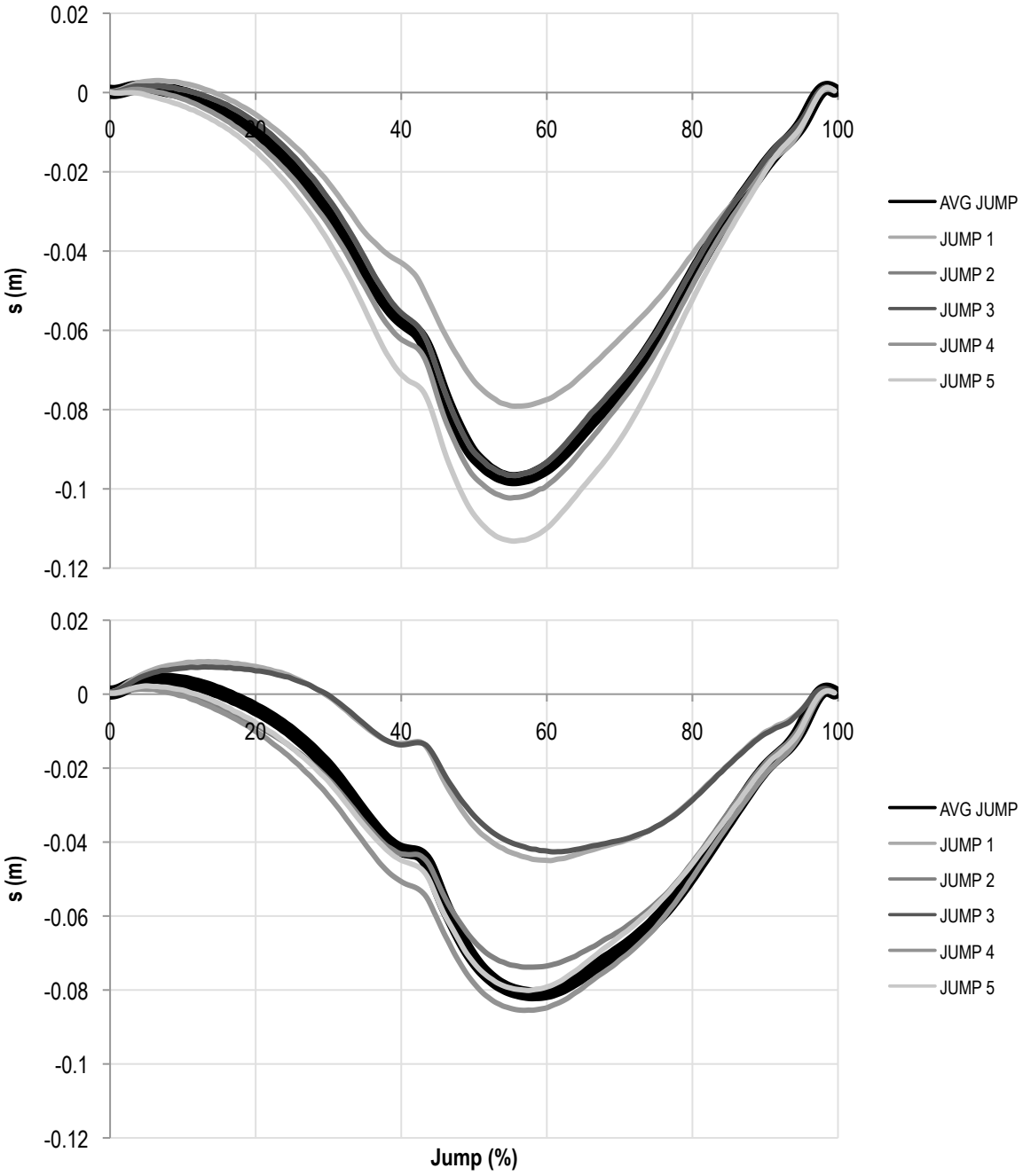

Figure 2.21: Subject 2 normal (upper graph) and controlled (lower graph) jumps. The mean curve of s (visceral mass displacement) for every trial and the mean of all the trials curve are shown for both the techniques.

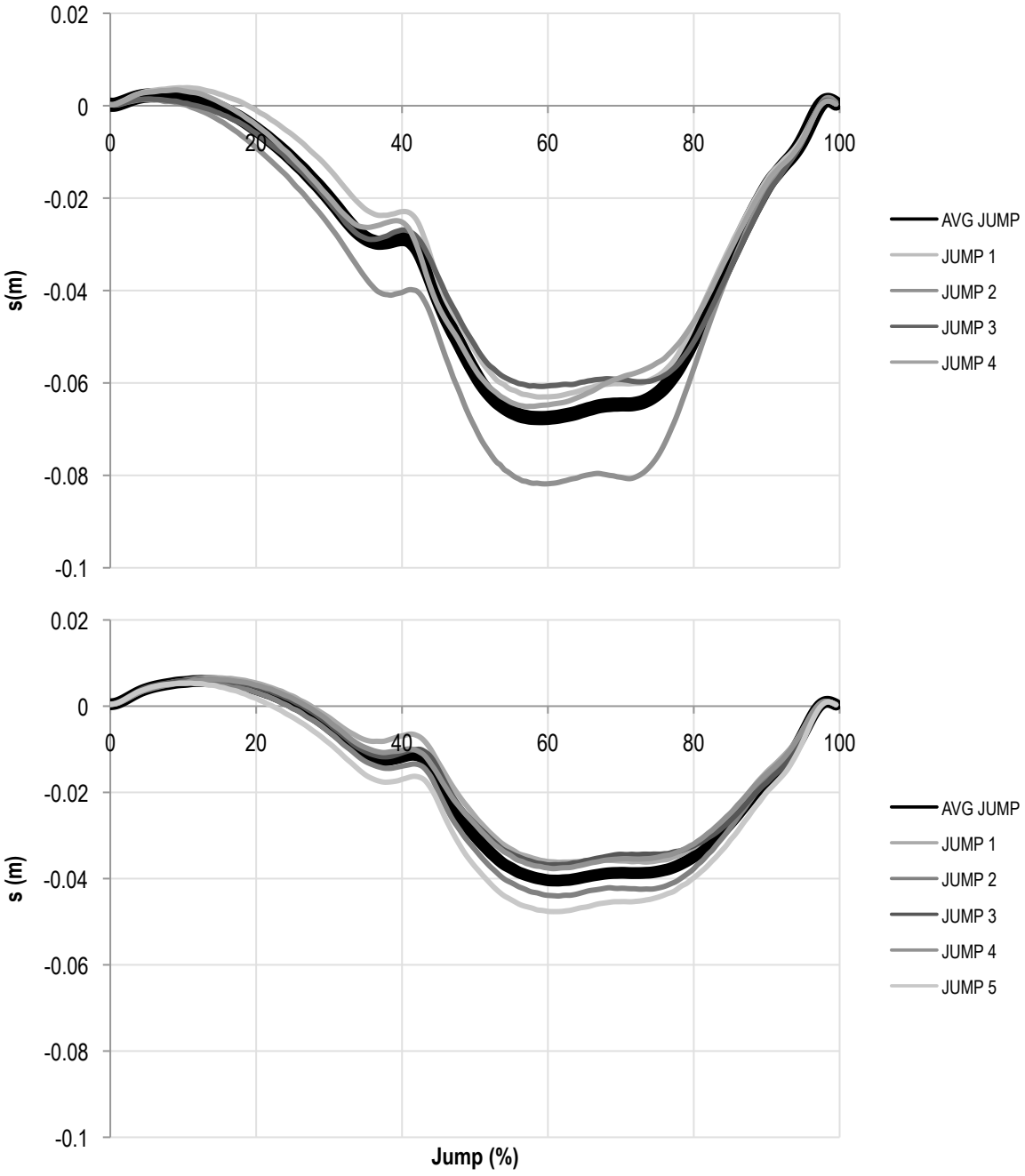

Figure 2.22: Subject 3 normal (upper graph) and controlled (lower graph) jumps. The mean curve of s (visceral mass displacement) for every trial and the mean of all the trials curve are shown for both the techniques.

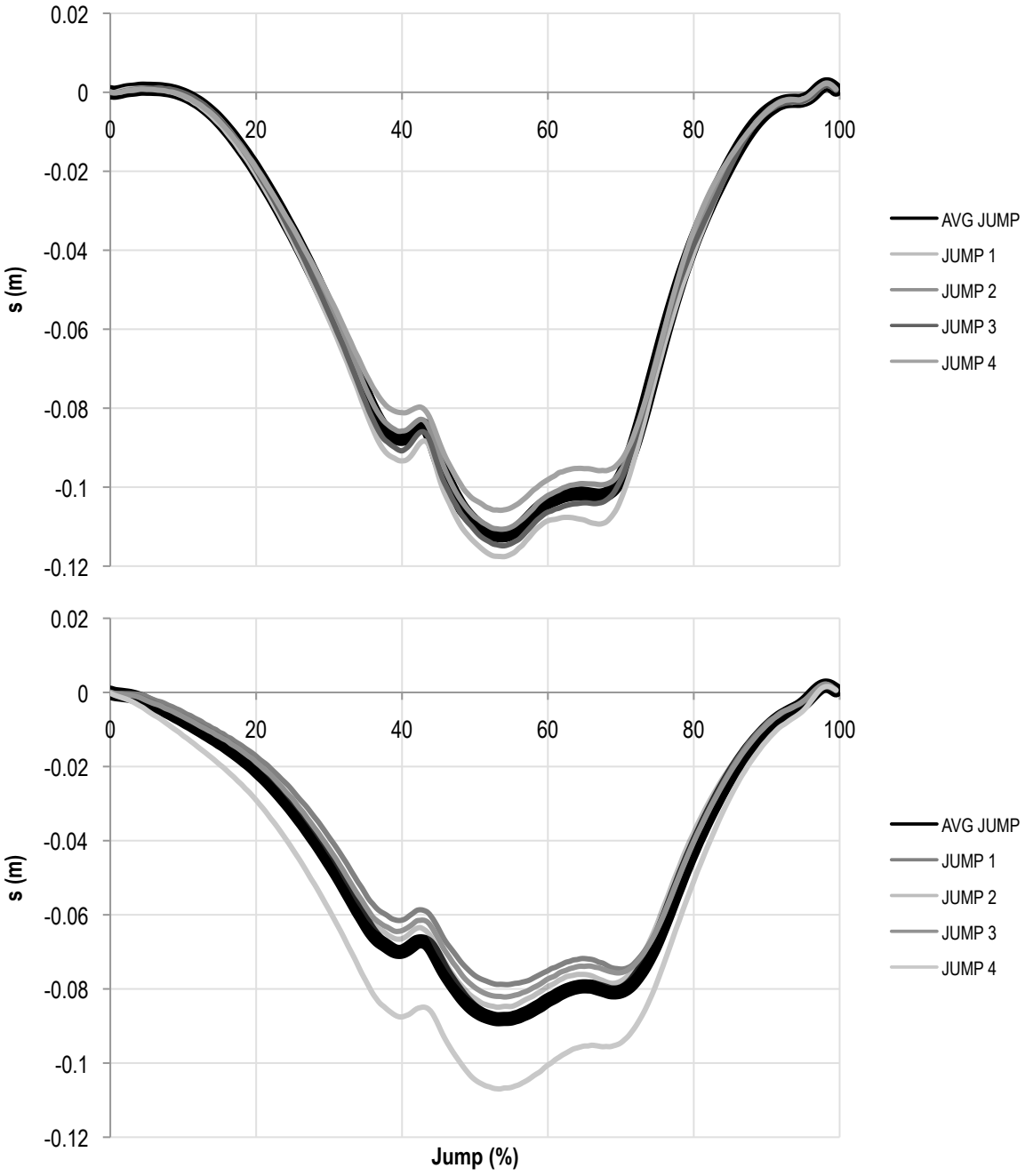

Figure 2.23: Subject 6 normal (upper graph) and controlled (lower graph) jumps. The mean curve of s (visceral mass displacement) for every trial and the mean of all the trials curve are shown for both the techniques.

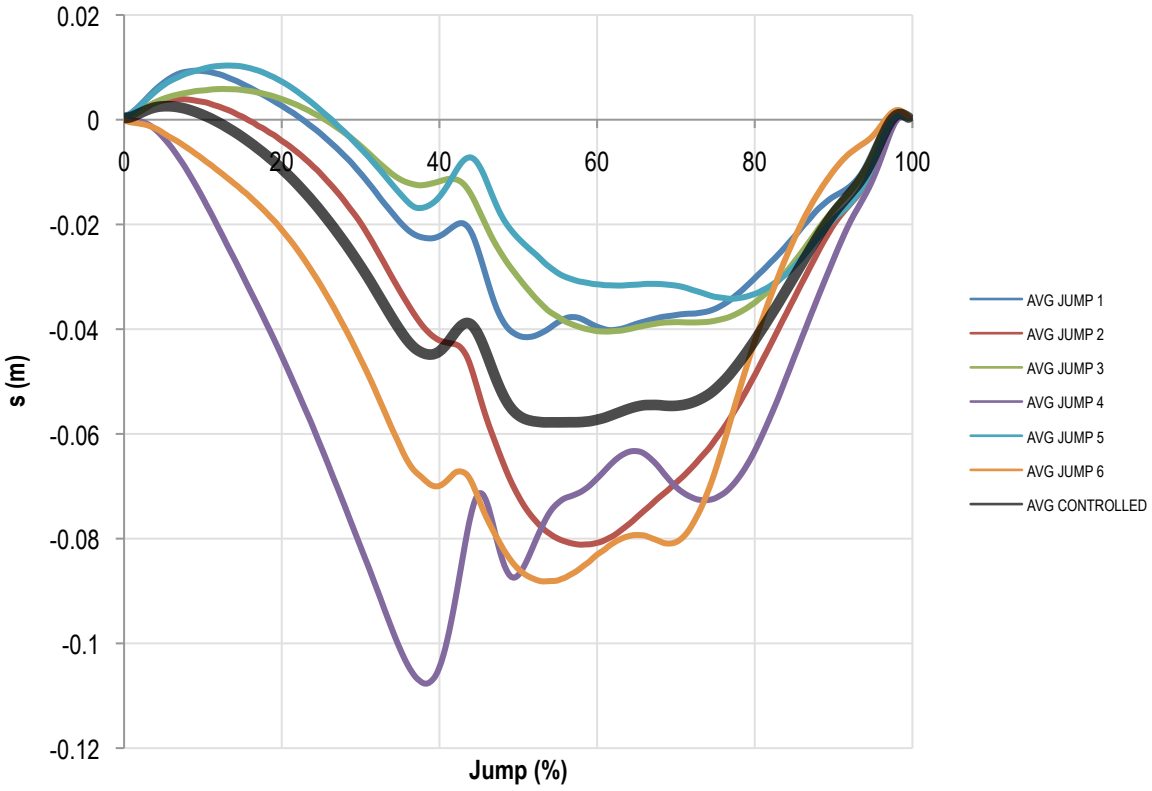

Figure 2.24: The overall mean curve of controlled jumps (black). All the mean curves of s (visceral mass displacement) for every subject (1-2-3-4-5-6) in normal jumps are also showed.

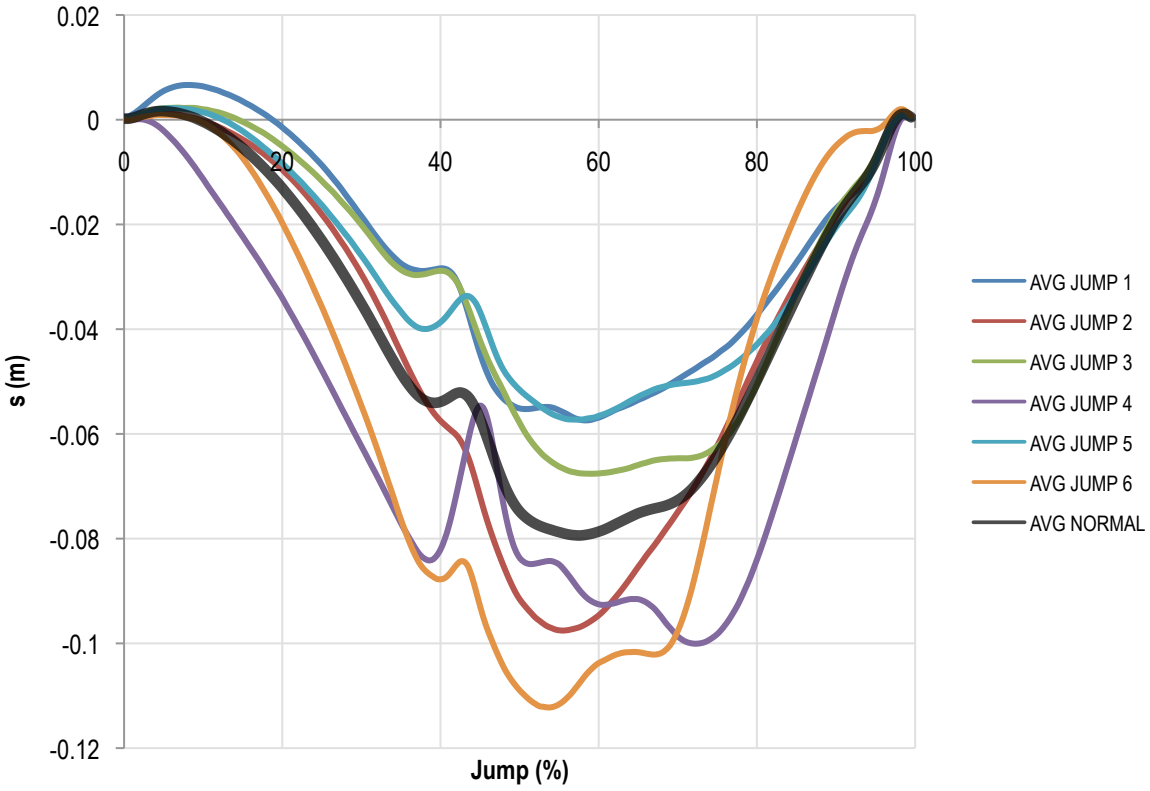

Figure 2.25: The overall mean curve of normal jumps (black). All the mean curves of s (visceral mass displacement) for every subject (1-2-3-4-5-6) in controlled jumps are also showed.

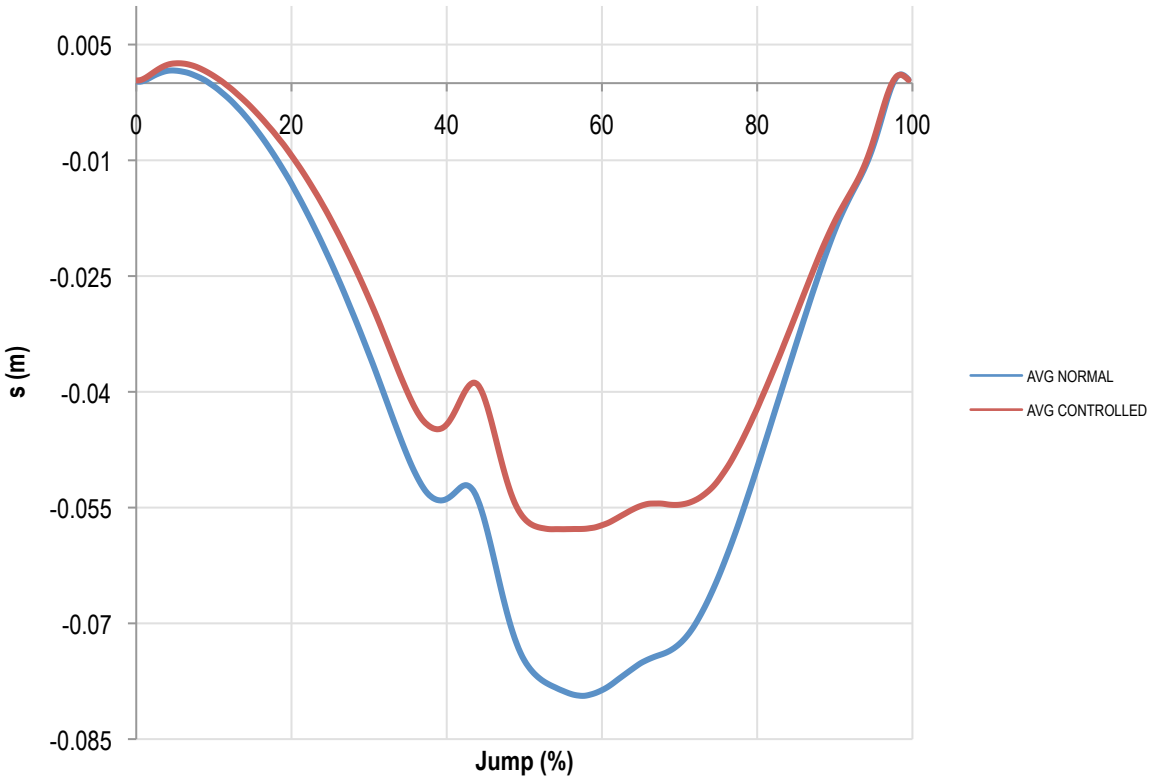

Figure 2.26: The overall mean curve of s (visceral mass displacement) in normal (blue) and controlled (red) jumps.

All the values show the relative viscera displacement with respect of the CoM. An intraclass-correlation shows a significant pattern (Fig. 2.27) for all the subjects (ICC= 0.791; p = 0.017): in 5 subjects, there is a higher mean nominal value of VMD in normal jumps, while in subject 4 the mean nominal value of VMD in controlled jumps, is slightly higher, compared to normal jumps (Fig. 2.19).

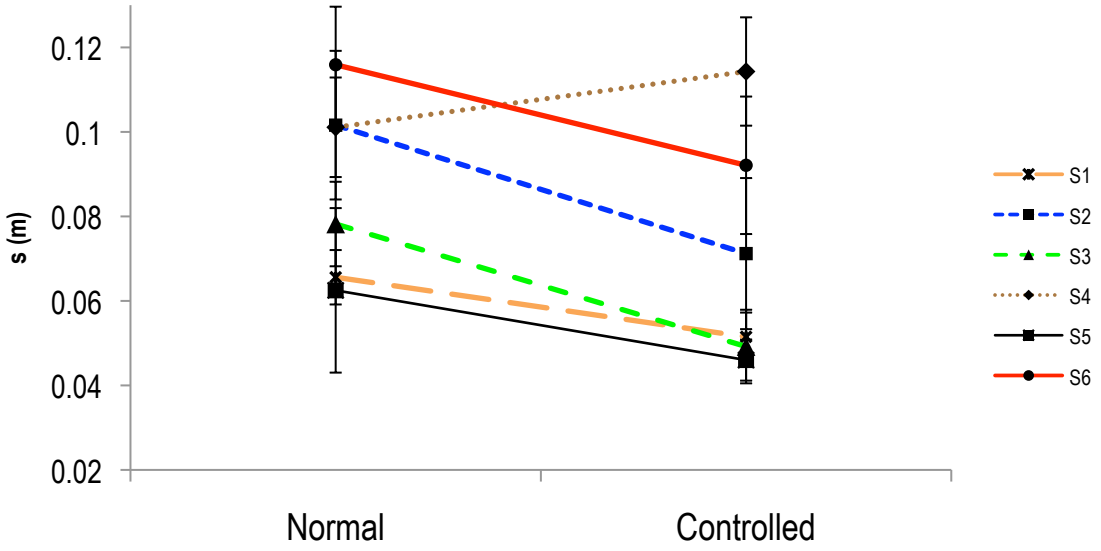

Figure 2.27: Correlation plot that show the pattern of s (visceral mass displacement) between normal and controlled jumps. Mean value and s.d. of all normal and controlled jumps trials are showed for every subject.

Moreover the same subject shows very high value both in normal (0.101 ± 0.011 m) and controlled jumps (0.114 ± 0.012 m), as the subject 6 (normal = 0.115 ± 0.013; controlled = 0.92 ± 0.016) but the descriptive analysis doesn't exhibit any outlier.

Finally, the viscera displacement mean curve both in normal and controlled jumps shown a local maximum ($\dot{s}(t) = 0$) around the 35% - 45% of the jump period due to the foot impact on the platform (Fig. 2.28). These peaks are due to the difference sampling frequency and sensitivity between the dynamometric platform (1.2 KHz) and the motion capture system (400 Hz). Moreover CoM displacement computed from kinematic is a weighted mean of anatomical segments centre of mass, hence it works as a low-pass filter for this vibration.

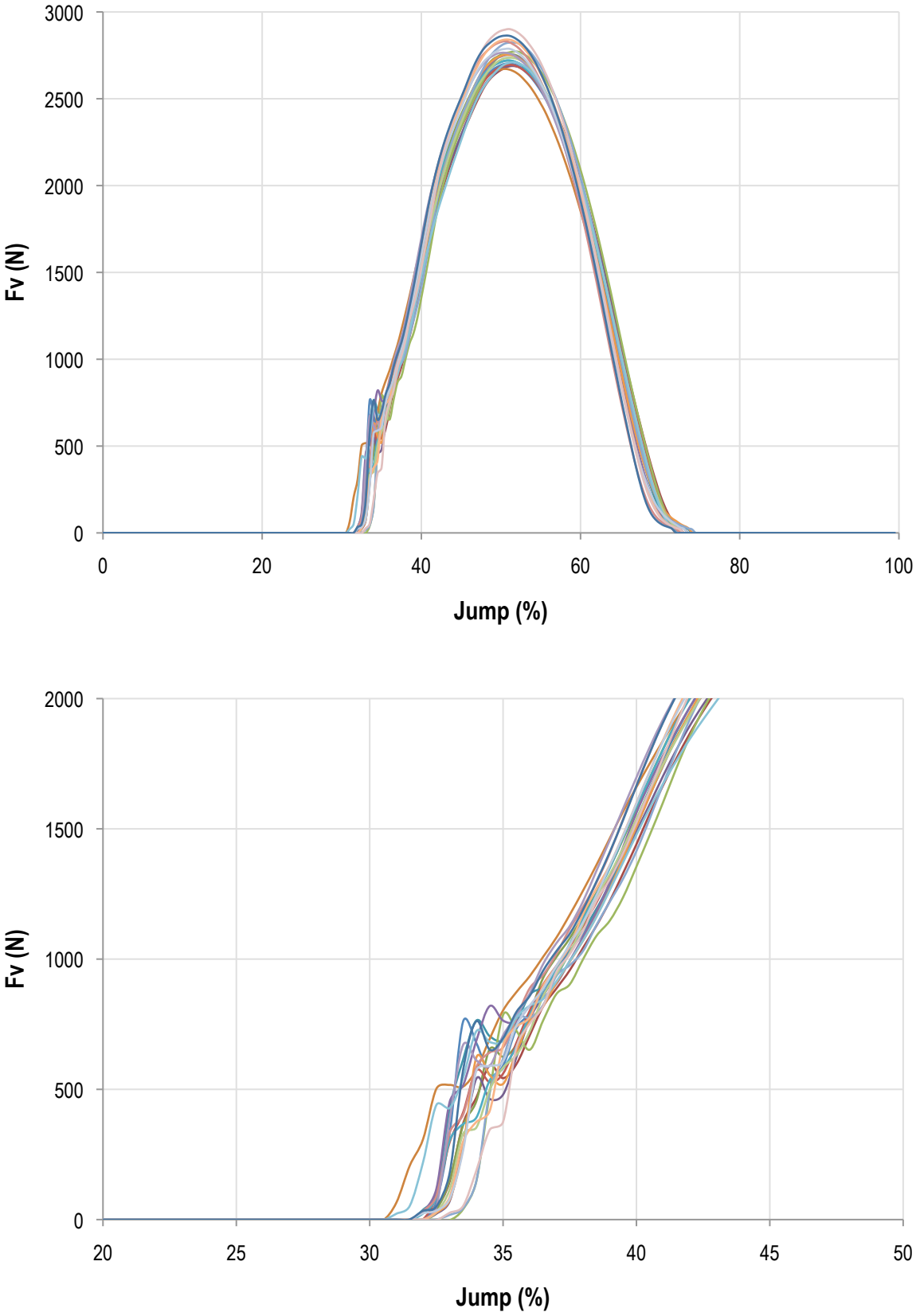

Figure 2.28: In figure are visible the repetitive high frequency peaks, due to the foot impact on the platform. The data shown are related to a single subject (S1) trial, as example of the force signal in respect of the percentage of jump movement.

3.4.2 Abdomen and pectoral motion

In Table 2.4 pectorals and abdomen displacements, weighted by the scaling factor ($m_e/m+m_e$) and divided for every subject, are shown.

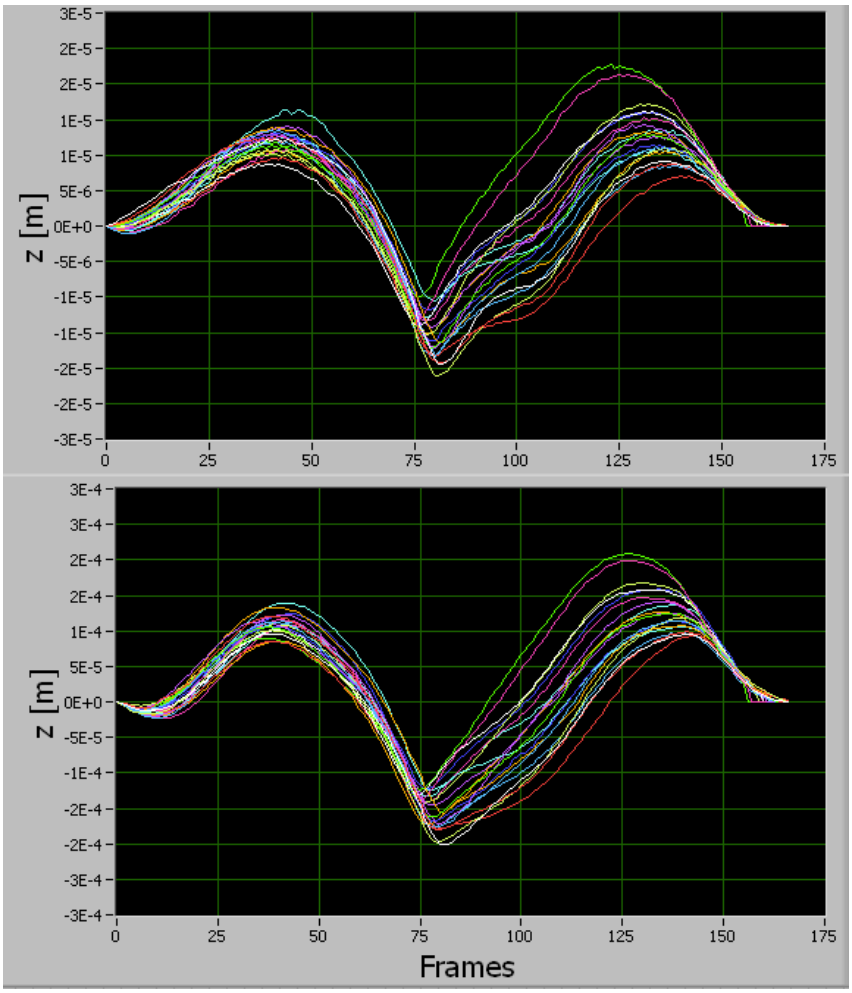

Figure 2.29: Exemplificative curves representing the right and left low abdominal fat displacement from a trials of normal jumps in subject 1. The displacement id weighted by the scaling factor $m_e/(M+m_e)$.

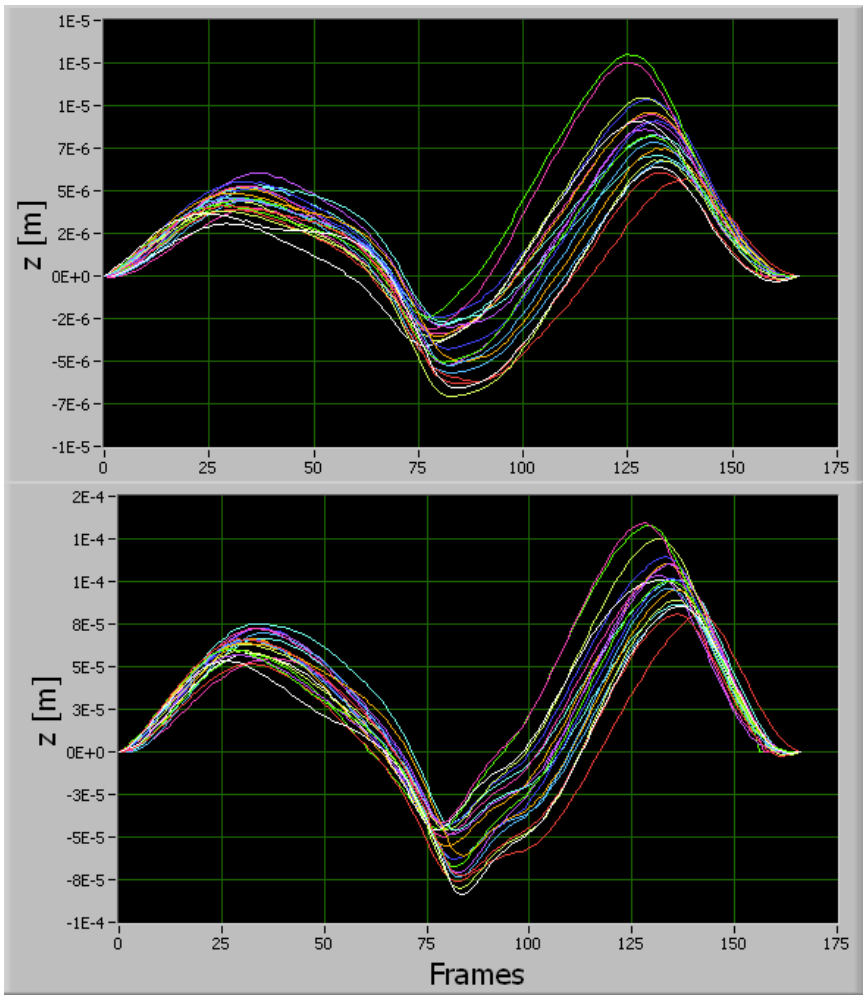

Figure 2.30: Exemplificative curves representing the right and left pectoral displacement from a trials of normal jumps in subject 1. The displacement id weighted by the scaling factor $m_e/(M+m_e)$.

The mean values of pectorals and abdomen displacements, weighted by the scaling factor $m_e/(M+ m_e)$, are 4.5×10^{-4} m and 8.9×10^{-4} m in normal jumps and 4.5×10^{-4} m and 9.6×10^{-4} m in controlled jumps respectively.

Accordingly to these low excursion values, we decide to consider pectoral and abdomen influence negligible on the overall motion. This choice has been done only to simplify vibration modeling, while external masses motion have been taken into account in equation (1) of VMD estimation.

The shape of external mass curve, both for pectoral and low abdomen show a different pattern, characterized by a minimum and a double maximum, hence a not exactly double signal frequency, in respect the viscera motion, is observable. A different motion pattern in

respect of the other internal wobbling mass is due to two reasons: (a) external masses are not closed in a box but free to move with no friction in the external side in respect of the body, but linked on the other side with constrains given by the skin and muscles; (b) vibration parameters as the low mass value and the constant k of the ideal spring (skin–muscles-abdominal fat) or the damping ratio ζ influence the movement.

NORMAL JUMP					
		Pect R	*Pect L*	*Abd R*	*Abd L*
S1	*Mean (m)*	1.34E-05	1.49E-04	3.37E-05	3.18E-04
	SD (m)	1.50E-06	1.27E-05	3.53E-06	3.02E-05
S2	*Mean (m)*	1.28E-05	1.25E-04	2.65E-05	2.71E-04
	SD (m)	2.11E-06	2.28E-05	5.23E-06	5.21E-05
S3	*Mean (m)*	1.31E-05	1.03E-04	2.75E-05	2.23E-04
	SD (m)	2.62E-06	2.03E-05	8.20E-06	5.14E-05
S4	*Mean (m)*	1.66E-05	1.59E-04	3.47E-05	2.97E-04
	SD (m)	2.80E-06	3.10E-05	6.98E-06	6.79E-05
S5	*Mean (m)*	1.27E-05	1.21E-04	2.04E-05	1.94E-04
	SD (m)	1.73E-06	1.54E-05	4.29E-06	3.83E-05
S6	*Mean (m)*	1.78E-05	1.56E-04	3.66E-05	2.99E-04
	SD (m)	3.36E-06	3.37E-05	7.50E-06	5.50E-05

CONTROLLED JUMP					
		Pect R	*Pect L*	*Abd R*	*Abd L*
S1	*Mean (m)*	1.47E-05	1.64E-04	3.51E-05	3.65E-04
	SD (m)	2.12E-06	1.70E-05	4.23E-06	4.10E-05
S2	*Mean (m)*	9.56E-06	1.12E-04	2.03E-05	1.96E-04
	SD (m)	1.32E-06	1.12E-05	3.46E-06	3.37E-05
S3	*Mean (m)*	1.25E-05	1.19E-04	2.81E-05	2.63E-04
	SD (m)	4.03E-06	2.27E-05	6.07E-06	8.70E-05
S4	*Mean (m)*	1.39E-05	1.37E-04	3.30E-05	2.70E-04
	SD (m)	2.41E-06	2.39E-05	7.65E-06	7.08E-05
S5	*Mean (m)*	1.14E-05	1.03E-04	2.40E-05	2.19E-04
	SD (m)	1.74E-06	1.41E-05	4.51E-06	6.04E-05
S6	*Mean (m)*	2.17E-05	1.82E-04	5.14E-05	4.33E-04
	SD (m)	5.72E-06	3.55E-05	1.28E-05	8.13E-05

Table 2.4: Mean values and standard deviations in normal and controlled jumps of right pectoral (Pect R), left pectoral (Pect L), right low abdominal fat (Abd R) and left low abdominal fat (Abd L) in every subject.

3.4.3 CoM and internal mass displacement: amplitude and delay

Visceral mass movement, from a qualitative analysis, shows a different pattern with respect to the container displacement both in normal and in controlled jumps for all the subjects. The time delay between the two curves is evident, and recalls a classical example of periodic signals phase shift. Its value seems to be constant after CoM maximum and minimum, following the 'periodic' CoM displacement. A paired t-test confirmed this hypothesis showing no significant difference of time delay (ms), both during the aerial (18.1 ± 5.73 ms) and landing (18.8 ± 9.8 ms) phases in both the jumping techniques.

A second paired t-test has been performed to evaluate the difference of ratio

$$r_{vm} = \frac{s(t)_{\max}}{y_1(t)_{\max}}$$

switching the technique, where respectively $s(t)_{max}$ and $y_1(t)_{max}$ are VMD and CoM maximum vertical displacement. VMD results significantly dependent on jump maximum vertical excursion, but the mean values of r_{vm} in normal jump are higher than in controlled jump, aside from subject 4 that shows the opposite trend. This is due to the high inter-subject variability as shown in table 2.5b, where the SD is higher then mean value difference.

r_{vm} Paired Samples Statistics

	Mean	N	Std. Deviation	Std. Error Mean
Normal Jump	0.3864	6	0.03496	0.01427
Controlled Jump	0.3363	6	0.0469	0.01915

r_{vm} Paired Samples Test

	Mean	Std. Deviation	Std. Error Mean	Sig. (2-tailed)
Normal - Controlled	0.05015	0.07333	0.02994	0.155

Table 2.5a, 2.5b: Statistic and paired samples test for r_{vm}.

3.3.5 Stiffness and damping parameters estimation

The total mean values and SD of natural frequency in normal and controlled jumps are 6.7 ± 2.5 Hz and 6.6 ± 1.8 Hz respectively, hence the calculated stiffness,

$$k = \left[\left(2\pi f_n \right)^2 m \right]$$

are k_1= 18.2 ± 13.5 KN/m and k_2= 17.9 ± 12.1 KN/m respectively. It has been calculated from the mean curve of every trial for all the subjects for normal and controlled jumps. A paired t-test doesn't exhibit a significant difference between the two techniques. The total mean values of damping ratio,

$$\zeta = \left[\frac{c}{2\sqrt{km}} \right]$$

are 73.6 ± 15.6 % and 73.8 ± 19.1 % for normal and controlled jumps respectively, hence c_1 300.3 ± 170.7 N/(m/s)is and c_2 is 287.3 ± 129.8 N/(m/s). Even damping resulted not different between the two techniques.

3.5 Discussion

3.5.1 Effects of jumping techniques in limiting visceral mass vertical displacement

In this work the effects of "controlled" jumping techniques on viscera displacement have been estimated. The technique is based on respiration and muscles contraction strategies, executed to compress viscera limiting their motion, and to increase the stiffness of the human body.

The method adopted estimates viscera displacement showing the result of the jumping technique, without a direct check on respiration and muscle contractions. For this reason the technique is based on a safe respiration control: the subject, after a deep diaphragmatic inspiration, doesn't breathe (apnea), aside from short and fast trunk expirations before every foot contact. These expirations provoke a higher abdominal muscles contraction to further compress viscera. Certainly, an inspiration and expiration volume measurement could be useful to test subjects' technical ability, but the addition of a spirometer during jumping could become invasive. In this case a previous volume variation measurement to check technique ability is recommended for future experiments.

However, even if a direct control on the technique was lacking, the methodology permitted to measure the decrease of viscera vertical displacement as effect of this technique. The results show a significant difference between the viscera displacement in normal and controlled jumps, but the paired t-test on the ratio r_{vm} does not show a significant difference. The small number of subjects and the inter-subjects variability do not allow to obtain a clear correlation between jump height and viscera motion: for every subject the r_{vm} mean value of all the normal jumps is higher then r_{vm} of controlled jump, except for subject 4, that shows an opposite trend. A significant difference could give a further evidence of technique effect on the system, in addition to the significant vertical excursion

difference. Hence, only the expansion of the sample size could demonstrate respiration and muscle contractions effect on viscera motion, but some evidences of its displacement control are already shown.

Only one out of six subjects shows no differences in the two jumping techniques, and a high mean value of viscera displacement in both the techniques (mean total jumps = 0.107 ± 0.013 m), and this could be seen as a difficulty in technique switch. Unfortunately this subject also shows unreal high values of viscera displacement in both the jumps, but couldn't be considered an outlier from a statistic descriptive analysis. This could be due to a measurement error, but we decided not to repeat the acquisitions of normal jumps after the training period, in order to avoid to influence the jumping technique.

For the other subjects, there is a significant correlation (ICC= 0.791; p = 0.017) in the patter of visceral mass motion between the two jumps to confirm the actual efficacy of the technique. The number of subjects should be increased to minimize the variance and to improve the significance, up to at least ten subjects. However, athletes with specific motor skills and free to attend the training period are difficult to be found.

3.5.2 Physiological data coherence

The viscera displacement mean values both in normal and in controlled jumps are higher when compared to literature values. As anticipated in the introduction, in the literature quantitative analysis have been done only in anatomical (Beillas, Lafon 2009) or slow-dynamic (Hostettler 2009) condition studies, where viscera motion is ranged between 0.03 m and 0.07 m. The unique value related to low repeated jumps has been shown by Minetti (Minetti & Belli 1994), and measured around 0.08 m.

The 'stroke' of the visceral mass is limited in the upper side by the diaphragm and downward by the pelvic floor. Even if the viscera displacement is mainly dependent on intestine and colon motion, because liver and stomach are strongly linked with diaphragm,

the estimation describes the viscera centre of mass displacement as a mean value dependent of all organ movements.

Obviously the higher vertical displacement depends on diaphragm motion, measured in a further study about deep breathing (Boussuges et al. 2009) showing a mean value of 0.070 ± 0.011 m and in an another work on maximum liver and spleen (organs strongly lined with diaphragm) displacement during free breathing (Hostettler, George 2010; Hostettler, Nicolau 2010) with a mean value of 0.0309 ± 0.0055 m.

The higher value measured in this work, (minimum value = 0.034 m – maximum value = 0.136 m; total mean = 0.076 ± 0.024 m) could be related to the different dynamic of the system with respect to previous studies: viscera are propelled by a higher force that in breathing or low jumps. The equation for its motion is:

$$f_v(t) = F_v(t) - M\ddot{y}_1(t) - Mg,$$

where M is the container mass, y_1 the container position and F_v the GRF.

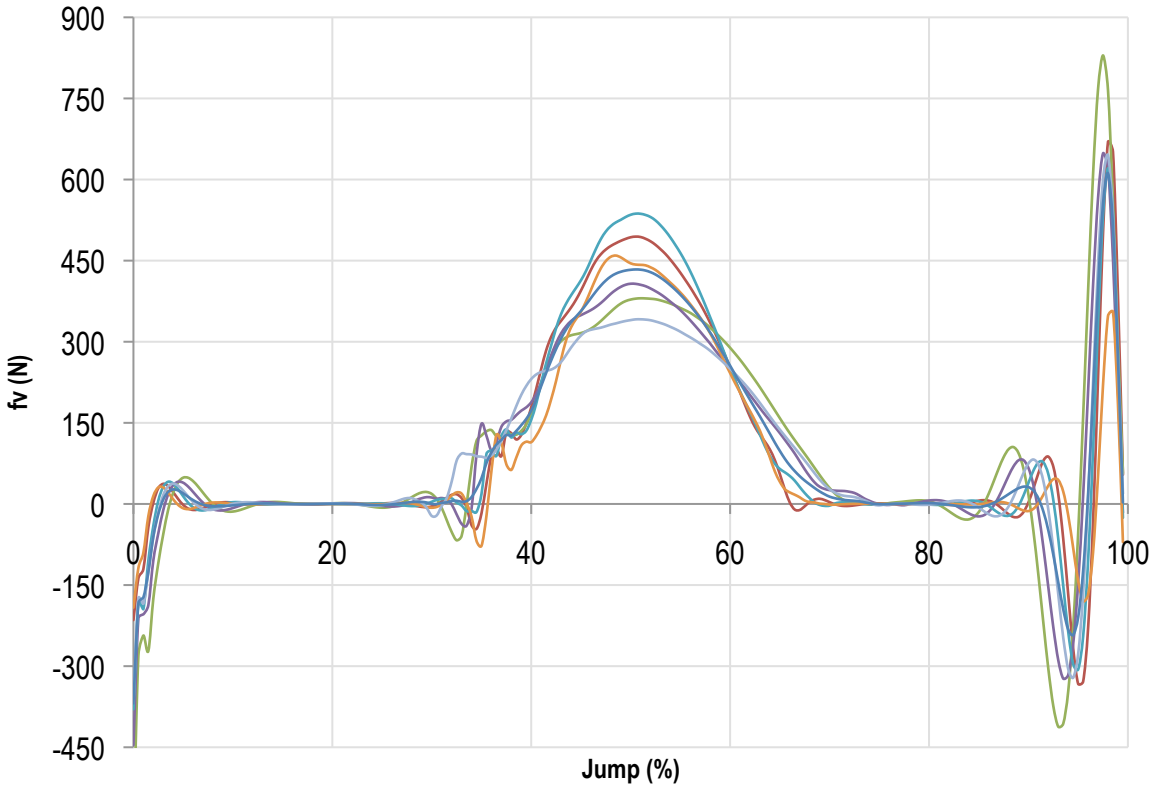

Figure 2.31: The mean f_v (N) profile of every subject in respect of the jump percentage (%).

This speculation is confirmed by the mean CoM excursions in normal and controlled jumps, which are respectively 0.232 ± 0.032 m, and 0.206 ± 0.024 m, revealing a comparable jumping performance of the subjects in both the techniques. This is relevant in sport activities where athlete performance has not to be influenced by the technique.

An important factor could be indentified in method accuracy, because even if the mathematical model has been designed without approximation, and the software has been tested with simulated data, the kinematic measurement with the optoelectronic system could suffer inaccuracy: skin motion and markers positioning couldn't assure a completed fixed reference to the articular joints (Cappozzo et al. 2005; Chiari et al. 2005; Della Croce et al. 2005; Leardini et al. 2005; Lucchetti et al. 1998), and the biomechanical model with 14 segments is an approximation of the human body system. At last, even if the subjects show similar anthropometric measures, minimizing the variance (0.570 ± 0.110 m) especially for trunk length (visceral piston stroke), the standard anthropometric data do not match exactly with individual parameters.

The data acquisition, instead, have been refined: compared with previous method, cinematography acquisition frequency has been quadrupled (400 Hz), providing a better spatial and temporal resolution, while the platform signal has been sampled at 1200 Hz and then decimated to match kinematics. Moreover, signals have been synchronized to fill the time gap due to platform signal double integration, further minimizing the measurement error.

In conclusion, ultrasonography or imaging methods (CT and MRI) are surely more accurate measurements, but also impractical to estimate the effects on a technique in jumping or running. A direct and concurrent measurement with an accelerometer into the abdominal cavity could reveal measurements error of the presented method. A 3 axis

miniaturized accelerometer with transmitting capabilities is at reach with modern technology.

3.5.3 Visceral mass curve analysis

The CoM and visceral mass displacement in periodic movements are not ideal periodic signals, but could be approximated with the Fourier series to compare their phases and amplitudes. In this study visceral mass and CoM curves are not decomposed but are analysed in the time domain, so a phase difference is described as a time delay. The time window chosen is the time between two consecutive CoM maximum. In this way all the signals are cut following CoM 'period', as well as the 'zero phase' reference. The results show, in both the jumping techniques, not significant time delays of viscera mass in respect of the first maximum and the following minimum of CoM, confirming an equal motion pattern of the system. This fact could confirm the hypothesis of a similar movement conditions in both up and down directions.

Anyway, some speculations on anatomical model of visceral mass could be done, although we do not have a precise description of it and, above all, we did not find a time delay. According to human anatomy, visceral mass motion is mainly represented by intestine and colon displacement, as a ball linked on the middle of the upper side of the trunk, but supported by the pelvic floor. Actually organs as liver and stomach could be design as rigid segments while intestine and colon are unshaped and slip each other. That said, this investigation could give rise to some speculations, but the values are estimation of real motion, very difficult to measure in an indirect mode. For example, a specific vibration model could be identified with distinct vibration parameters, depending on physical features and mechanical interactions, for upward and downward motion. Probably the upper side of 'viscera stroke', mainly represented by diaphragm, could have a higher stiffness and could be more regulated by specific respiration technique. Moreover the more

static and limited organs are in the upper side, while the more soft and compliant on the pelvic floor. The pelvic floor does not present marked elastic component, but its interaction with intestine could be modelled as heavy damped due to intestine physical features.

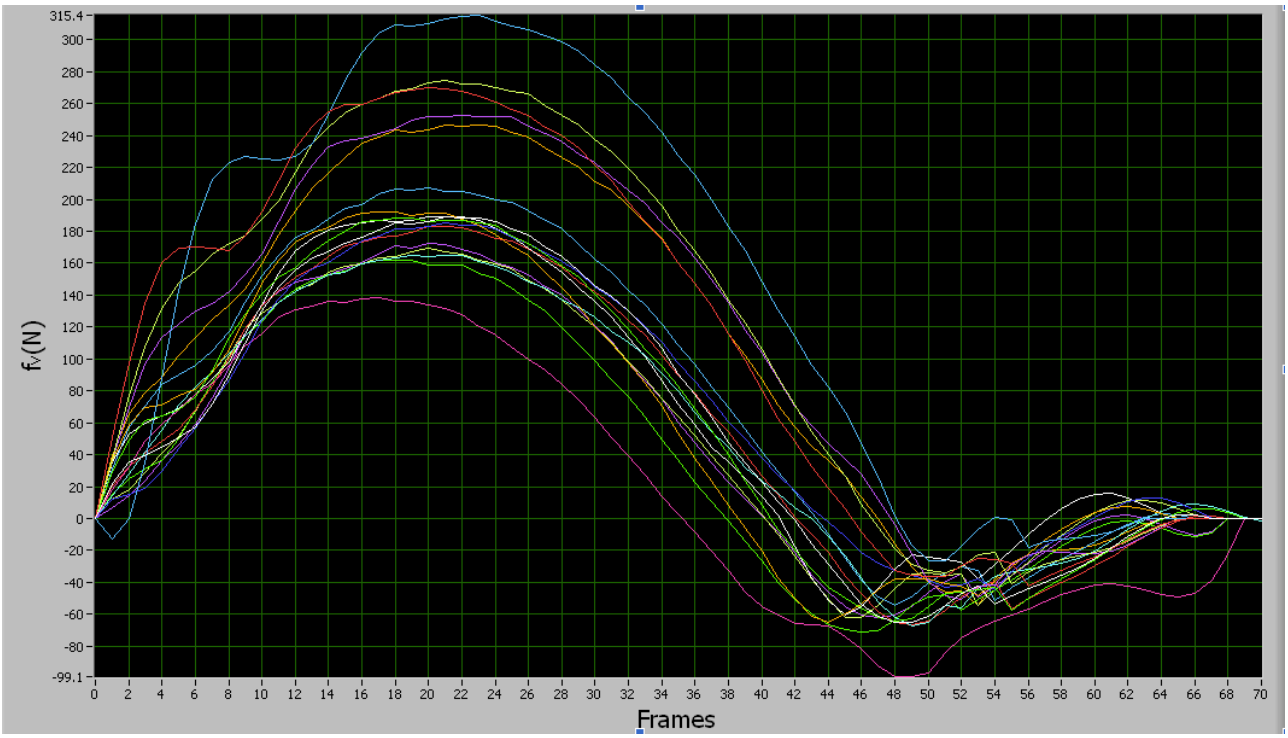

Figure 2.32: The f_v force acting on visceral mass, during the contact time.

A more qualitative description based on curves shape could be done to find general pattern or to focus on specific variations between subjects. A quantitative analysis needs a great database to describe significant patterns.

As described before, VMD shows a constant 'phase shift', in respect of CoM vertical displacement, in all the jumps of all the subjects. As well as in the VMD curve, a local maximum at 40 % of jump movement is exhibited in all the jumps and it's due to foot impact on the dynamometric platform. It could be more accentuated (subject 4 - 5), or smooth (subject 2 - 3), but with a comparable amplitude and shape for normal and controlled jumps within every subject.

The intra-class-correlation analysis, as described in figure 2.27, indicates an approach to describe and to correlate the VMD computed. This analysis exhibits a significant pattern but considering the vertical excursion value and variation in both normal and controlled jumps, two groups could be found: (a) group 'A' made up of subject s 1 - 3 - 5; (b) group 'B' made up of subjects 2 and 5 - 6. The group A presents the lowest VMD excursions, but also dividing the jump in two half, a more visible maximum in the first half for all the jumps. The group B, instead, shows a direct descent and higher excursions. This fact could be related with diaphragm control and its stiffness.

However, in both the groups the most visible pattern change is shown in the second half of the jump: in all the subjects, after the foot contact in controlled jumps, a plateau characterizes viscera displacement as if the viscera has been blocked or pushed up. This pushing force, is really evident in subject 4, where even if a particular pattern is shown, it is evident the ascent profile in controlled jumps, in respect of the descent in normal jump. For this reason, even if a statistically significant evidence was not found for the last curve shape analysis, the technique effect given by a specific respiration and muscle contractions strategy could be detected even in this case. Indeed the maximum inspiration and the concurrent abdominal muscles contraction before foot contact, could produce a plateau in VMD, and exactly block or push up the visceral mass. Moreover this pattern is supported by a significant difference in VMD that shows a limited vertical displacement in controlled jumps.

3.5.3 Vibration parameters of the body: normal and controlled jump influence

As described before, there was no significant difference in vibration parameters between the two techniques. The *k* and *c* mean values could have a physical relevance but are higher in respect of other values found in literature (Cavagna et al. 1997; Muksian & Nash

1974). Moreover standard deviation is very high hence no hypothesis could be inferred. A simple test could be done, estimating the constant k in a free vibration without damping. The constant k is proportional to the force-displacement ratio:

$$k = \frac{f_{v-peak}}{VMD},$$

where the mean value of fv-peak is around the 500 N and of VMD in both the techniques is 0.076 m hence mean k value is around the 6500 N/m.

It could be said that we are in presence of a damped harmonic motion, hence the stiffness should be computed from the equation of a damped harmonic oscillator,

$$f = \left(\frac{1}{2\pi}\right)\sqrt{\frac{k}{m} - \left(\frac{c}{2m}\right)^2},$$

and the harmonic decrease is an exponential decrease:

$z_{vm} = A \cdot \exp^{\frac{-ct}{2m}}$, where A is a constant and z_{vm} the harmonic decrease.

Unfortunately repeated jumps does not show a harmonic oscillations decrease, hence a direct extrapolation from VMD response is not applicable.

Anyway, it's well known that with damping the maximum amplitude ratio occurs at a frequency lower then the resonant frequency $\omega = \omega_n$. The maximum amplitude ratio occurs when

$$\frac{\omega}{\omega_n} = \sqrt{1 - 2\zeta^2}$$

which is lower then the damped natural frequency, $\omega_d = \omega_n\sqrt{1-\zeta^2}$ by a small amount.

Finally, the frequency response method needs different data measurements (accelerometers applied on the body and a huge number of trials) to estimate vibration parameters with an acceptable accuracy.

For this reason in locomotion and biomechanical application theoretical methods are more accurate depending on the optimization of simulated response of vibrational system. In ‘Perspectives’ chapter, this topic will be more precisely discussed.

3.6 Perspectives

In this work we decided to model the system as a SDOF (single-degree-of-freedom) to simplify the vibration analysis and to show preliminary data, but a more complete description could be done in the future using a MDOF (multi-degree-of-freedom) system. The characteristic frequency response of human body should depend on all the mass-spring-damper model acting on the system. The inaccuracy both of measurements and SDOF model potentially caused an unreal variance and an inappropriate data analysis.

In a MDOF system, there are n coupled oscillators and n independent modes of oscillation, hence a frequency domain analysis of the system, shows all the principal mode of vibration. This approach is called principal modes analysis, and allows to decompose an oscillating motion in simple harmonic components, revealing the dynamics of the system.

Hence, a MDOF system oscillates with a motion that contains all the frequencies of its principal modes and can be seen as the superimposition of simple oscillations, everyone at a different frequency. The number of principal modes that exist will correspond to the number of degree of freedom, and in this case are two.

The coordinates used to describe motion also describe modes, and are not stated in absolute quantities, but as numerical ratios $\frac{X_2}{X_1}$, where X2 and X1 are the maximum values of displacement during the harmonic motion of every part of the system. That ratio is the value of one coordinate relative to all the others fixed for any given mode, and the absolute value of any one coordinate determines the value of all the other coordinates.

In conclusion, it is possible to compute the modes of the system by starting from the equation of motion exhibiting the natural frequencies.

A first free-vibration demonstration of container and viscera model is shown:

From the equation of motion,

$$\begin{cases} M\ddot{x}_1 - k_1 x_1 - k_2\left(x_1 - x_2\right) = 0 \\ m\ddot{x}_2 + k_2\left(x_2 - x_1\right) = 0 \end{cases}$$

and for harmonic motion at frequency ω

$$x_1 = X_1 \sin\omega t$$
$$x_2 = X_2 \sin\omega t$$

Substituting for x1 and x2 in the equation of motion,

$$\frac{X_2}{X_1} = \frac{\left(M\omega^2 - k_1 - k_2\right)}{-k_2} = \frac{-k_2}{\left(m\omega^2 - k_2\right)}$$

and eliminating X1 and X2, frequency equation is:

$$\omega_{1,2}^2 = \frac{1}{2}\left[\left(\frac{M+m}{Mm}\right)k_2 + \frac{k_1}{M}\right] \pm \frac{1}{2}\sqrt{\left(\frac{M+m}{Mm}\right)k_2^2 + 2k_1k_2\left(\frac{m-M}{M^2m}\right) + \frac{k_1^2}{M^2}}$$

From this equation is possible to calculate, knowing the masses M and m and estimating k_1 and k_2, the two natural frequencies of the system in an ideal condition of a perfect harmonic motion and without damping.

These are not the real condition of the system, because the response is damped, hence another method has to be found.

Generally, the model parameters could be estimated with two methods:

- Theoretical method: the elementary components of the system (every single oscillator) and their interactions must be modelled, to obtain a system of equations that contains the parameters, and to resolve them in order to confront the effective motion of the system with that one previewed.
- Experimental method: the resonances of the system must be investigated, exciting the system in opportune way and to measure the frequency response in order to confront the experimental data with the theoretical model.

Obviously, it's not simple to excite all the human body because specific force generator devices are needed, for this reason we approached the problem with the theoretical method. An interesting approach is represented by the system identification, that is a general term to describe mathematical algorithms that build dynamical models from measured data: the system could be still described with an input/output relation even in time than in frequency domain, with the same input and output of frequency response method. Two types of models are common in the field of system identification:

- Grey box model: although the peculiarities of what is going on inside the system are not entirely known, a certain model based on both insight into the system and experimental data is constructed. This model does however still have a number of unknown free parameters which can be estimated using system identification. Grey box modelling is also known as 'semi-physical modelling'.
- Black box model: No prior model is available. Most system identification algorithms are of this type.

In the visceral mass example a grey box-model will be chosen, starting from the equation of motion previous shown. The system is described as:

$$\dot{\xi}(t) = A\xi(t) + Bu(t)$$
$$y(t) = C\xi(t)$$

where y(t) is the output/response and u(t) is the input/force. A, B and C are the following matrix:

$$\xi_1 = x_1$$
$$\xi_2 = \dot{x}_1$$
$$\xi_3 = x_2$$
$$\xi_4 = \dot{x}_2$$

$$\dot{\xi}_1 = \xi_2$$

$$\dot{\xi}_2 = \frac{1}{M}\left[F + k_1\xi_1 + c_1\xi_2 + k_2\xi_1 + c_2\xi_2 - k_2\xi_3 - c_2\xi_4\right]$$

$$\dot{\xi}_3 = \xi_4$$

$$\dot{\xi}_4 = \frac{1}{m}\left[-k_2\xi_1 + c_2\xi_2 + k_2\xi_3 + c_2\xi_2 - c_2\xi_4\right]$$

$$\dot{\xi} = \begin{bmatrix} 0 & 1 & 0 & 0 \\ \frac{k_1 + k_2}{M} & \frac{c_1 + c_2}{M} & \frac{-k_2}{M} & \frac{-c_2}{M} \\ 0 & 0 & 1 & 0 \\ \frac{-k_2}{m} & \frac{c_2}{m} & \frac{k_2}{m} & \frac{-c_2}{m} \end{bmatrix}\xi + \begin{bmatrix} 0 \\ 1 \\ 0 \\ 0 \end{bmatrix}F;$$

$$y = \begin{bmatrix} \frac{M}{m+M} & 0 & \frac{m}{M+m} & 0 \end{bmatrix}\xi;$$

The LABVIEW 2009 System Identification Toolkit, will minimize the error between the real response and the one simulated by the software, optimizing the parameters value.

Finally, I foresee an increasing interest in sports biomechanics to improve athletes jumping performance, as well as in the energetics and biomechanics of locomotion.

A more complete and accurate CoM displacement calculation could include viscera motion, adding a not negligible anatomical segment influence (14% of body mass). From an energetic approach, the time delay between body CoM and viscera generates energy losses that confirm an extra-mechanical work done by the system, and could evaluate the 'economy' of different motor strategies. That said, CoM displacement especially in movements characterized by a considerable vertical excursion, could exhibit an oscillation influenced by a component due to viscera relative motion. In this case the classical periodic, ascent or descent profile shown by CoM in running on level or at extreme slopes, could change as well as the related mechanical external work 'WEXT' done. Moreover, visceral mass is accelerated in respect with CoM as the other anatomical segments, enhancing also the mechanical internal work 'WINT' of the system, thanks to its high mass value.

A large database of normal subjects viscera displacement, standardized for anthropometric measures, could be generated to validate a specific motion pattern in running: the influence of this 'visceral mass work', could be correlated with some biomechanical variables as body CoM speed, step frequency, duty factor, or path gradient. In this way an equation model to estimate viscera motion dependent on accessible biomechanical parameters could be inferred, and both CoM displacement and WTOT calculations could be refined.

Obviously, in this case the size effect has a relevant influence, particularly in obese subjects where both internal and external mass oscillations are critical: external mass already shows a different vibration pattern in vertical jump with normal subject, due to the lack of a physical guide on the body, as the abdomen cavity for the internal mass. In this way, visceral mass intervention in mechanical work and CoM computation in obese subjects, could minimize measurements errors, normally quite difficult to prevent.

In the end, this method is based on motion capture and dynamometric platform concurrent measurements, that are traditional instruments of gait analysis. This fact allows to measure viscera motion without other invasive sensors and to easy add its influence in locomotion energetics.

CHAPTER 4

SUMMARY

In this last chapter, an analysis on biomechanical and physiological speculations regarding the relations between the two studies will be presented, while in 'PART I' and 'PART II' sections, specific topics about each study have been debated.

As already mentioned, running energetic in level and non-level gaits has been largely analyzed, as well as the computational methods to estimate total mechanical energy changes 'WTOT' (Ardigo, Lafortuna 1995; Cavagna & Kaneko 1977; Cavagna, Saibene 1964; Cavagna, Thys 1976; Minetti 1995; Minetti 1998; Minetti, Ardigo 1994; Minetti et al. 2002; Minetti & Saibene 1992; Saibene & Minetti 2003). In the past human locomotion has been studied also in relation of effect of size (Cavagna et al. 1983; Minetti, Saibene 1994), age (Cavagna et al. 2008; DeJaeger et al. 2001), gravitational acceleration variation (Cavagna et al. 1998; Griffin et al. 1999; Margaria & Cavagna 1964; Margaria & Cavagna 1967; Minetti 2001), and finally with the application of passive aids in an enhanced leg locomotion (di Prampero 2000; Formenti & Minetti 2007; Smith 1992).

In addiction, mechanics and energetic of human movements in particular conditions, need specific data measurements or analysis of unusual factors, as the mechanical turning work 'WTURN' in skyscraper running, or the estimation of viscera mass displacement 'VMD' in vertical jumps.

This approach allows to improve and refine methods for the calculation of the centre of mass displacement or to estimate the energies involved in a specific locomotion, but also to infer physiological and biomechanical evidences related to race strategies.

Indeed, the viscera motion could be seen as a further anatomical segment to include in the centre of mass computation, with a potential high influence due to its mass (14 % total body mass). In fact as observed in 'PART II', visceral mass displacement curve shows a 'phase shift' in respect of CoM curve, that could generate an extra-mechanical work done by the system: the higher the phase shift the greater the energy lost. In vertical jump the

higher phase shift is found in normal jump, where the subject doesn't add any further control on viscera motion, but it could be obviously associated as well with running.

The CoM displacement alterations due to viscera influence are more significant in applied conditions, because of its relation with performance. As well as in running on curves, where the athletes performance is related to the curvature radius of the path (Usherwood & Wilson 2006) and to the loss of force peak in internal leg (Chang & Kram 2007), the visceral mass motion could take action in running on step and respiratory frequencies, and indirectly on race strategy.

In running competitions and particularly in 'run up' races, the race strategy is a key factor, and for this reason athletes should manage at most their aerobic and anaerobic resource (Capelli 1999; Capelli & di Prampero 1991).

As described in 'PART I', Wilkie's model demonstrates as a subject could express the maximum mechanical power with respect of race duration (Minetti, Cazzola 2009), but a specific strategy has to be chosen: best athletes are keen not to change the vertical speed, or to shift the speed inflection point as far as possible in respect of race duration. The step frequency chosen is strongly linked with race speed, and also correlated with vibration (Cavagna et al. 2005; Cavagna, Mantovani 1997; Farley & Gonzalez 1996; Minetti, Capelli 1995; Minetti, Cazzola 2009) and energetic of running (Dalleau et al. 1998) and walking (Minetti, Capelli 1995).

In skyscraper running, the leading component of the speed is the vertical one and the step frequency $f_{step} = 2\left(\frac{stride}{s}\right)$ is related to the number of stair-step, of height $h_{stair/step}$, in a half stride $N_{stair-step} = \left(\frac{num_{stair-step}}{s}\right)\left(\frac{1}{f_{step}}\right)$.

The best way for an athlete to keep a regular vertical speed profile is to impose a constant stair-step frequency and hence a constant stair-step vertical length

$$l_{stair-step} = \left(\frac{\left(num_{stair-step} * h_{stair-step} \right)}{2 * stride} \right),$$

even if other mechanical determinants could occur (Cavagna, Mantovani 1997; Cavagna et al. 1991).

Moreover different stair-step frequencies lead to different CoM displacements and in particular, the lower the stair-step frequency the lower the CoM vertical oscillations frequency.

In addition, showing the vertical speed as

$$v_{vert-stair} = \frac{num_{stair-step}}{s} = N_{stair-step} * f_{step},$$

the most useful way, for a 'skyscraper runner', to reach the higher speed related to a specific race strategy is to increase $N_{stair\text{-}step}$, rather then f_{step}, that leads to a mechanical internal work and energy expenditure increment.

It is known that during running on positive gradient for extreme slopes the CoM vertical trajectory becomes almost totally ascent (Minetti, Ardigo 1993; Minetti, Moia 2002; Saibene & Minetti 2003), decreasing its oscillations in vertical direction. Improving $f_{stair\text{-}step}$ and in presence of a predominantly CoM ascending profile, also the internal mass oscillation could decrease: flight time is almost nil, and the visceral mass is forced by a more constant stimulus, generating a lower vibration and low energy loss due to phase shift.

An interesting analysis could be suggested: run up runners probably select a specific $N_{stair\text{-}step}$, optimal for both short and long races depending on biomechanical and physiological variables, while f_{step} changes with race duration, and hence in relation with the optimal speed for a specific race. These variables depend on metabolic/mechanical work

minimization, evidently linked to vertical CoM displacement and anatomical segments relative accelerations.

Indeed, the acceleration of a particular anatomical segment as visceral mass could influence both mechanical work and respiration frequency: the mechanical interactions between viscera mass and diaphragm have been verified in bipedal and quadruped locomotion, and its effect has also been shown in 'PART II' of this thesis.

Hence, besides the mechanical optimization, run up runners select naturally also a particular respiration frequency, depending on $N_{stride\text{-}step}$ and correlated to viscera motion. The number of stair-step in an half stride could be extrapolated from 'Skyscraper running' study, and the mean value is 2 (stair-step/stride). Finally this number of stair-step could be correlated with the most advantageous mechanical lever of the leg during foot contact, and with the length-force relationship in the skeletal muscle.

All these speculations could become perspectives for future experiments both about skyscrapers running and viscera displacement in human locomotion.

A simple, not invasive sensor for respiration frequency measurement could be used during run up races to verify the relationships inferred before. Moreover, specific respiration and contraction strategies have to be verified by a direct test with a spirometer: inspiration and expiration flows and volume will be measured performing different respiration techniques.

From a more general biomechanical point of view, the influence of visceral mass motion could be modeled as an equation dependent on specific factors as gradient, speed, frequency and anatomical features as body size and BMI. In this way the estimation of the total external mechanical work, and the computation of CoM displacement could be refined for different gaits and in specific conditions.

Reference

Alexander RM. Wallabies vibrate to breathe. *Nature*. 1987: **328**: 477.

Alexander RM. Breathing while trotting. *Science*. 1993: **262**: 196-197.

Ardigo LP, Lafortuna C, Minetti AE, Mognoni P, Saibene F. Metabolic and mechanical aspects of foot landing type, forefoot and rearfoot strike, in human running. *Acta Physiol Scand*. 1995: **155**: 17-22.

Baudinette RV, Gannon BJ, Runciman WB, Wells S, Love JB. Do cardiorespiratory frequencies show entrainment with hopping in the tammar wallaby? *J Exp Biol*. 1987: **129**: 251-263.

Beillas P, Lafon Y, Smith FW. The effects of posture and subject-to-subject variations on the position, shape and volume of abdominal and thoracic organs. *Stapp Car Crash J*. 2009: **53**: 127-154.

Bernasconi P, Kohl J. Analysis of co-ordination between breathing and exercise rhythms in man. *J Physiol*. 1993: **471**: 693-706.

Bonsignore MR, Morici G, Abate P, Romano S, Bonsignore G. Ventilation and entrainment of breathing during cycling and running in triathletes. *Med Sci Sports Exerc*. 1998: **30**: 239-245.

Boussuges A, Gole Y, Blanc P. Diaphragmatic motion studied by m-mode ultrasonography: methods, reproducibility, and normal values. *Chest*. United States, 2009:391-400.

Bramble DM, Carrier DR. Running and breathing in mammals. *Science*. 1983: **219**: 251-256.

Capelli C. Physiological determinants of best performances in human locomotion. *Eur J Appl Physiol Occup Physiol*. 1999: **80**: 298-307.

Capelli C, di Prampero PE. Maximal explosive power and aerobic exercise in humans. *Schweiz Z Sportmed*. 1991: **39**: 103-111.

Cappozzo A, Della Croce U, Leardini A, Chiari L. Human movement analysis using stereophotogrammetry. Part 1: theoretical background. *Gait Posture*. 2005: **21**: 186-196.

Cavagna GA, Franzetti P, Fuchimoto T. The mechanics of walking in children. *J Physiol*. 1983: **343**: 323-339.

Cavagna GA, Heglund NC, Willems PA. Effect of an increase in gravity on the power output and the rebound of the body in human running. *J Exp Biol*. 2005: **208**: 2333-2346.

Cavagna GA, Kaneko M. Mechanical work and efficiency in level walking and running. *J Physiol*. 1977: **268**: 467--481.

Cavagna GA, Legramandi MA, Peyre-Tartaruga LA. Old men running: mechanical work and elastic bounce. *Proc Biol Sci*. England, 2008:411-418.

Cavagna GA, Mantovani M, Willems PA, Musch G. The resonant step frequency in human running. *Pflugers Arch*. 1997: **434**: 678-684.

Cavagna GA, Saibene FP, Margaria R. External work in walking. *J Appl Physiol*. 1963: **18**: 1-9.

Cavagna GA, Saibene FP, Margaria R. MECHANICAL WORK IN RUNNING. *J Appl Physiol*. 1964: **19**: 249-256.

Cavagna GA, Thys H, Zamboni A. The sources of external work in level walking and running. *J Physiol*. 1976: **262**: 639-657.

Cavagna GA, Willems PA, Franzetti P, Detrembleur C. The two power limits conditioning step frequency in human running. *J Physiol*. 1991: **437**: 95-108.

Cavagna GA, Willems PA, Heglund NC. Walking on Mars. *Nature*. 1998: **393**: 636.

Chang YH, Kram R. Limitations to maximum running speed on flat curves. *J Exp Biol*. England, 2007:971-982.

Chiari L, Della Croce U, Leardini A, Cappozzo A. Human movement analysis using stereophotogrammetry. Part 2: instrumental errors. *Gait Posture*. 2005: **21**: 197-211.

Daley MA, Biewener AA. Muscle force-length dynamics during level versus incline locomotion: a comparison of in vivo performance of two guinea fowl ankle extensors. *J Exp Biol*. 2003: **206**: 2941-2958.

Daley MA, Usherwood JR. Two explanations for the compliant running paradox: reduced work of bouncing viscera and increased stability in uneven terrain. *Biol Lett*. England, 2010:418-421.

Dalleau G, Belli A, Bourdin M, Lacour JR. The spring-mass model and the energy cost of treadmill running. *Eur J Appl Physiol Occup Physiol*. 1998: **77**: 257-263.

DeJaeger D, Willems PA, Heglund NC. The energy cost of walking in children. *Pflugers Arch*. 2001: **441**: 538-543.

Della Croce U, Leardini A, Chiari L, Cappozzo A. Human movement analysis using stereophotogrammetry. Part 4: assessment of anatomical landmark misplacement and its effects on joint kinematics. *Gait Posture*. 2005: **21**: 226-237.

DeLorey DS, Kowalchuk JM, Paterson DH. Adaptation of pulmonary O2 uptake kinetics and muscle deoxygenation at the onset of heavy-intensity exercise in young and older adults. *J Appl Physiol*. United States, 2005:1697-1704.

DeLorey DS, Paterson DH, Kowalchuk JM. Effects of ageing on muscle O2 utilization and muscle oxygenation during the transition to moderate-intensity exercise. *Appl Physiol Nutr Metab*. Canada, 2007:1251-1262.
di Prampero PE. Cycling on Earth, in space, on the Moon. *Eur J Appl Physiol*. 2000: **82**: 345-360.
di Prampero PE. Factors limiting maximal performance in humans. *Eur J Appl Physiol*. 2003: **90**: 420-429.
Donelan JM, Kram R, Kuo AD. Mechanical work for step-to-step transitions is a major determinant of the metabolic cost of human walking. *J Exp Biol*. 2002: **205**: 3717-3727.
Farley CT, Gonzalez O. Leg stiffness and stride frequency in human running. *J Biomech*. 1996: **29**: 181-186.
Formenti F, Minetti AE. Human locomotion on ice: the evolution of ice-skating energetics through history. *J Exp Biol*. England, 2007:1825-1833.
Gabaldon AM, Nelson FE, Roberts TJ. Mechanical function of two ankle extensors in wild turkeys: shifts from energy production to energy absorption during incline versus decline running. *J Exp Biol*. 2004: **207**: 2277-2288.
Giuliodori MJ, Lujan HL, Briggs WS, DiCarlo SE. A model of locomotor-respiratory coupling in quadrupeds. *Adv Physiol Educ*. 2009: **33**: 315-318.
Gottschall JS, Kram R. Mechanical energy fluctuations during hill walking: the effects of slope on inverted pendulum exchange. *J Exp Biol*. 2006: **209**: 4895-4900.
Griffin TM, Tolani NA, Kram R. Walking in simulated reduced gravity: mechanical energy fluctuations and exchange. *J Appl Physiol*. 1999: **86**: 383-390.
Gurd BJ, Peters SJ, Heigenhauser GJ, LeBlanc PJ, Doherty TJ, Paterson DH, Kowalchuk JM. O2 uptake kinetics, pyruvate dehydrogenase activity, and muscle deoxygenation in young and older adults during the transition to moderate-intensity exercise. *Am J Physiol Regul Integr Comp Physiol*. United States, 2008:R577-584.
Hill AR, Adams JM, Parker BE, Rochester DF. Short-term entrainment of ventilation to the walking cycle in humans. *J Appl Physiol*. 1988: **65**: 570-578.
Hostettler A, George D, Remond Y, Nicolau SA, Soler L, Marescaux J. Bulk modulus and volume variation measurement of the liver and the kidneys in vivo using abdominal kinetics during free breathing. *Comput Methods Programs Biomed*. Ireland: 2010 Elsevier Ireland Ltd, 2010:149-157.
Hostettler A, Nicolau SA, Remond Y, Marescaux J, Soler L. A real-time predictive simulation of abdominal viscera positions during quiet free breathing. *Prog Biophys Mol Biol*: 2010 Elsevier Ltd, 2010.
Jones RH, Molitoris BA. A statistical method for determining the breakpoint of two lines. *Anal Biochem*. United States, 1984:287-290.
Koopman B, Grootenboer HJ, de Jongh HJ. An inverse dynamics model for the analysis, reconstruction and prediction of bipedal walking. *J Biomech*. 1995: **28**: 1369-1376.
Kostka T, Drygas W, Jegier A, Zaniewicz D. Aerobic and anaerobic power in relation to age and physical activity in 354 men aged 20-88 years. *Int J Sports Med*. 2009: **30**: 225-230.
Kram R, Taylor CR. Energetics of running: a new perspective. *Nature*. 1990: **346**: 265-267.
Lafortuna CL, Reinach E, Saibene F. The effects of locomotor-respiratory coupling on the pattern of breathing in horses. *J Physiol*. 1996: **492 (Pt 2)**: 587-596.
Larsen AH, Sorensen H, Puggaard L, Aagaard P. Biomechanical determinants of maximal stair climbing capacity in healthy elderly women. *Scand J Med Sci Sports*. Denmark, 2009:678-686.
Laursen B, Ekner D, Simonsen EB, Voigt M, Sjogaard G. Kinetics and energetics during uphill and downhill carrying of different weights. *Appl Ergon*. 2000: **31**: 159-166.
Leardini A, Chiari L, Della Croce U, Cappozzo A. Human movement analysis using stereophotogrammetry. Part 3. Soft tissue artifact assessment and compensation. *Gait Posture*. 2005: **21**: 212-225.
Lucchetti L, Cappozzo A, Cappello A, Della Croce U. Skin movement artefact assessment and compensation in the estimation of knee-joint kinematics. *J Biomech*. 1998: **31**: 977-984.
Margaria R, Aghemo P, Rovelli E. Measurement of muscular power (anaerobic) in man. *J Appl Physiol*. 1966: **21**: 1662-1664.
Margaria R, Cavagna GA. HUMAN LOCOMOTION IN SUBGRAVITY. *Aerosp Med*. 1964: **35**: 1140-1146.
Margaria R, Cavagna GA. Human locomotion on the moon surface. *Riv Med Aeronaut Spaz*. 1967: **30**: 629-644.
McDermott WJ, Van Emmerik RE, Hamill J. Running training and adaptive strategies of locomotor-respiratory coordination. *Eur J Appl Physiol*. 2003: **89**: 435-444.
McFadyen BJ, Winter DA. An integrated biomechanical analysis of normal stair ascent and descent. *J Biomech*. 1988: **21**: 733-744.
McIntosh AS, Beatty KT, Dwan LN, Vickers DR. Gait dynamics on an inclined walkway. *J Biomech*. 2006: **39**: 2491-2502.
Mian O, Thom J, Ardigò L, Narici M, Minetti A. Metabolic cost, mechanical work, and efficiency during walking in young and older men. *Acta Physiol (Oxf)*. 2006: **186**: 127-139.

Minetti A, Belli G. A model for the estimation of visceral mass displacement in periodic movements. *J Biomech*. 1994: **27**: 97-101.
Minetti AE. Optimum gradient of mountain paths. *J Appl Physiol*. 1995: **79**: 1698-1703.
Minetti AE. A model equation for the prediction of mechanical internal work of terrestrial locomotion. *J Biomech*. 1998: **31**: 463-468.
Minetti AE. Walking on other planets. *Nature*. 2001: **409**: 467, 469.
Minetti AE, Ardigo LP. The transmission efficiency of backward walking at different gradients. *Pflugers Arch*. 2001: **442**: 542-546.
Minetti AE, Ardigo LP, Saibene F. Mechanical determinants of gradient walking energetics in man. *J Physiol*. 1993: **472**: 725-735.
Minetti AE, Ardigo LP, Saibene F. Mechanical determinants of the minimum energy cost of gradient running in humans. *J Exp Biol*. 1994: **195**: 211-225.
Minetti AE, Ardigo LP, Saibene F. The transition between walking and running in humans: metabolic and mechanical aspects at different gradients. *Acta Physiol Scand*. 1994: **150**: 315-323.
Minetti AE, Capelli C, Zamparo P, di Prampero PE, Saibene F. Effects of stride frequency on mechanical power and energy expenditure of walking. *Med Sci Sports Exerc*. 1995: **27**: 1194-1202.
Minetti AE, Cazzola D, Seminati E, Giacometti M, Roi GS. Skyscraper running: physiological and biomechanical profile of a novel sport activity. *Scand J Med Sci Sports*. 2009.
Minetti AE, Moia C, Roi GS, Susta D, Ferretti G. Energy cost of walking and running at extreme uphill and downhill slopes. *J Appl Physiol*. 2002: **93**: 1039-1046.
Minetti AE, Saibene F. Mechanical work rate minimization and freely chosen stride frequency of human walking: a mathematical model. *J Exp Biol*. 1992: **170**: 19-34.
Minetti AE, Saibene F, Ardigo LP, Atchou G, Schena F, Ferretti G. Pygmy locomotion. *Eur J Appl Physiol Occup Physiol*. 1994: **68**: 285-290.
Muksian R, Nash CD, Jr. A model for the response of seated humans to sinusoidal displacements of the seat. *J Biomech*. 1974: **7**: 209-215.
O'Connell ER, Thomas PC, Cady LD, Karwasky RJ. Energy costs of simulated stair climbing as a job-related task in fire fighting. *J Occup Med*. 1986: **28**: 282-284.
Paterson DJ, Wood GA, Morton AR, Henstridge JD. The entrainment of ventilation frequency to exercise rhythm. *Eur J Appl Physiol Occup Physiol*. 1986: **55**: 530-537.
Pontzer H. Effective limb length and the scaling of locomotor cost in terrestrial animals. *J Exp Biol*. England, 2007:1752-1761.
Pontzer H. Predicting the energy cost of terrestrial locomotion: a test of the LiMb model in humans and quadrupeds. *J Exp Biol*. England, 2007:484-494.
Rand MK, Ohtsuki T. EMG analysis of lower limb muscles in humans during quick change in running directions. *Gait Posture*. Netherlands, 2000:169-183.
Rousanoglou EN, Boudolos KD. Rhythmic performance during a whole body movement: dynamic analysis of force-time curves. *Hum Mov Sci*. Netherlands, 2006:393-408.
Sabapathy S, Schneider DA, Comadira G, Johnston I, Morris NR. Oxygen uptake kinetics during severe exercise: a comparison between young and older men. *Respir Physiol Neurobiol*. Netherlands, 2004:203-213.
Saibene F, Minetti AE. Biomechanical and physiological aspects of legged locomotion in humans. *Eur J Appl Physiol*. 2003: **88**: 297-316.
Smith GA. Biomechanical analysis of cross-country skiing techniques. *Med Sci Sports Exerc*. 1992: **24**: 1015-1022.
Teh KC, Aziz AR. Heart rate, oxygen uptake, and energy cost of ascending and descending the stairs. *Med Sci Sports Exerc*. 2002: **34**: 695-699.
Usherwood JR, Wilson AM. Accounting for elite indoor 200 m sprint results. *Biol Lett*. 2006: **2**: 47-50.
Willems PA, Cavagna GA, Heglund NC. External, internal and total work in human locomotion. *J Exp Biol*. 1995: **198**: 379-393.
Williams KR, Cavanagh PR. A model for the calculation of mechanical power during distance running. *J Biomech*. 1983: **16**: 115-128.
Winter DA. A new definition of mechanical work done in human movement. *J Appl Physiol*. 1979: **46**: 79-83.
Young IS, Alexander R, Woakes AJ, Butler PJ, Anderson L. The synchronization of ventilation and locomotion in horses (Equus caballus). *J Exp Biol*. 1992: **166**: 19-31.
Yu B, Kienbacher T, Growney ES, Johnson ME, An KN. Reproducibility of the kinematics and kinetics of the lower extremity during normal stair-climbing. *J Orthop Res*. 1997: **15**: 348-352.

Ringraziamenti

Spesso la musica è più diretta di mille parole:

Grazie Elena, solo Faber è capace di raccontarla così . . .

Ti ho trovata lungo il fiume
che suonavi una foglia di fiore
che cantavi parole leggere, parole d'amore
ho assaggiato le tue labbra di miele rosso rosso
ti ho detto dammi quello che vuoi, io quel che posso.
F. De Andrè

Grazie Prof, per il 'Tutto è possibile', per 'Le tre vite da vivere' e per '…charm'

Non conosce paura l'uomo che salta
e vince sui vetri e spezza bottiglie e ride e sorride,
perchè ferirsi non è impossibile,
morire meno che mai e poi mai.
F. De Gregori

Grazie Mamma e Babbo,

E con le stesse scarpe camminare
per diverse strade
o con diverse scarpe
su una strada sola
F. De Gregori

Grazie Paolino, solo tu. . .

Ma quando vide l'amico legato intorno al ramo
trafitto dai coltelli come un San Sebastiano
Niso dovette uscire che troppo era il furore
quattro ne fece fuori prima di cadere.
M. Bubola

Grazie Gabri, Darione, Teo, Fra, Carmensita, AnTonno, Cristine, Fabrizio, Sara, Gaspare e il Telli,

La storia siamo noi, nessuno si senta offeso,
siamo noi questo prato di aghi sotto il cielo.
La storia siamo noi, attenzione, nessuno si senta escluso….
…La storia siamo noi, siamo noi che scriviamo le lettere,
siamo noi che abbiamo tutto da vincere, tutto da perdere.
F. De Gregori

Grazie Carlito Suarez,

Alla fiera dell'est, per due soldi un topolino mio padre comprò. E venne il cane, che morse il gatto che si mangiò il topo, che al mercato mio padre comprò.
A. Branduardi

Grazie Pietro, Riccardo, Mario, Galli, Sandra, Marina e Anna,

Viva l'Italia, l'Italia liberata,
l'Italia del valzer, l'Italia del caffè.
L'Italia derubata e colpita al cuore,
viva l'Italia, l'Italia che non muore.

F. De Gregori

Grazie a “I Re della Cantina” : Maxsfiga, Coe, Merk, Paolino, Clara Jones, Benedicts, Lillas, Damianito Gordito e Kaz,

Ahi, permette signorina, siamo i re della cantina
vampiri nella vigna, sottrattor nella cucina
son monarca e son boemio, se questa è la miseria
mi ci tuffo, con dignità da rey …
V. Capossela

Grazie “Daniele Gallo y compadres”,

Siamo santi o peccatori
Siamo grandi o irrisolti
Siamo noi il Sole e la Luna….
l'eletto e la fortuna
D. Gallo

Grazie Paro, Laura e Giada,

Il capitano non tiene mai paura, dritto sul cassero,
fuma la pipa, in questa alba fresca e scura che rassomiglia un pò alla vita.
E poi il capitano, se vuole, si leva l'ancora dai pantaloni
e la getta nelle onde e chiama forte quando vuole qualcosa,
c'è sempre uno che gli risponde.
F. De Gregori

Grazie Eziaz, Leozinho, Luca Ardigò,

Io la sera mi addormento
e qualche volta sogno perché voglio sognare
e nel sogno stringo i pugni
tengo fermo il respiro e sto ad ascoltare.
Qualche volta sono gli alberi d'Africa a chiamare
altre notti sono vele piegate a navigare.
Sono uomini e donne piroscafi e bandiere
viaggiatori viaggianti da salvare.
I. Fossati